

8-2012

# THE POWER OF THERMONUCLEAR SUPERNOVAE AFTER ONE YEAR

Ginger Bryngelson

Clemson University, rhizomaroma@gmail.com

Follow this and additional works at: [https://tigerprints.clemson.edu/all\\_dissertations](https://tigerprints.clemson.edu/all_dissertations)



Part of the [Astrophysics and Astronomy Commons](#)

---

## Recommended Citation

Bryngelson, Ginger, "THE POWER OF THERMONUCLEAR SUPERNOVAE AFTER ONE YEAR" (2012). *All Dissertations*. 998.  
[https://tigerprints.clemson.edu/all\\_dissertations/998](https://tigerprints.clemson.edu/all_dissertations/998)

This Dissertation is brought to you for free and open access by the Dissertations at TigerPrints. It has been accepted for inclusion in All Dissertations by an authorized administrator of TigerPrints. For more information, please contact [kokeefe@clemson.edu](mailto:kokeefe@clemson.edu).

THE POWER OF THERMONUCLEAR SUPERNOVAE AFTER ONE YEAR

---

A Thesis  
Presented to  
the Graduate School of  
Clemson University

---

In Partial Fulfillment  
of the Requirements for the Degree  
Doctor of Philosophy  
Physics

---

by  
Ginger Bryngelson  
August 2012

---

Accepted by:  
Dr. Mark D. Leising, Committee Chair  
Dr. Jeremy King  
Dr. Dieter Hartmann  
Dr. Jens Oberheide

## ABSTRACT

Type Ia supernovae (SNe Ia), the thermonuclear explosion of a white dwarf, shape our understanding of the expansion of the universe with the use of their uniformity in distance determinations. Powered by radioactivity synthesized in the explosion, they fade slowly over hundreds of days. Sometime after 200 days, the continually expanding ejecta allows  $\gamma$ -rays from  $^{56}\text{Ni}$  and  $^{56}\text{Co}$  decays to escape, and soon any radioactive power contributing to lighting up the SN comes from positrons formed in 19% of  $^{56}\text{Co}$  decays.

While at first it seemed that positrons escaped through the thinning ejecta, it has become apparent that conclusions can only be drawn from accounting for all the power from the near-infrared (NIR) as well as the optical. Only a handful of SNe have been observed during epochs at a year after explosion in both the optical and NIR. These seem to make an argument for the complete trapping of positrons while also suggesting there is more power unobserved in other bands.

This dissertation discusses observations of three nearby SNe; 2006E, 2006ce, and 2006mq, which were all discovered after maximum light, but bright enough to be observed to late times (the latest at  $\sim 525$  days after peak). The late multi-wavelength observations are converted to fluxes and luminosity and we assess the behavior of different wavelength regimes. A simple positron deposition model is employed to estimate the feasibility of positron escape. We find that we cannot rule out positron escape, but that it seems likely that there is a color evolution that shifts power away from observed bands. This shifting of power seems to vary from SN to SN and is not uniform across all normal SNe Ia.

## DEDICATION

This thesis is dedicated to my parents and brother. Your unconditional love and support carry me through any trial I choose to face. And sharing the joy of my successes with you makes it worth the journey. I love you so much.

And also to you, Jeremy, who has loved me more than I deserve, and treated me better than anyone has. You have surprised me with your generosity, delighted me with your wit, and inspired me with your loving heart.

## ACKNOWLEDGEMENTS

I would like to express my gratitude to my advisor, Dr. Mark Leising. Your guidance and patience have helped me to understand the intricacies of SNe Ia, and also enhanced my general curiosity. I appreciate your tireless willingness to answer my questions. I also owe so much Peter Milne who was a mentor in observing, reducing, and assessing SN images. I am so grateful to have had the opportunity to work with him - it was enjoyable and enlightening.

I want to thank my committee, Dr. Jeremy King and Dr. Dieter Hartmann, and Dr. Jens Oberheide for their continual guidance and interest in my graduate career.

I also want to thank the many graduate students whose help was instrumental in putting a world coordinate system on the R band images of SN2006E. Thanks for your 3 hours of clicking on stars, Amber Porter, Julie Djordjevic, Dina Drozdov, Amanpreet Kaur, Tianhong Yu, Joe Liskowsky, Josh Wood, Wresha Parajuli, and Ana Delgado!

And thanks to the amazing non-graduate student – Jeremy Davis – who not only helped put WCS on 2006E images, and helped make badpixel files for them, but for doing the dishes, laundry, cooking and helping me stay sane and happy.

# TABLE OF CONTENTS

	Page
TITLE PAGE . . . . .	i
ABSTRACT . . . . .	ii
DEDICATION . . . . .	iii
ACKNOWLEDGMENTS . . . . .	iv
LIST OF TABLES . . . . .	vii
LIST OF FIGURES . . . . .	viii
1. INTRODUCTION . . . . .	1
1.1 SN Ia Explosion . . . . .	2
1.2 SN Ia Light Curve . . . . .	3
1.2.1 Visible Spectra . . . . .	5
1.3 Unanswered Questions . . . . .	9
1.4 Late Epochs . . . . .	9
1.4.1 The Importance of the Infrared . . . . .	11
2. OBSERVATIONS . . . . .	14
2.1 Telescopes and Instruments . . . . .	14
2.1.1 Super-LOTIS . . . . .	14
2.1.2 Kuiper 1.5m Telescope . . . . .	14
2.1.3 Bok 2.3m Telescope . . . . .	15
2.1.4 Mayall 4m Telescope . . . . .	15
2.1.5 The WIYN 3.5m Telescope . . . . .	15
2.2 The Supernovae . . . . .	15
2.2.1 SN2006E . . . . .	15
2.2.2 SN2006ce . . . . .	18
2.2.3 SN2006mq . . . . .	19
2.3 Image Analysis . . . . .	20
2.3.1 Reductions . . . . .	20
2.3.2 Image Subtraction . . . . .	20
2.3.3 Photometry . . . . .	22
2.4 SN2006E Light Curves . . . . .	22
2.5 SN2006ce Light Curves . . . . .	24
2.6 SN2006mq Light Curves . . . . .	26
3. ANALYSIS . . . . .	33
3.1 Epoch Determination . . . . .	33
3.2 Color Evolution . . . . .	37

3.3	Bolometric Flux . . . . .	38
3.4	Deposited Positron Energy . . . . .	45
4.	CONCLUSIONS . . . . .	54
4.1	Future Work . . . . .	56
	APPENDICES . . . . .	57
A.	DATA REDUCTION How-To's . . . . .	58
	BIBLIOGRAPHY . . . . .	100

## LIST OF TABLES

Table		Page
2.1	SN2006E Observations Log . . . . .	17
2.2	SN2006ce Observations Log . . . . .	18
2.3	SN2006mq Observations Log . . . . .	19
2.4	SN2006E Calculated Visible Magnitudes . . . . .	23
2.5	SN2006E Calculated Near Infrared Magnitudes . . . . .	24
2.6	SN2006ce Calculated Visible Magnitudes . . . . .	24
2.7	SN2006ce Calculated Near Infrared Magnitudes . . . . .	26
2.8	SN2006mq Calculated Visible Magnitudes . . . . .	26
2.9	SN2006mq Calculated Near Infrared Magnitudes . . . . .	27
3.1	Vega and A <sub>0</sub> Star Fluxes by Band . . . . .	39



## LIST OF FIGURES

Figure	Page
1.1 Decay Scheme of $^{56}\text{Ni} \rightarrow ^{56}\text{Co} \rightarrow ^{56}\text{Fe}$ . . . . .	4
1.2 SN Ia Light Curves in $U, B, V, R, I, J, H, K$ . . . . .	6
1.3 Early Spectra of SNe Ia . . . . .	7
1.4 Progression of SNe Ia Spectrum . . . . .	8
1.5 Light Curves of Different Deposition Assumptions . . . . .	10
1.6 <i>UVOIR</i> Light Curve of SN2000cx with Models of Positron Escape . . . . .	12
2.1 SN2006E Before Subtraction . . . . .	20
2.2 Image Subtraction for SN2006E . . . . .	22
2.3 SN2006E B-band Light curve . . . . .	25
2.4 SN2006E V-band Light Curve . . . . .	28
2.5 SN2006E R-band Light Curve . . . . .	28
2.6 SN2006E I-band Light Curve . . . . .	29
2.7 SN2006E J-band Light Curve . . . . .	29
2.8 SN2006E H-band Light Curve . . . . .	30
2.9 SN2006ce Visible Light Curve . . . . .	30
2.10 SN2006ce NIR Light Curve . . . . .	31
2.11 SN2006mq Visible Light Curve . . . . .	31
2.12 SN2006mq NIR Light Curve . . . . .	32
3.1 SN2006E Fit to SN1992A . . . . .	34
3.2 SN2006E Multi-band Lightcurve . . . . .	34
3.3 SN2006ce Multi-band Lightcurve . . . . .	35
3.4 SN2006mq Multi-band Lightcurve . . . . .	36
3.5 V-J Color Evolution of SNe 2006E, 2006ce, and 2006mq . . . . .	37
3.6 SN2003hv with Filter Passbands . . . . .	38
3.7 SN2006E NIR, Visible, and Total Flux from $B, V, R, I, J, H$ Observations . . . . .	41

List of Figures (Continued)

Figure	Page
3.8 SN2006ce NIR, Visible, and Total Flux from $B, V, R, I, J, H$ Observations . . .	41
3.9 SN2006mq NIR, Visible, and Total Flux from $B, V, R, I, J, H$ Observations . . .	42
3.10 Luminosities of SNe 2006E, 2006ce, and 2006mq . . . . .	43
3.11 NIR Plateaus of 8 SNe Ia . . . . .	44
3.12 Power Provided by $\gamma$ -rays and Positrons in SNe Ia . . . . .	46
3.13 Electron Continuous Slowing Down Approximation Range . . . . .	47
3.14 1-Zone Model Column Density . . . . .	47
3.15 1-Zone Model Positron Energy Deposition . . . . .	48
3.16 SN2006ce Luminosity Compared with Positron Energy Deposition . . . . .	49
3.17 SN2006E Luminosity Compared with Model Energy Deposition . . . . .	50
3.18 SN2006mq Luminosity Compared with Positron Energy Deposition . . . . .	50
3.19 SN2003hv $BVRIJH$ Luminosity Compared with the 2006 SNe Ia . . . . .	51
3.20 Late Decline Rates of Bolometric SNe Magnitudes . . . . .	53

# CHAPTER 1

## INTRODUCTION

Type Ia Supernovae (SNe Ia) are thought to be the thermonuclear explosions of degenerate white dwarfs in a binary system. While it is currently unclear whether the majority of SNe Ia derive from a white dwarf (WD) with a stellar companion at a different point in its evolution, or from the double degenerate scenario where both stars are WDs, the observed behavior of these events are phenomenologically similar (Hillebrandt and Niemeyer, 2000). The similarity of each event's absolute peak brightness led to their use as distance indicators. Even after variations in their intrinsic magnitudes were discovered, their usefulness was salvaged and intensified by the realization that SN Ia peak brightness correlates with decline rate (Phillips, 1993),(Perlmutter et al., 1997),(Riess et al., 1996). The shape of a light curve can provide a reliable way of determining SN Ia absolute magnitude, and thus the distance to their host galaxies.

Combined with observations of host galaxy redshift, distant SN Ia distance measurements have resulted in unexpected and dramatic cosmological conclusions. Using Cepheid variables, Hubble (1929) discovered a linear correlation between galaxy distance and velocity in the direction away from us (barring galaxies within the Local Group). Because of SNe Ia, observations have expanded out to distances of hundreds of Mpc and refined the slope of this relationship. At close distances, the relationship is linear, but Riess et al. (1998) found that galaxies moving at the greatest speeds are found to be 0.28 magnitudes dimmer – or 14% farther – than predicted by the linear curve, indicating our universe is accelerating in its expansion (Perlmutter et al., 1997),(Riess et al., 1996).

SNe Ia have been suggested as a possible source of positrons to power the mysterious 511 keV galactic bulge emission. Knödlseder et al. (2005) map out the emission corresponding to electron-positron annihilation and find a strong concentration in the bulge of the Galaxy. The source for the positrons is unknown.

## 1.1 SN Ia Explosion

The light curve that is instrumental in determining SN Ia distance information also tells us a great deal about the physics of this event. The explosion results from a runaway thermonuclear reaction triggered when some part of the degenerate material reaches a high temperature or density. A WD left to its own devices would simply cool down forever, but in a close enough binary system, a WD can accrete mass from its companion star. As its own mass increases, the degenerate material contracts and the gravitational pressure increases. The degeneracy pressure supporting the star against collapse can withstand only so much. For a WD composed of carbon and oxygen (or with equal parts protons and electrons), the mass limit is  $1.44 M_{\odot}$ , known as the Chandrasekhar mass limit. Thus, an explosion would have to occur when or before the WD accretes to this mass. Once ignition occurs somewhere in the WD, the nuclear burning increases the temperature which induces more nuclear burning which quickly spreads throughout the star. The electron degenerate material is not able to expand and cool quickly enough to abate the burning front, and soon the runaway nuclear burning engulfs the star resulting in an explosion.

The burning front moves sub-sonically (a deflagration) through the star, creating iron peak elements in the central regions where the density is the highest. In the outer layers, the density is lower, and nuclear burning produces only intermediate mass elements (IME) such as  $^{40}\text{Ca}$ ,  $^{32}\text{S}$ ,  $^{28}\text{Si}$ , &  $^{20}\text{Ne}$  and may even leave unburned  $^{12}\text{C}$  &  $^{16}\text{O}$ , &  $^{24}\text{Mg}$  (Hillebrandt and Niemeyer, 2000).

Almost the entirety of the released nuclear energy is used up in the expansion of the SN ejecta. If it weren't for the radioactive elements created in the nuclear burning, there wouldn't be much to observe after the initial explosion.

While 1-D single-degenerate Chandrasekhar-mass deflagration models seem to agree very well with many observed light curves and spectra, More complicated models have been invoked to explain the ever increasing nuances of SNe Ia, including double degenerate models, delayed detonation models, and a slew of more recent 3-D models with mixing and asymmetries.

Nuances for SNe Ia include sub-luminous SNe which do not follow the peak-width relationship, SNe with carbon signatures, or with Fe-peak elements in outer layers; and

SNe with fast or slow expansion velocities. However, the majority of SNe Ia fall into the "normal" category. This kind of SN will be examined in the remainder of the thesis.

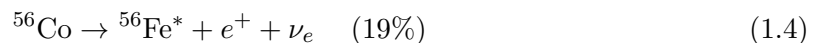
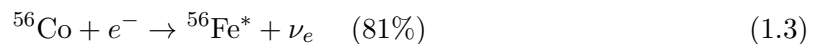
## 1.2 SN Ia Light Curve

The largest source of power for the light curve comes from radioactive  $^{56}\text{Ni}$  – first proposed by Colgate and McKee (1969). A normal SN Ia produces  $\sim 0.6 M_{\odot}$  of  $^{56}\text{Ni}$  (Hoefflich and Khokhlov, 1996), though, depending on the SN, the range can be  $0.07 M_{\odot}$  (Mazzali et al., 1997) to  $1.4 M_{\odot}$  (Filippenko et al., 1992).

The decay schemes of  $^{56}\text{Ni} \rightarrow ^{56}\text{Co} \rightarrow ^{56}\text{Fe}$  (Nadyozhin, 1994) are shown in Figure 1.1.  $^{56}\text{Ni}$  electron capture decays with a lifetime of  $\tau_{\text{Ni}} = 8.80$  days to an excited state of  $^{56}\text{Co}$ , which decays — cascading through subsequent excited states — to the ground state, releasing photons of average energy 1.72 MeV.



$^{56}\text{Co}$  then decays with a lifetime of  $\tau_{\text{Co}} = 111.3$  days into an excited state of  $^{56}\text{Fe}$  through electron capture 81% of the time, and through beta decay 19% of the time.



The excited state ( $^{56}\text{Fe}^*$ ) decays through multiple photon emissions to the stable ground state of  $^{56}\text{Fe}$ .



The decay produces gamma rays of average energy  $\sim 1$  MeV, while the positron may have kinetic energy ranging from 0-1.459 MeV (with a typical energy of 0.632 MeV) (Nadyozhin, 1994).

At early times the SN Ia ejecta are optically thick, and all gamma rays produced by radioactive decay deposit all of their energy, predominantly through Compton scattering. This creates energetic electrons which then thermalize mainly through exciting and ionizing

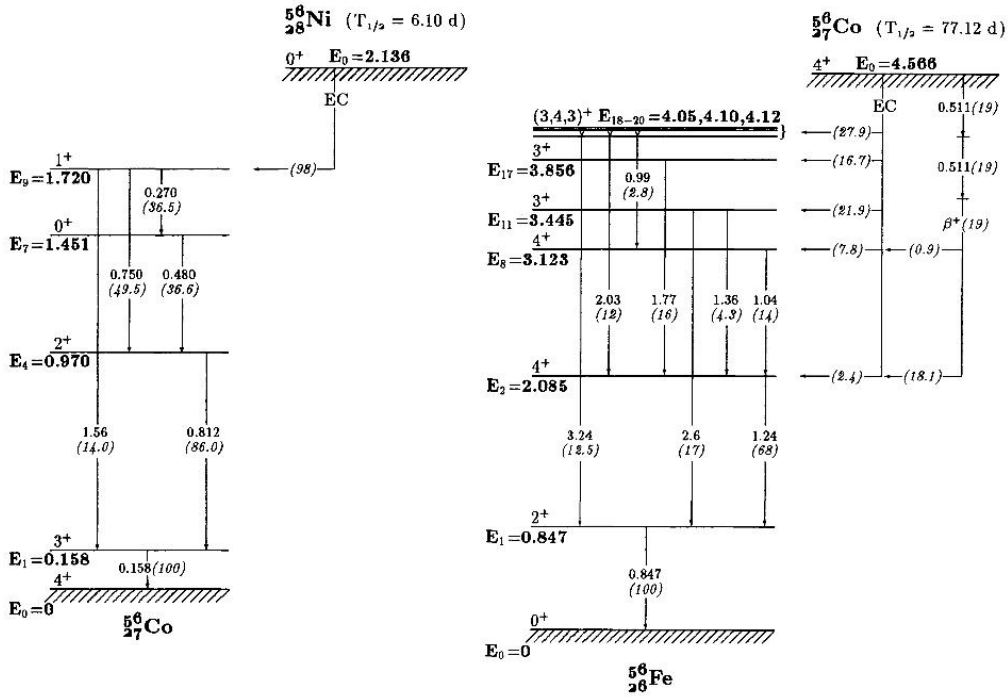


Figure 1.1 The simplified decay schemes of  $^{56}\text{Ni} \rightarrow ^{56}\text{Co}$  (left) and of  $^{56}\text{Co} \rightarrow ^{56}\text{Fe}$  (right) from Nadyozhin (1994). The number in parentheses at each transition is the percentage of photons per decay that undergo that transition, while the number in bold (if present) indicates the energy (in MeV) of the photon emitted.

bound electrons. Visible photons created from de-excitation and recombination diffuse through and eventually escape from the outer photosphere-like layers of the ejecta. At this “photospheric” phase, the radiative output can be approximated as a blackbody. But the ejecta, traveling at 11-13,000 km/s, continue to expand, and after 200 days past maximum light, the SN transitions to a nebular phase. The optical depth decreases, the diffusion timescale is shortened, trapping is less-efficient, and light escapes from deeper and deeper in the ejecta. Once in the nebular phase, the material is optically thin and completely transparent to the gamma rays. Now, only the deposition of kinetic energy of the positrons from the  $^{56}\text{Co} \rightarrow ^{56}\text{Fe}$  decay power the light curve. The fraction of positrons that do not escape is dependent on the configuration of the magnetic field (Milne et al., 2001).

Thus, the light curve shapes are built from the evolution of escaping thermal photons. In the beginning, the ejecta is optically thick, so the random walk of these photons requires a long time before they reach the surface. Consequently, the light curve is initially dim, but progressively increases in luminosity as more and more of these photons are able to escape. The number of escaping photons peaks roughly 18 days after explosion. The decrease that follows is due, in part, to the decreasing density. More gamma rays escape, thus fewer are energizing the ejecta.

The opacity in the UV and blue wavelengths is very large, so any photons radiated in the ejecta at this regime are absorbed and their energy is redistributed through repeated fluorescences (Pinto and Eastman, 2000). An energetic photon excites a high-energy atomic transition, which de-excites in a cascade of lower energy transitions. The amount of light seen in an energy band depends on the number of transitions resulting in, and the monochromatic opacity for, each line in that energy band. Thus, each band exhibits a differently shaped light curve, which evolves differently with time. Figure 1.2, taken from Kasen (2006), shows the evolution of the early light curve in several bands – from the visible to near-infrared (NIR).

### 1.2.1 Visible Spectra

While light curves reveal much about the energy release, spectra afford a complementary peek into the chemical make-up.

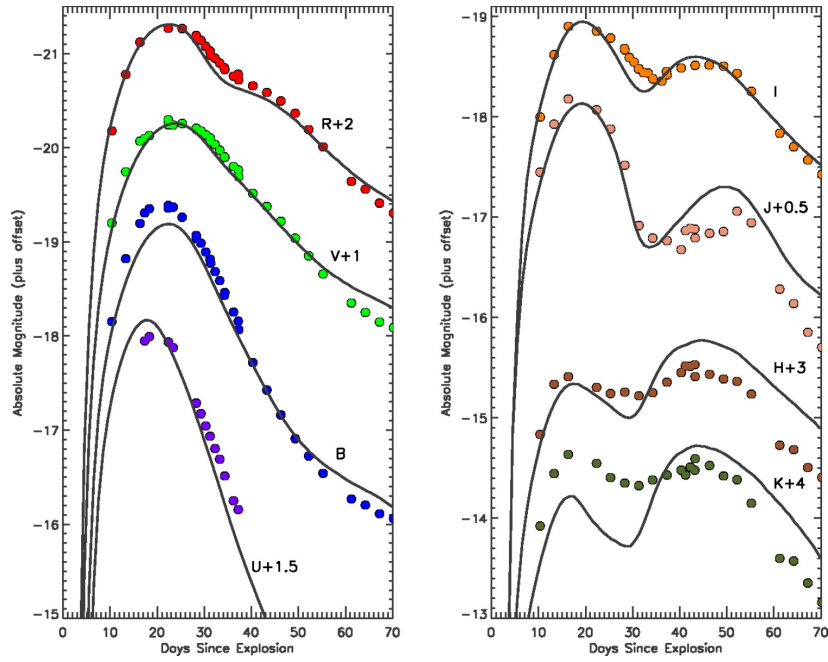


Figure 1.2 Taken from Kasen (2006), the light curves of the normally luminous SN Ia SN2001el (circles) plotted with models for  $U, B, V, R, I, J, H, K$  bands. Note the different timing of maximum light and dissimilar shapes for each band — particularly, the secondary maximum in the NIR.



Early spectra reveal deep Si II absorption lines and those of other IME, indicating that burning does not reach nuclear statistical equilibrium (NSE) in outer layers (Branch, 1982). Figure 1.3 shows the early spectrum of three typical SNe Ia. All exhibit the tell-tale deep Si absorption lines (at 6150 Å) which is what designates them as Ia. They also show other IME lines (e.g., Ca II at ~ 8300 Å). Note how remarkably similar these spectra are.

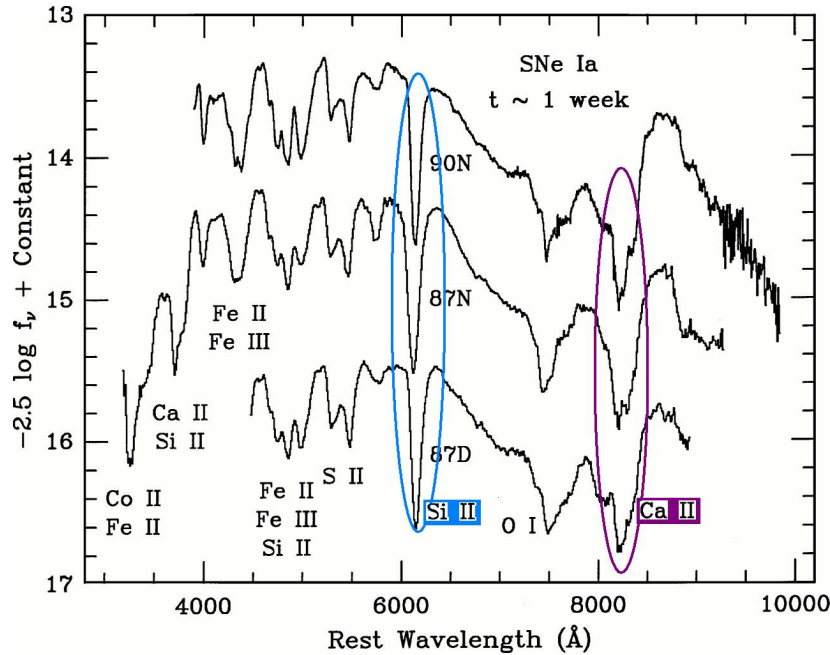


Figure 1.3 From Filippenko (1997), the visible spectra of SNe Ia (from top to bottom: SN1990N, SN1987N, SN1987D) arbitrarily offset vertically for better viewing. The deep Si II trough at 6150 Å is from blue-shifted Si II 6347 Å and 6371 Å lines — collectively called  $\lambda 6355$  Å. The early Si signature indicates incomplete nuclear burning in the outer layers of SNe Ia. The homogeneity of SNe Ia is evident in the notches present in each spectra (e.g., near 4550 Å, 4650 Å, and 5150 Å)

As time progresses, and the photosphere recedes further into the ejecta, we see fewer IME and more iron-group elements. Figure 1.4 shows the progression of spectra for a typical SN Ia.

Note at early times, the Si II absorption at  $\lambda 6355$  Å is strong, but starts to weaken after 2 weeks ( $t \geq 14$  days). Also at 2 weeks, Fe II emission ( $\lambda \sim 6500$  Å) and absorption

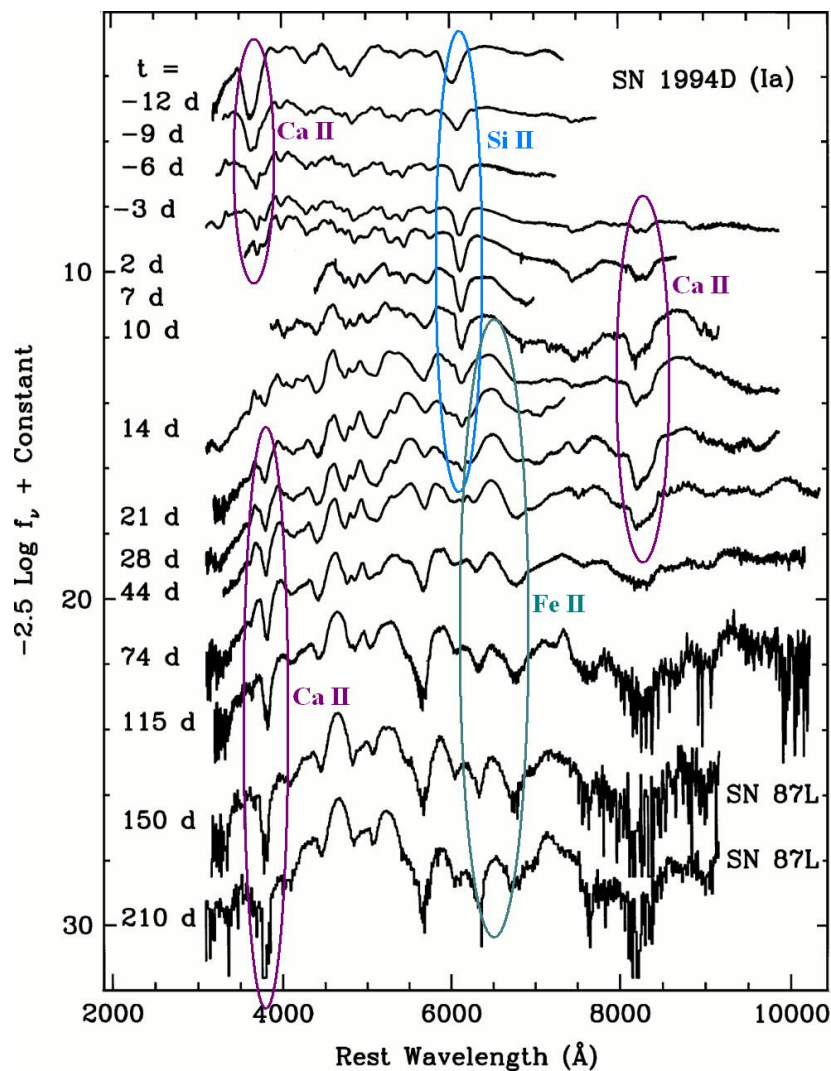


Figure 1.4 The progression of the visible spectra of normal SN Ia SN1994D from Filippenko (1997). Time is labeled on the left with  $t = 0$  occurring at maximum light. See text for qualitative explanation. The last two spectra are of the similar SN1987L.

emerges, which is a hint that we're beginning to see the iron-rich core. There are still Ca II lines visible ( $\lambda \sim 3800 \text{ \AA}$ ), but Co lines dominate and dozens of forbidden Fe emission lines can be seen. The decrease of Co lines is at a rate consistent with radioactive decay of  $^{56}\text{Co}$ .

### 1.3 Unanswered Questions

Despite their use as cosmological distance indicators, much is still not understood about SNe Ia. The progenitor of a SN Ia explosion has long been thought to be a WD with a companion star (perhaps a Red Giant). However, observations such as Brown et al. (2012) are beginning to suggest that the double degenerate scenario is more likely.

The location of the point of ignition starting the thermonuclear explosion is still unknown as well. Ignition may occur at the center, where the density is the highest, or at the surface where accretion is taking place. Recent 3-D models utilize multiple ignition points scattered through the star. How the burning front propagates is another open question. The delayed detonation model proposed that the burning front begin as a deflagration and then transition at some critical density to a detonation (Khokhlov, 1991). Different burning propagation has been invoked to explain different observations.

A related question involves the location of the synthesized  $^{56}\text{Ni}$ . Depending on the location of the  $^{56}\text{Ni}$  within the SN ejecta, one could expect to see different light curve behavior – either fast rise and fall times from quickly-escaping gamma rays or a slower rise and fall from the deeply buried radioactive material.

At late epochs, the SN ejecta becomes more transparent, and light originates from deeper and deeper. Late-time observations offer a new window on the location of radioactivity, the densities of the ejecta, and thus early explosion physics.

### 1.4 Late Epochs

At early times, all gamma rays from radioactive decays are deposited in the ejecta and their energies go towards powering the light curve. However, as the ejecta expands, more gamma rays escape. Though they may deposit a minimal amount of energy on their way out, via Compton scattering, most of their energy is lost. At later epochs, all gamma rays escape the ejecta, and it is only the deposition of the kinetic energy of positrons (from

19% of  $^{56}\text{Co}$  decays) that powers the light curve. It is the nature of the magnetic field that determines how far positrons may travel before thermalizing or, at late times, what fraction of positrons escape the ejecta. Figure 1.5, reproduced from Milne et al. (2001), models the bolometric light curve of SNe Ia, showing the luminosity evolution for different assumptions of gamma ray and positron depositions. Note that beginning at  $t \sim 500$  days, the light curve is steeper without positron deposition, because the energy that would be added to power the light curve instead escapes. Thus by measuring the amount of energy

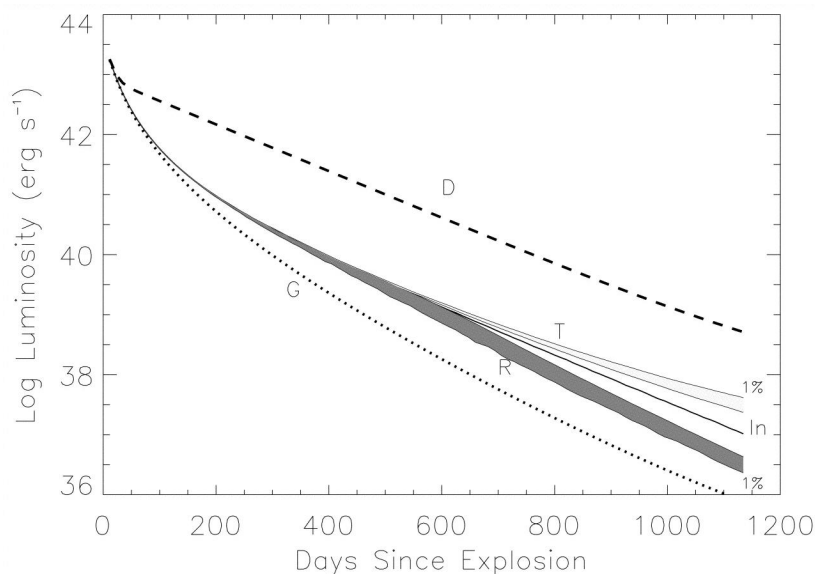


Figure 1.5 From Milne et al. (2001), predicted bolometric light curves assuming instantaneous deposition of all decay energy (dashed line **D**), gamma-ray deposition accounting for escape due to late-time diffuse ejecta (dotted line **G**), and gamma-ray deposition with varying degrees of positron deposition (middle lines **R** through **T**). The dark band (**R**) shows the range of curves for a radial field configuration, the light band (**T**) is the range for a trapping field, while the line in-between (labeled **In**) is the curve for instantaneous in-situ deposition of positron energy. Ranges correspond to different ionization fractions of the ejecta.

output during the SN's positron dominated time, one can determine the amount of positron trapping, and thus constrain the magnetic field configuration. Milne et al. (2001) compared the  $V$ -band light curves of 22 SNe Ia with models of different magnetic field configurations,

and concluded that they were better fit by the radially escaping positron model. These conclusions rested on the assumption that the  $V$ -band scales with the total luminosity, and there is little to no color evolution. After day 50, the  $V$ -band did account for a consistent 25% of the visible light, so this assumption seemed reasonable.

#### 1.4.1 The Importance of the Infrared

However, Axelrod (1980) suggested that at late epochs there may be a significant shift in emission to the  $IR$ . Because the rate of collisions in the ejecta is fast relative to radiative transitions, thermal emissions dominate. At early times, the thermal ejecta is hot and emissions are mainly in the visible bands, however at later times, the ejecta has cooled, and the emission in the  $IR$  becomes more important. At low temperatures, visible atomic levels aren't excited, and the fine structure transitions of iron dominate emission. Axelrod (1980) suggests that all emission will shift quickly to the far- $IR$ , which cannot currently be observed. This instability is termed the infrared catastrophe.

Lair et al. (2006) observed seven normally luminous and super-luminous SNe Ia, and found that while the  $B$ ,  $V$ , and  $R$  bands declined at 1.4 mag per 100 days at epochs of 200-500 days, the  $I$  decline rate was shallower at 0.94 mag per 100 days. Sollerman et al. (2004) observed SN2000cx in  $UVOIR$  out to 480 days past maximum, and determined that the visible light curves continually declined by about 1.4 mag per 100 days, the  $I$ -band light curve only declined by  $\sim 0.8$  mag per 100 days, and the  $J, H$ -band light curves actually increased in magnitude!

Sollerman et al. (2004) combined their observations from each band into a  $UVOIR$  light curve that included the UV, visible, and NIR bands,  $UBVRIJHK$  as shown in Figure 1.6. They then compared this  $UVOIR$  curve to models of gamma ray and positron energy deposition and concluded that the late decline rate was  $\sim 1.0$  mag/100 days which is the same as the decay rate of  $^{56}\text{Co}$ . If one interprets this as resulting directly from all of the kinetic energy of positrons produced in the  $^{56}\text{Co}$  decay, this would suggest that all (or at least a constant fraction of) positrons were trapped in the SN ejecta. Because of the inclusion of the NIR, Sollerman et al. (2004) arrived at the opposite conclusion of Milne et al. (2001). It would seem that the color evolution (rising importance of the NIR) is

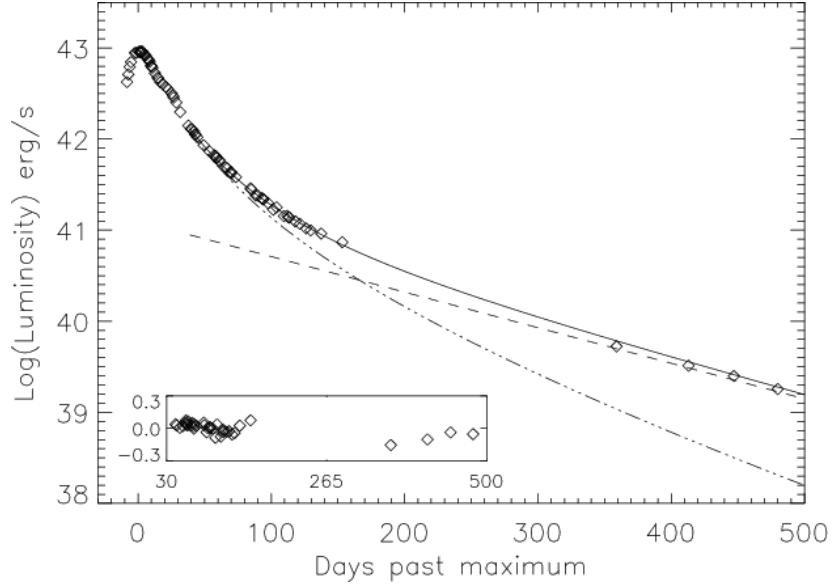


Figure 1.6 From Sollerman et al. (2004), the (*UVOIR*) light curve of SN2000cx (diamonds) plotted against a model of  $^{56}\text{Co}$  decay (solid line). The dot-dashed line shows the contribution from gamma rays, and the dashed line is the contribution from the positrons assuming all energy is deposited in the ejecta. The fit of SN2000cx seems to indicate positron trapping is occurring.

such that it mimics the effect of positron escape in the *BVRI*. It may be worth noting that Sollerman et al. (2004) used the assumption that the late light curve power derived from the complete positron energy deposition to calculate the amount of  $^{56}\text{Ni}$  that was synthesized in the explosion. This derived  $^{56}\text{Ni}$  mass is smaller than that derived around peak light, which indicates that there is still missing power in the *UBVOIR* light curve. They estimate that at 500 days there is 40% of emission that is not caught in the bands they observed, and suggest it may be red-ward of *K*.

SN2001el, a normal SN Ia, was also observed to have a significant contribution from the near-*IR* (Stritzinger and Sollerman, 2007). From 310 to 445 days, the percentage of flux from the *JHK* bands increased from 6% to 25%. The decline rate of Stritzinger and Sollerman (2007)'s *UVOIR* light curve also seemed to indicate the majority of positrons were deposited in the ejecta, favoring a trapping magnetic field configuration. SN2004S

exhibits practically identical characteristics to SN2001el (Krisciunas et al., 2007), though only extends out to around a year in the NIR.

SN2003hv was one of the brightest SNe Ia discovered in 2003 and was observed in the visible and NIR in imaging and spectroscopy out to 786 days past peak date (Leloudas et al., 2009). A UBVOIR light curve was also built for it, which was measured to have a decline rate of 0.99 mag/100 days - the same as the  $^{56}\text{Co}$  decay. Again, there was a discrepancy between the amount of synthesized  $^{56}\text{Ni}$  derived from peak and the amount derived from the late light curve. Leloudas et al. (2009) observed spectra in the visible, NIR, and mid-infrared (MIR) at 320, 394, and 358 days past peak respectively. The flux of the visible and NIR spectra were scaled down to match the MIR spectrum epoch, and then the entire spectral flux was integrated. Leloudas et al. (2009) found that at these late epochs there was an additional  $34 (\pm 17)\%$  extra energy in the MIR compared to the observed UBVOIR light curve. This indicates that the missing flux has at least in part moved on to longer wavelengths.

Though a significant decrease in the late visible light curves indicating the beginning of the infrared catastrophe has not yet been observed, there is no doubt that important energy information is contained in the NIR at late times. The observations in this dissertation widen the pool of well-observed SNe Ia in the late visible and NIR. The handful of SNe with these observations are similar in their late UBVOIR decline rates, and their missing power. We look for further uniformity at late times, and more information about the positron trapping and total late power. Are positrons trapped in all SNe Ia? Can positrons escape the ejecta while depositing enough of their kinetic energy into the ejecta to create the observed late power?

## CHAPTER 2

### OBSERVATIONS

We took observations of the supernovae 2006E, 2006ce, and 2006mq using telescopes in a range of sizes, capturing light that ranged from the near edge of ultra-violet to the near infra-red.

#### 2.1 Telescopes and Instruments

The following telescopes were used for our SN Ia observations.

##### Steward Observatory Telescopes

Steward Observatory facilities were used chiefly by Peter Milne from University of Arizona.

##### 2.1.1 Super-LOTIS

Super-LOTIS (Livermore Visible Transient Imaging System) is a robotic telescope situated at Kitt Peak National Observatory (KPNO) which is 56 miles southwest of Tucson, AZ in the Tohono O’odham Nation. Super-LOTIS nightly observes SNe, novae, and GRBs. It is currently supported by a collaboration that includes Steward Observatory, Lawrence Livermore National Laboratory, NASA GSFC, Clemson University, and UC Berkeley Space Sciences Laboratory. It has a 0.6m aperture, a 17’ x 17’ field of view, and can take about 250 60-second exposures each night. Observations obtained with Super-LOTIS were in  $B, V, R, I$ . However, since 2007, the telescope has only  $V, R, I$  and  $H\alpha$  filters.

##### 2.1.2 Kuiper 1.5m Telescope

The Kuiper Telescope with its 1.5m diameter mirror is located on Mount Bigelow in the Catalina Mountains north of Tucson, AZ. It is operated by Steward Observatory. Visible observations ( $B, V, R, I$ ) were taken with the Mont4k instrument which uses a charge-coupled device (CCD) of 4096 x 4097 pixels with a plate scale of 0.14 arcsec/pixel and a



field of view of  $580 \times 580$  arcsec<sup>2</sup> NIR observations ( $J, H, K$ ) were taken with the 256x256 Near-Infrared Camera which has a plate scale of 0.36 or 0.9 arcsec/pixel.

### 2.1.3 Bok 2.3m Telescope

The 2.3m Bok Telescope is also located at KPNO. Visible observations were taken using 90Prime, a prime focus imaging system with a mosaic of four 4k x 4k CCDs. It affords a field of view of 1 square degree, and has a plate scale of 0.45 arcsec/pixel. NIR observations on the Bok also used the 256x256 Near-Infrared Camera. On this telescope the pixel scale is 0.24 or 0.6 arcsec/pixel.

## National Visible Astronomical Observatory Telescopes

### 2.1.4 Mayall 4m Telescope

KPNO is also home to the Mayall telescope, which has an aperture of 4m and can support a number of instruments. The two used in this study were MOSAIC and FLAMINGOS. The MOSAIC instrument, designed for wide-field visible imaging, is made of an array of 8 CCD chips with a field of view of 36 arcminutes. FLAMINGOS is a wide-field NIR imager and multi-slit spectrometer. For imaging, it affords a field of view of 10 arcminutes by 10 arcminutes in filters:  $J, H, K, Ks$ . While the portion needed to observe SNe is small relative to both fields of view, the large view allows a SN field to be shifted without worry that it will be accidentally positioned off the CCD.

### 2.1.5 The WIYN 3.5m Telescope

Also located at KPNO, the WIYN 3.5m Telescope gets comparable seeing to the Mayall 4m due to many technological advances. The NIR observation taken with WIYN used the WHIRC camera which has a field of view of 3.3 arcminutes by 3.3 arcminutes and a pixel scale of 0.1 arcseconds/pixel.

## 2.2 The Supernovae

### 2.2.1 SN2006E

SN2006E was discovered in the host galaxy NGC 5338 independently by two survey teams – by Tim Puckett and Vishnu Reddy using the Puckett Observatory 0.6m automated

supernova patrol telescope on January 12.45 UT at an unfiltered magnitude of 14.3, and by Miloudi Baek and Weidong Li using the 0.76m Katzman Automatic Imaging Telescope (KAIT) for the Lick Observatory Supernova Search (LOSS) on January 13.58 UT at the same magnitude (Puckett et al., 2006). A pre-discovery image of the SN taken by Yamaoka and Itagaki (2006) with a 0.3m reflector telescope on January 2.835 UT gave an unfiltered red magnitude of about 13.6. Aldering et al. (2006) took a spectrum of SN2006E with the Supernova Integral Field Spectrograph (SNIFS) on the University of Hawaii 2.2m telescope on January 14.6 UT. They determined it was a Type Ia supernova that appeared to be a few weeks past maximum light. The Swift-satellite team (Immler et al., 2006) observed the field on January 13.83 UT with the Ultraviolet/Visible Telescope (UVOT) and the X-Ray Telescope (XRT). They found a magnitude of 17.27 mag in the UVW1 filter (spanning 181-321 nm), a magnitude of 18.41 in the UVW2 filter (spanning 112-264 nm) and a non-detection in the X-ray. Comparing the color to that of SN2005am (Brown et al., 2005), they found it resembled the 25 day mark with an uncertainty of +/- 5 days. The spectrum of Aldering et al. (2006) implies SN2006E's maximum light occurred on January 1, 2006, whereas the color comparison drawn by Immler et al. (2006) implies a maximum light date between December 15 and December 25, 2005.

Our observations were taken with the telescopes and instruments described in Section 2.1 and are detailed in Table 2.1.

Table 2.1 SN2006E Observations Log

Date	Telescope	Instrument	Filters
2006-04-19	Kuiper 1.5m	Mont4K	BVRI
2006-04-24	Kuiper 1.5m	Mont4K	BVRI
2006-05-12	Kuiper 1.5m	Mont4K	BVRI
2006-05-13	Kuiper 1.5m	Mont4K	BVRI
2006-04-14	Bok 2.3m	256x256	H
2006-07-14	Bok 2.3m	256x256	J
2006-12-20	Bok 2.3m	90Prime	VRI
2007-01-09	Mayall 4m	FLAMINGOS	JHK
2007-01-10	Mayall 4m	MOSAIC	BV
2007-01-25	Bok 2.3m	90Prime	V
2007-02-04	Bok 2.3m	256x256	JH
2007-02-15	Kuiper 1.5m	Mont4K	I
2007-02-25	Kuiper 1.5m	256x256	J
2007-03-09	Bok 2.3m	90Prime	UBVRI
2007-03-28	Mayall 4m	FLAMINGOS	J
2007-03-29	Mayall 4m	FLAMINGOS	JH
2007-04-05	Kuiper 1.5m	256x256	H
2007-04-17	Kuiper 1.5m	Mont4K	BVR
2007-04-18	Kuiper 1.5m	Mont4K	BV
2007-05-06	Kuiper 1.5m	256x256	JH
2007-05-09	Kuiper 1.5m	Mont4K	BVRI
2007-05-23	Mayall 4m	MOSAIC	BVRI
2007-05-24	Mayall 4m	FLAMINGOS	JH
2007-06-06	Bok 2.3m	90Prime	V
2007-06-06	Bok 2.3m	90Prime	BVR
2008-04-07	Kuiper 1.5m	Mont4K	BVRI
2010-01-31	Mayall 4m	FLAMINGOS	JH
2011-03-18	WIYN 3.5m	WHIRC	K

### 2.2.2 SN2006ce

SN2006ce was discovered May 10.14 UT by Ponticello et al. (2006) using the 0.76m KAIT for LOSS at a magnitude of 12.4. Nothing was seen at its location prior to April 1, 2006. Blackman et al. (2006) took a spectrum of SN2006ce on June 6.83 UT that indicated it was a SN Ia. Comparing it with a library of spectra, they concluded it was  $35 \pm 5$  days after maximum light.

Our observations began August 28, 2006 and are listed in Table 2.2.

Table 2.2 SN2006ce Observations Log

Date	Telescope	Instrument	Filters
2006-08-28	Mayall 4m	FLAMINGOS	JH
2006-08-29	Kuiper 1.5m	Mont4K	BVRI
2006-09-11	Kuiper 1.5m	256x256	JH
2006-09-27	Kuiper 1.5m	Mont4K	BVRI
2006-10-07	Bok 2.3m	256x256	JH
2006-10-22	Bok 2.3m	90Prime	BVRI
2006-11-24	Kuiper 1.5m	Mont4K	BVRI
2006-12-07	Bok 2.3m	256x256	J
2006-12-20	Bok 2.3m	90Prime	BVRI
2007-01-09	Mayall 4m	FLAMINGOS	JH
2007-01-25	Bok 2.3m	90Prime	BVRI
2007-02-02	Kuiper 1.5m	Mont4K	BVRI
2007-02-04	Bok 2.3m	256x256	J
2007-02-15	Kuiper 1.5m	Mont4K	BI
2007-09-12	Bok 2.3m	90Prime	UBVRI
2007-11-03	Bok 2.3m	90Prime	BVR
2007-12-17	Mayall 4m	MOSAIC	BV
2007-12-19	Bok 2.3m	256x256	J

### 2.2.3 SN2006mq

SN2006mq was discovered by Lee and Li (2006) using KAIT for LOSS on November 5.50 206 UT at a magnitude of 13.2. They also found it in an earlier observation of its host galaxy, ESO 494-G26, on October 22.56 2006 (mag 12.7). An visible spectrum taken by Watson et al. (2006) with the Hiltner 2.4m telescope at the MDM Observatory on November 6.5 UT resembled that of a SN Ia around two weeks after maximum. However, Prieto (2006) reported an improved analysis of this, with the conclusion that SN2006mq spectrum was more like a SN Ia 40 days after maximum.

Our observations began on November 7, 2006 and are listed in Table 2.3.

Table 2.3 SN2006mq Observations Log

Date	Telescope	Instrument	Filters
2006-11-07	Kuiper 1.5m	256x256	JHK
2006-12-07	Bok 2.3m	256x256	JHK
2006-12-20	Bok 2.3m	90Prime	BVRI
2007-01-09	Mayall 4m	FLAMINGOS	JHK
2007-01-24	Bok 2.3m	90Prime	BVRI
2007-02-02	Kuiper 1.5m	Mont4K	BVRI
2007-02-04	Bok 2.3m	256x256	JH
2007-04-17	Kuiper 1.5m	Mont4K	BVRI
2007-11-03	Bok 2.3m	90Prime	BVRI
2007-11-20	Kuiper 1.5m	256x256	JH
2007-12-02	Kuiper 1.5m	Mont4K	VR
2007-12-18	Bok 2.3m	256x256	JH
2008-01-15	Bok 2.3m	90Prime	BVRI
2008-01-19	Kuiper 1.5m	256x256	J
2008-01-23	Mayall 4m	FLAMINGOS	JH
2008-02-13	Kuiper 1.5m	Mont4K	VRI
2008-03-14	Bok 2.3m	90Prime	BVRI
2008-04-06	Kuiper 1.5m	Mont4K	RI

## 2.3 Image Analysis

### 2.3.1 Reductions

Visible and NIR images were reduced using the Image Reduction and Analysis Facility (IRAF) software package.<sup>1</sup> Each image was trimmed, overscan strip corrected, bias subtracted, dark subtracted, flattened and had bad pixels fixed. Visible images were then combined for greater signal to noise, while NIR images underwent more complicated steps in order to perform sky background determination and subtraction. Then NIR images are aligned and combined as well. Appendix A contains more explicit steps for standard visible images (A.1), multi-extension fits files (Section A.2), and NIR images (Section A.3).

### 2.3.2 Image Subtraction

Because of the proximity of SN2006E to the center of its host galaxy, there was a worry that its signal would be confused with galaxy light, as is shown in Figure 2.1.

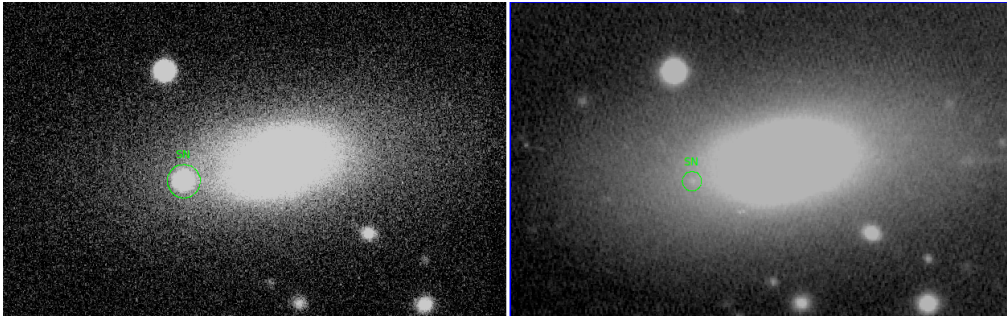


Figure 2.1 SN2006E’s position in the host galaxy means that at late times the SN light gets overwhelmed by galaxy light. Both images are a B band image of SN2006E taken with the Kuiper telescope. The one on the left was taken on April 19, 2006, while the right image was taken on May 9, 2007. The SN position is circled in both. Notice how difficult it is to separate the SN from the background galaxy light - especially at late epochs.

---

<sup>1</sup> IRAF is distributed by the National Optical Astronomy Observatories, which are operated by the Association of Universities for Research in Astronomy, Inc., under cooperative agreement with the National Science Foundation, <http://iraf.noao.edu>

Thus additional visible and NIR images of the field were taken well after the SN disappeared. These images were then used as subtraction images – images that were subtracted from science images of the SN with the hope of removing unwanted galaxy light. This proved to be a challenging task as the subtraction images were taken with different instruments than some of the science images. Considerable work went into matching the respective size, orientation, point spread function, and flux of a subtraction image to those of each science image.

First, a world coordinate system (WCS) was assigned to every science and subtraction image using the IRAF task CCMAP and CCSETWCS. If an image already had a WCS assigned to it (an automated process from the instrument it was taken with), it was corrected using MSCCMATCH. Then, for each science image, a separate subtraction image was made - copied from the appropriate filter original subtraction image. The subtraction image was aligned to the science image according to both image's WCS using WREGISTER. This included stretching, translation, and rotation of the subtraction image. Afterward, the full-width half-maximum (FWHM) of several stars were measured in each image. The subtraction image was then convolved with the appropriate Gaussian (using GAUSS) in an attempt to match the seeing conditions in which the science image was taken. In the rare cases where the subtraction image was more blurry (had a greater FWHM), the science image was convolved with a Gaussian to match the subtraction image seeing conditions. Using IMARITH, an offset value was then added or subtracted to images to make the background counts roughly zero, and then the subtraction image was scaled appropriately so that the maximum values of stars or galaxies matched those in the science image. Finally, the subtraction image was subtracted from the science image (again using IMARITH) and an arbitrary offset of 30 counts was added to minimize the number of negatively valued pixels. An example of the results is shown in Figure 2.2

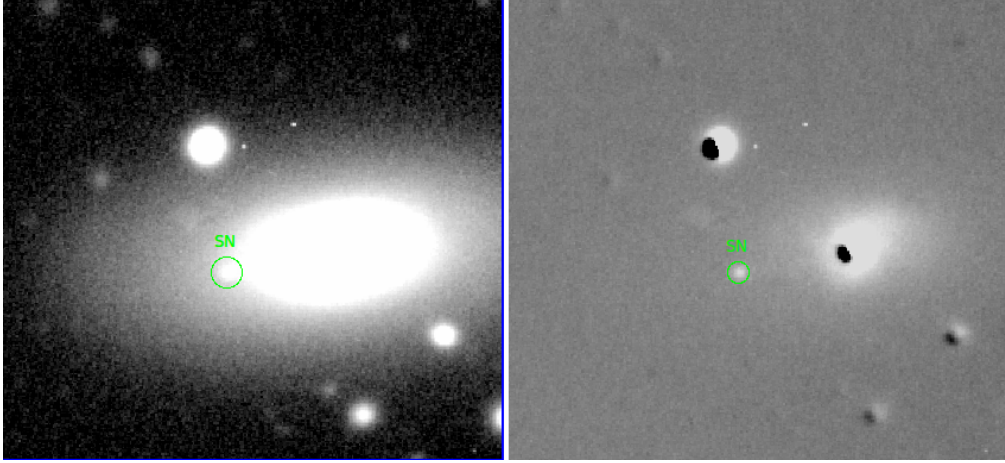


Figure 2.2 Images of SN2006E taken on December 20, 2006 with the Bok telescope. The image on the left is the original reduced science image, while the image in the right is the same image after having the subtraction image subtracted from it. This removes the background galaxy light in the area of the SN. The SN position SN is circled in both images.

### 2.3.3 Photometry

The instrumental magnitudes of local field stars, the supernova, and standard stars were measured with aperture photometry using IRAF. In the visible bands, local stars and the SN were calibrated with observations of standard star fields using Landolt transformation equations. In the NIR band observations, additional field stars and the SN were calibrated using stars in the field with known magnitudes from the Two Micron All Sky Survey (2MASS) catalog. A guide on performing photometry on reduced images is included in Appendix Section A.4.

## 2.4 SN2006E Light Curves

Calculated magnitudes of SN2006E from aperture photometry are recorded in Tables 2.4 (Visible) and 2.5 (NIR).



Table 2.4 SN2006E Calculated Visible Magnitudes

Date	B	B error	V	V error	R	R error	I	I error
2006-04-19	16.866	0.003	16.584	0.003	17.169	0.005	17.126	0.008
2006-04-24	16.958	0.003	16.671	0.003	16.925	0.004	17.330	0.010
2006-05-12	17.336	0.005	17.045	0.004	17.523	0.008	17.496	0.020
2006-05-13	17.299	0.004	17.003	0.004	17.439	0.005	17.769	0.016
2006-12-20	.....	.....	20.051	0.020	21.511	0.081	22.572	0.222
2007-01-10	20.652	0.037	20.747	0.045	.....	.....	.....	.....
2007-01-25	.....	.....	20.872	0.031	.....	.....	.....	.....
2007-02-15	.....	.....	.....	.....	.....	.....	21.266	0.216
2007-03-09	.....	.....	21.470	0.044	22.578	0.162	.....	.....
2007-04-17	22.626	0.127	22.016	0.064	23.065	0.193	.....	.....
2007-04-18	22.611	0.049	22.248	0.104	24.146	0.262	20.645	0.132
2007-05-09	22.847	0.096	23.116	0.209	22.745	0.211	.....	.....
2007-05-23	22.960	0.047	22.831	0.030	23.560	0.090	24.892	0.061
2007-06-06	.....	.....	22.975	0.162	.....	.....	.....	.....
2007-06-07	23.035	0.269	22.952	0.142	.....	.....	.....	.....

The following figures show the B (2.3), V (2.4), R (2.5), I (2.6), J (2.7), H (2.8) magnitudes of SN2006E. Both the photometry of the unsubtracted and subtracted images are included for a comparison. Subtraction tends to result in lower magnitudes as there is less galaxy light contained in the SN measurement. Also plotted with visible magnitudes are typical SN Ia 100-200 day decline rates anchored at 100 days by the first data point in each band, followed by 200-500 day Ia decline rates from Lair et al. (2006). The NIR plots include some late J or H points (connected in a line) of SN2003hv from Leloudas et al. (2009) for comparison. The determination for the epochs is discussed in the upcoming Section 3.1.

Table 2.5 SN2006E Calculated Near Infrared Magnitudes

Date	J	J error	H	H error
2006-04-14	.....	.....	17.488	0.468
2006-07-14	17.931	0.524	.....	.....
2007-01-09	18.556	0.191	18.006	0.162
2007-02-04	18.574	0.103	18.125	0.208
2007-02-25	19.508	0.906	.....	.....
2007-03-29	19.877	0.074	18.874	0.103
2007-04-05	20.566	0.283	18.597	0.525
2007-05-24	19.508	0.418	19.744	0.257

### 2.5 SN2006ce Light Curves

Tables 2.6 and 2.7 contain the magnitude measurements of SN2006ce in visible and NIR respectively. Figure 2.9 shows the visible light curve while Figure 2.10 exhibits the NIR curve. The different bands have been arbitrarily offset in magnitude as designated in the plot for easy viewing of their relative shapes. Much like in section 2.4, also plotted are typical decline rates (in visible) or late SN2003hv data (in NIR).

Table 2.6 SN2006ce Calculated Visible Magnitudes

Date	B	B error	V	V error	R	R error	I	I error
2006-08-29	17.005	0.004	16.457	0.003	16.776	0.004	16.612	0.012
2006-09-27	17.116	0.007	16.885	0.004	17.289	0.007	17.344	0.016
2006-10-22	17.704	0.006	17.283	0.006	18.064	0.017	17.615	0.029
2006-11-24	.....	.....	17.978	0.006	19.031	0.014	18.171	0.031
2006-12-20	18.662	0.005	18.265	0.007	19.299	0.023	17.864	0.023
2007-01-25	19.191	0.031	18.804	0.041	20.029	0.136	18.397	0.121
2007-02-02	19.224	0.043	19.206	0.020	19.911	0.056	19.424	0.087
2007-02-15	19.715	0.017	.....	.....	.....	.....	19.626	0.153

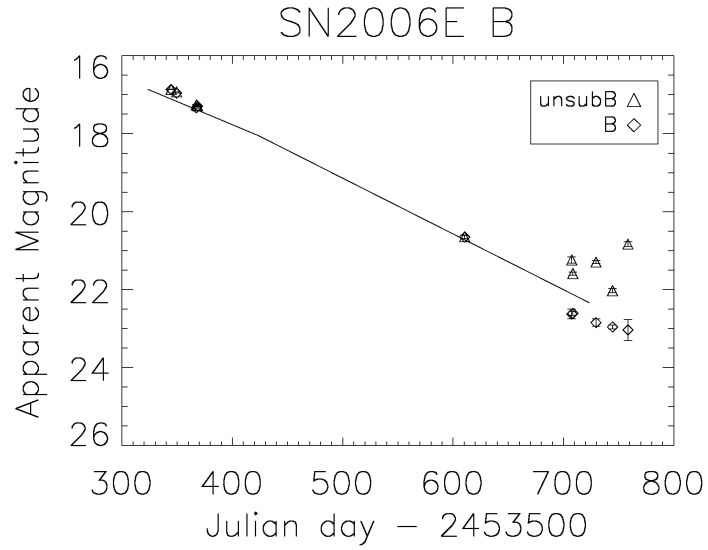


Figure 2.3 The measured magnitudes of SN2006E from both the B band unsubtracted (triangles) and subtracted (diamonds) images are plotted according to their Julian date.

Apart from the I band, the visible curves seem to follow the decline rate of normal SNe Ia quite well. While the H band seems to decline steadily, the J band flattens for about 100 days.

Table 2.7 SN2006ce Calculated Near Infrared Magnitudes

Date	J	J error	H	H error
2006-08-28	18.374	0.045	16.143	0.046
2006-09-11	19.059	0.420	17.246	0.187
2006-11-07	19.580	0.322	.....	.....
2006-12-07	19.501	0.121	.....	.....
2007-01-09	19.440	0.107	18.661	0.155
2007-02-04	19.616	0.233	.....	.....
2007-12-19	17.151	0.039	.....	.....

## 2.6 SN2006mq Light Curves

The results from visible and NIR photometry are in Tables 2.8 and 2.9 respectively. The visible and NIR light curves follow in Figures 2.11 and 2.12 and are plotted similarly to those in Section 2.5.

Table 2.8 SN2006mq Calculated Visible Magnitudes

Date	B	B error	V	V error	R	R error	I	I error
2006-12-20	15.318	0.002	16.164	0.003	15.030	0.002	15.450	0.002
2007-01-24	16.192	0.007	16.689	0.005	16.144	0.011	16.665	0.039
2007-02-02	16.385	0.010	16.858	0.013	16.362	0.008	16.976	0.018
2007-03-09	16.970	0.007	17.371	0.006	17.230	0.013	17.619	0.017
2007-04-17	17.618	0.025	17.954	0.032	17.578	0.029	18.457	0.086
2007-11-03	20.353	0.030	20.630	0.032	21.094	0.091	20.047	0.079
2007-12-02	.....	.....	20.612	0.686	20.508	0.295	16.612	0.012
2008-01-15	21.277	0.118	21.676	0.112	21.632	0.239	16.612	0.012
2008-03-15	21.933	0.302	21.782	0.260	22.367	0.535	16.612	0.012
2008-04-07	.....	.....	.....	.....	.....	.....	20.489	0.261

The visible bands of all three SNe follow the decline rates from Lair et al. (2006) very well, except the I band where measured magnitudes float both above and below the

Table 2.9 SN2006mq Calculated Near Infrared Magnitudes

Date	J	J error	H	H error	K	K error
2006-11-07	13.395	0.005	12.454	0.005	12.510	0.011
2006-12-07	15.695	0.016	.....	.....	13.683	0.015
2007-01-09	17.313	0.023	15.422	0.010	14.979	0.019
2007-02-04	18.586	0.157	16.734	0.059	.....	.....
2007-02-05	19.334	0.281	17.078	0.120	.....	.....
2007-02-25	16.950	0.596	16.056	0.117	17.164	0.232
2007-11-20	18.803	0.070	18.461	0.111	.....	.....
2007-12-18	19.024	0.059	.....	.....	.....	.....
2008-01-19	19.045	0.074	18.931	0.229	.....	.....
2008-01-23	18.906	0.078	18.726	0.201	.....	.....

plotted decline. The I band has a great deal of fringing (interference patterns caused by the way light travels through the detector) that is difficult to remove from images and often makes it difficult to determine the level of the sky compared to the star. This is especially true at late times when the SN is faint enough that it is comparable to the level of fringing. The error bars plotted for each observation are calculated with IRAF and include uncertainties including SN, local star, and standard star signal to noise in observations and uncertainties in the known standard star magnitudes. These uncertainties are folded into transformation equations which assesses how differently the instrument sees stars of different colors at different airmasses. With these observations, we did not have enough observations at different airmasses to accurately measure an airmass dependence. The fringing adds an error on top of this. Early on, this additional error is miniscule, however at late times it is not unreasonable to think it adds half a magnitude to the error bars.

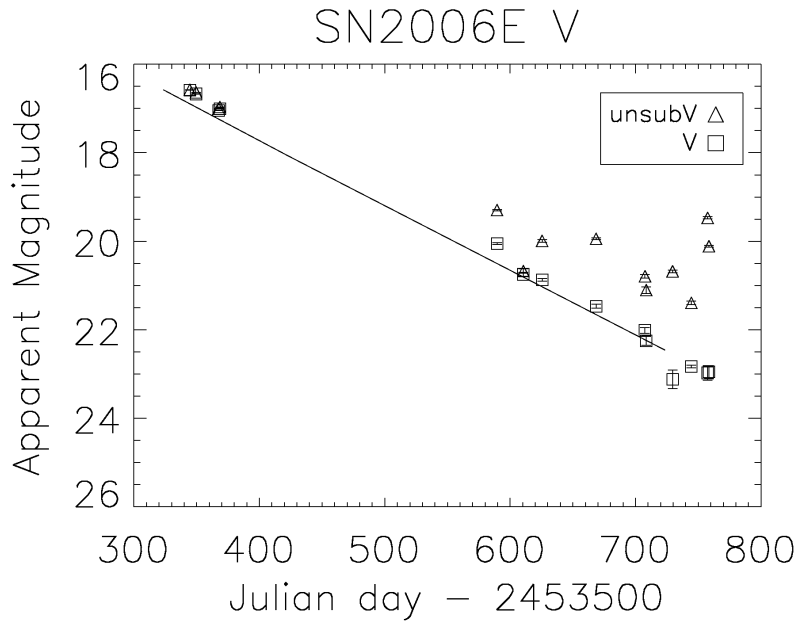


Figure 2.4 The measured magnitudes of SN2006E from both the V band unsubtracted (triangles) and subtracted (squares) images are plotted according to their Julian date.

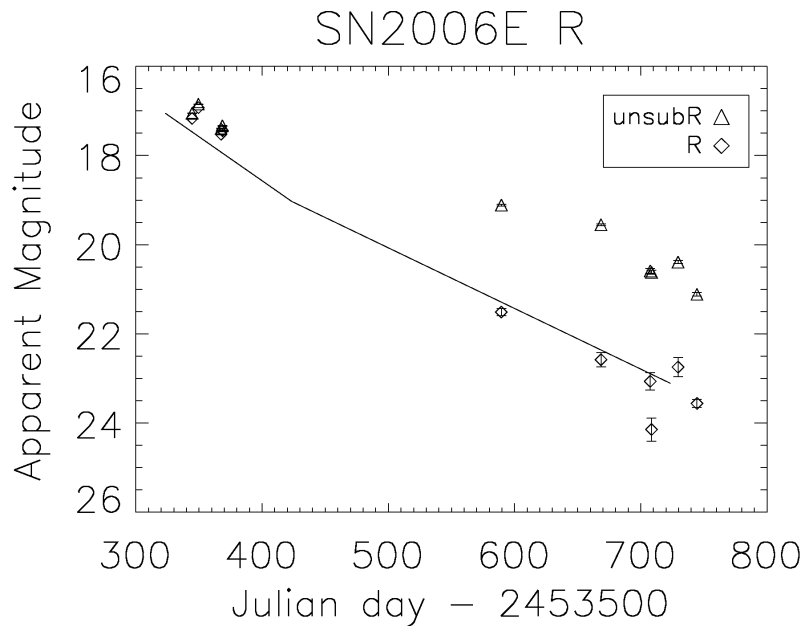


Figure 2.5 The measured magnitudes of SN2006E from both the R band unsubtracted (triangles) and subtracted (diamonds) images are plotted according to their Julian date.

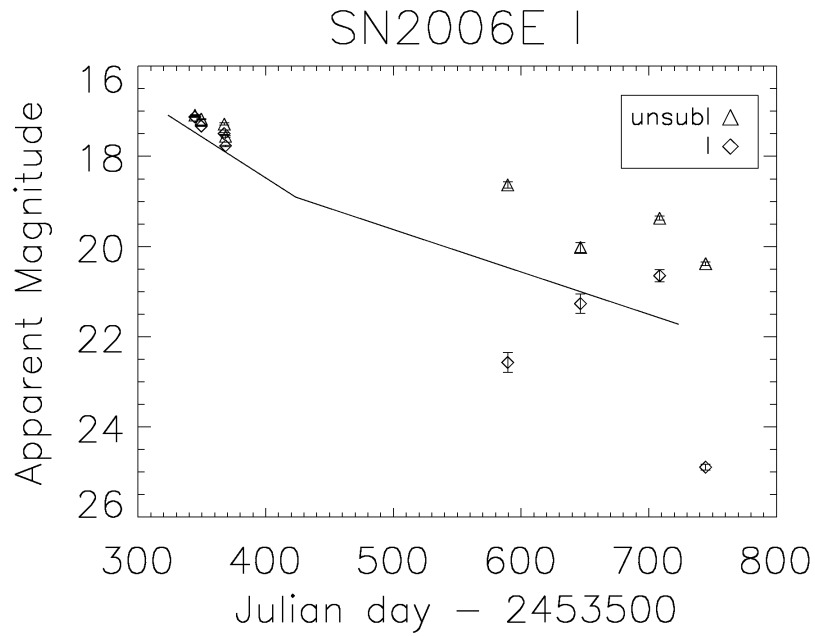


Figure 2.6 The measured magnitudes of SN2006E from both the I band unsubtracted (triangles) and subtracted (diamonds) images are plotted according to their Julian date.

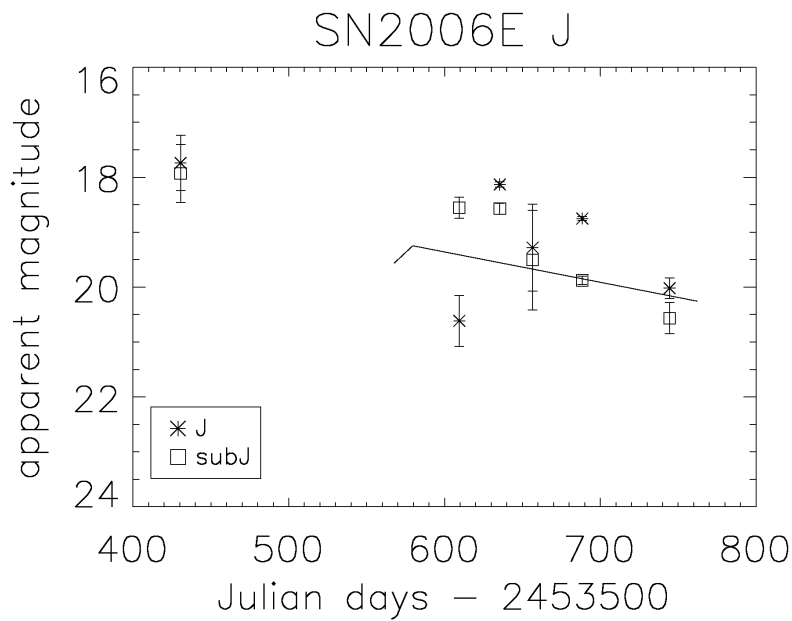


Figure 2.7 The measured magnitudes of SN2006E from both the J band unsubtracted (asterisks) and subtracted (diamonds) images are plotted according to their Julian date.

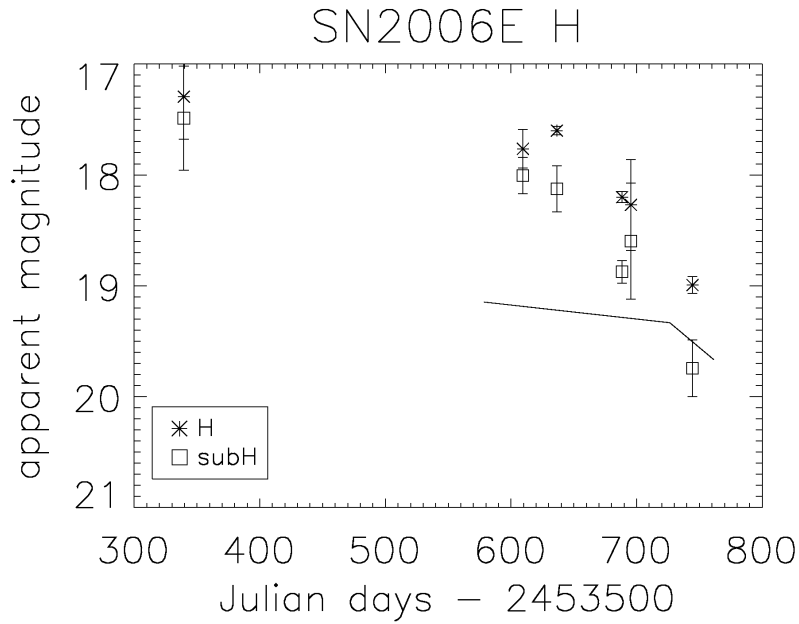


Figure 2.8 The measured magnitudes of SN2006E from both the H band unsubtracted (asterisks) and subtracted (squares) images are plotted according to their Julian date.

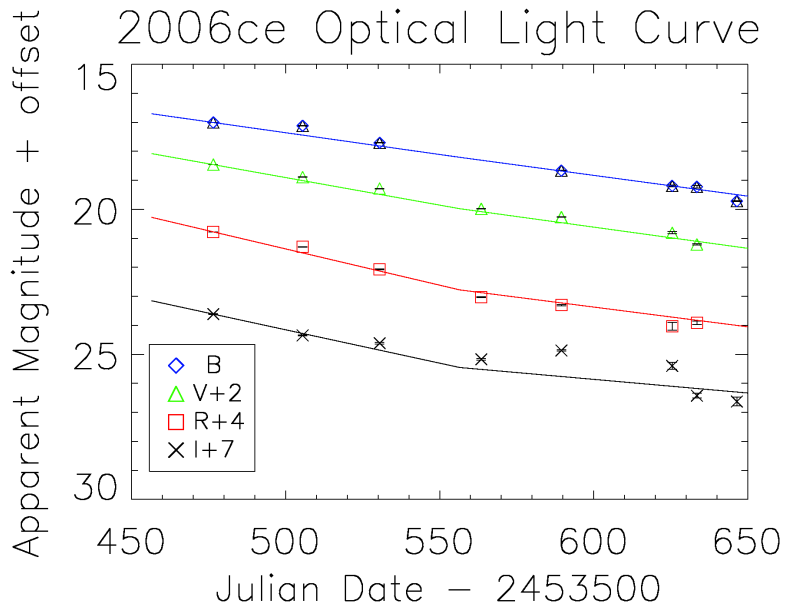


Figure 2.9 The visible light curve of SN2006ce from our observations in *BVRI*. The individual bands are arbitrarily offset as stated to allow better comparison. The lines are typical decline rates for SNe Ia from 100-200 days and from 200-500 days.



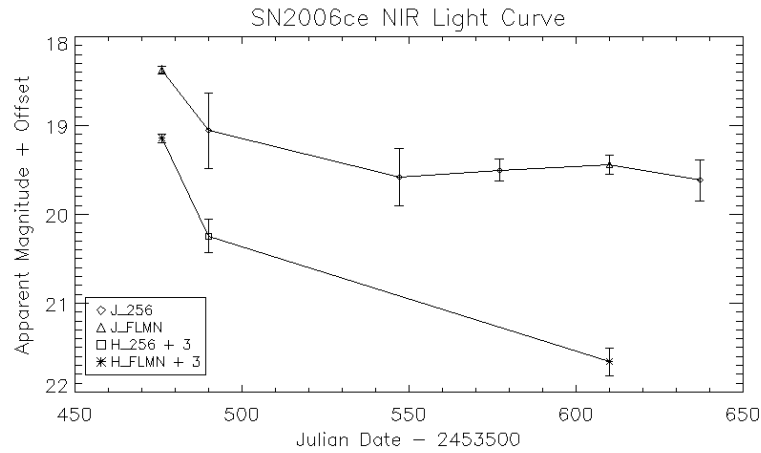


Figure 2.10 The light curve of SN2006ce from our observations in  $J, H$ . The H band points are arbitrarily offset by 3 magnitudes in order to facilitate better comparison.

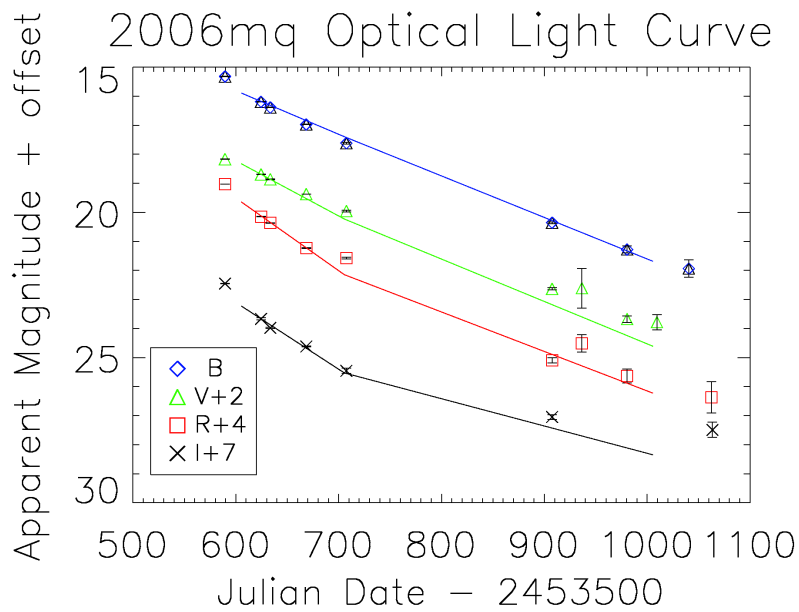


Figure 2.11 The light curve of SN2006mq from our observations in  $B, V, R, I$ . The individual bands are arbitrarily offset as stated to allow better comparison. The lines are typical decline rates for SNe Ia from 100-200 days and from 200-500 days.

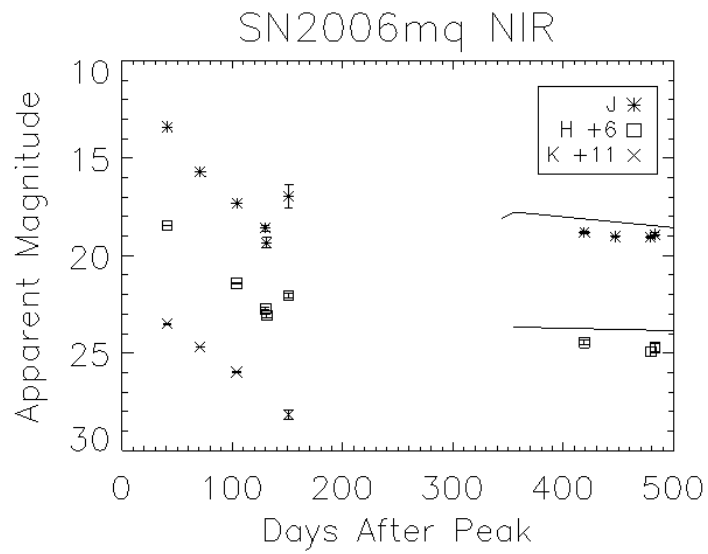


Figure 2.12 The light curve of SN2006mq from our observations in *JHK*. The H band points are arbitrarily offset by 6 magnitudes, as are the *K* band by 11magnitudes. The lines beginning at roughly 350 days are the *J* and *H* light curves of SN2003hv from Leloudas et al. (2009)

## CHAPTER 3

### ANALYSIS

#### 3.1 Epoch Determination

All three SNe were discovered post peak which means some information like peak brightness, peak date, and peak decline rate are not known. Both SNe 2006ce and 2006mq had fairly definitive peak dates determined from early spectral observations. SN2006E, however had competing groups assign it different peak dates (see Section 2.2.1). Due to the uniformity of SNe Ia, we can hope to gather this information by comparing with other well-studied Ia light curves. We use the earliest light curve information which is visible data from Super-LOTIS observations. We can fit the early 2006E  $B, V, R, I$  light curves to those of the normal SN1992. In the fit, the peak date and amount of extinction is allowed to vary.

Extinction is due to dust, either in the SN host galaxy or our own Milky Way. This dust scatters different wavelengths of light to various degrees. Bluer light is scattered more easily, while longer wavelengths are less affected. We assume a Milky Way galaxy distribution of sizes of dust particles for the dust in the SN host galaxy, (though see Elias-Rosa et al. (2006) for an example of a SN host galaxy with perhaps a different distribution) which tells us the relationship between extinction for each band.

Figure 3.1 shows the best fit of the SN2006E light curves to the SN1992A template taken from Hamuy et al. (1996). This resulted in a peak date of December 19, 2005 which falls in the estimation from Immler et al. (2006).

Now we can look at the light curve data in terms of the epoch since peak light. Figure 3.2 shows the multi-band light curve of SN2006E at the newly-defined epochs.

Figure 3.3 shows the multi-band light curve of SN2006ce at the epochs defined by Blackman et al. (2006) and Figure 3.4 shows the multi-band light curve of SN2006mq at epochs determined by the Prieto (2006) estimated peak date.

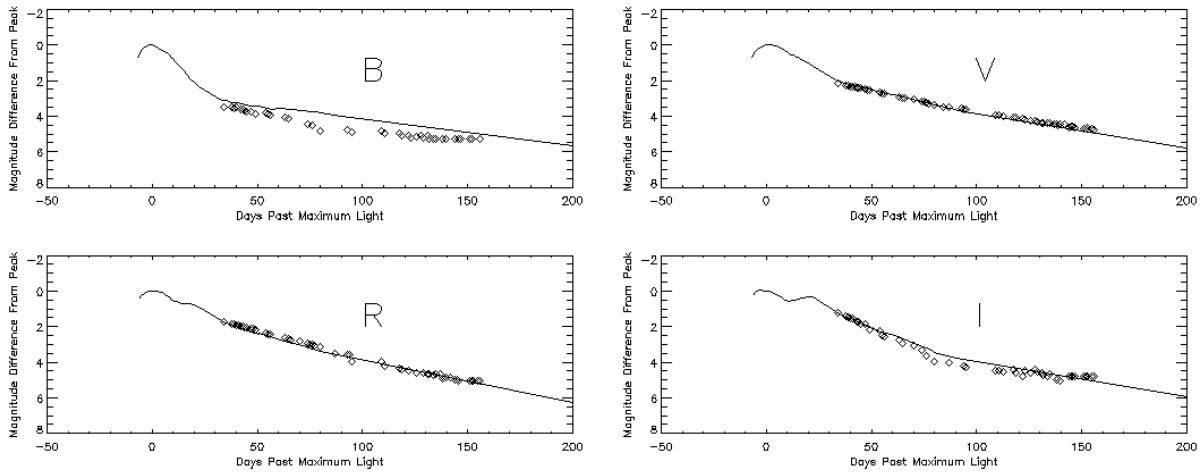


Figure 3.1 SN2006E Super-LOTIS  $B, V, R, I$  data (diamonds) fit to the normal SN Ia 1992A (solid line)

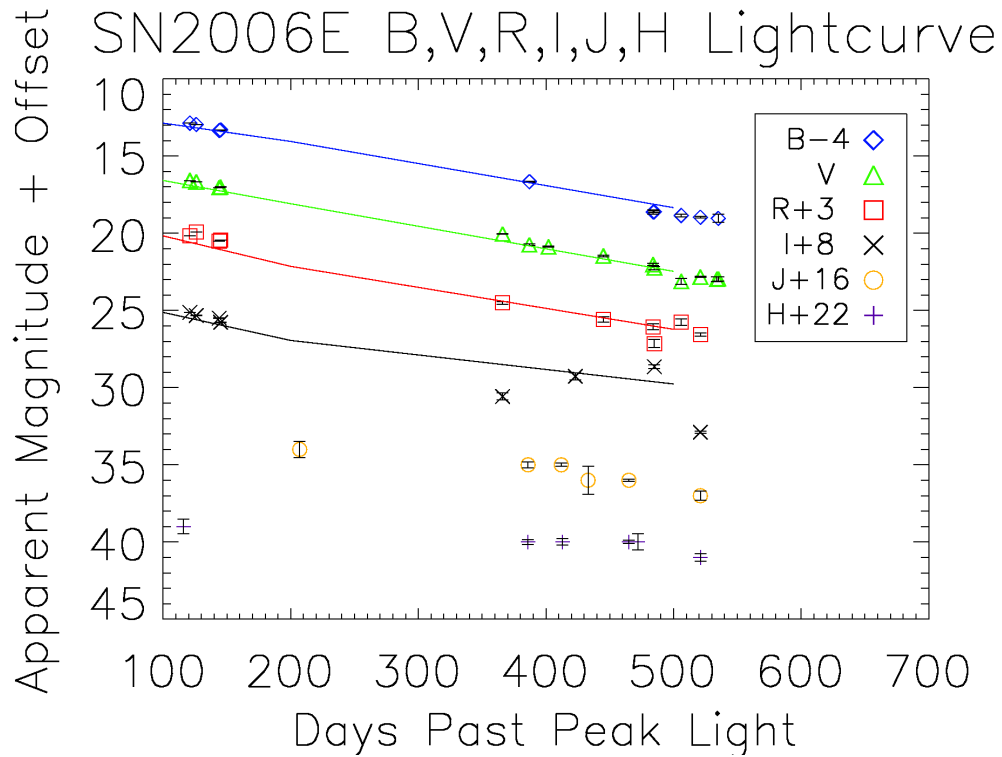


Figure 3.2 The  $B, V, R, I, J, H$  light curve of SN2006E. The bands are arbitrarily offset as marked to avoid confusion.

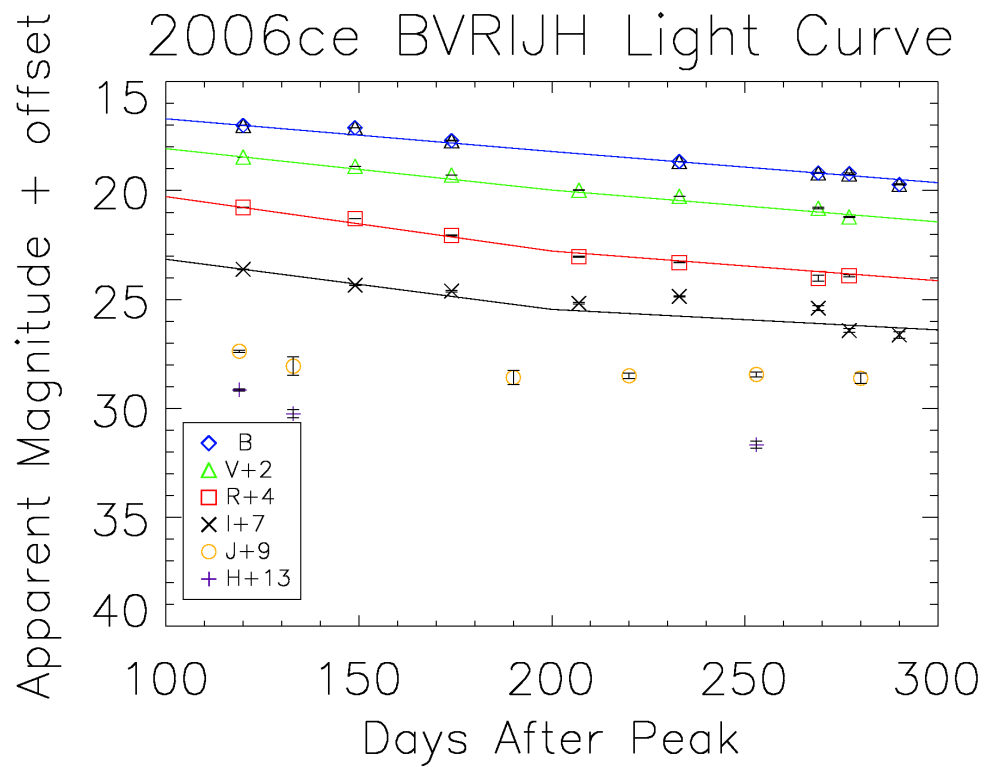


Figure 3.3 The  $B, V, R, I, J, H$  light curve of SN2006ce. The bands are arbitrarily offset as marked to avoid confusion.

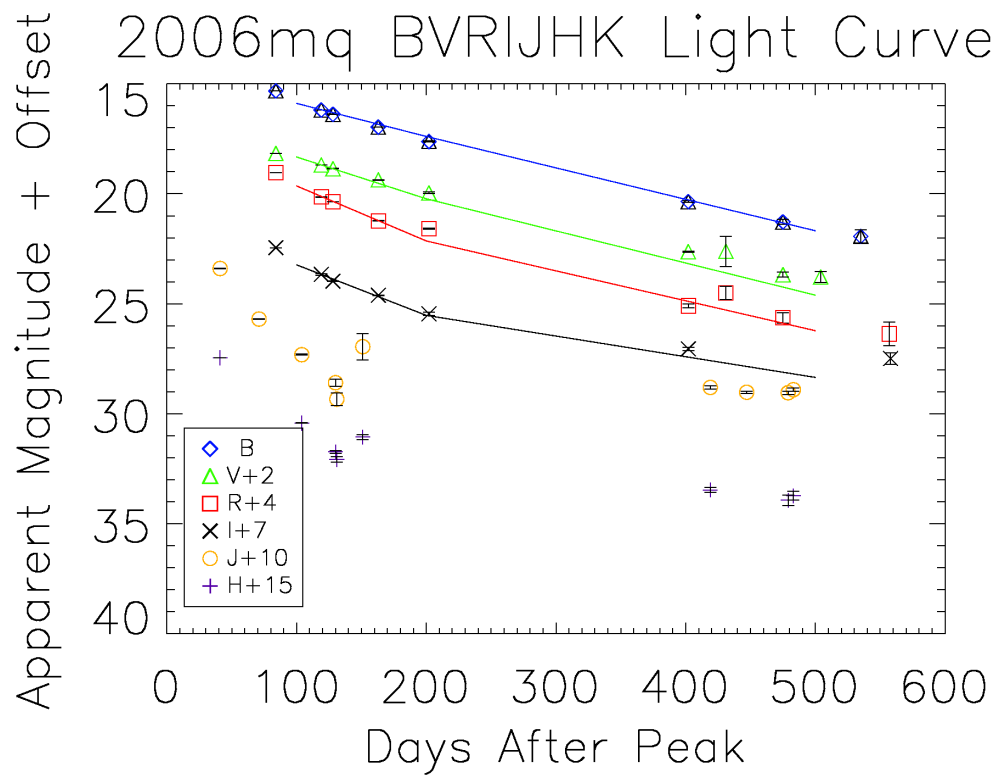


Figure 3.4 The  $B, V, R, I, J, H$  light curve of SN2006mq. The bands are arbitrarily offset as marked to avoid confusion.

### 3.2 Color Evolution

We can compare a representative of the visible bands to a representative band for the NIR to get a sense of the color evolution. Figure 3.5 shows the  $V-J$  magnitudes as a function of epoch for our three SNe. In each one, the NIR appears to transition to a greater

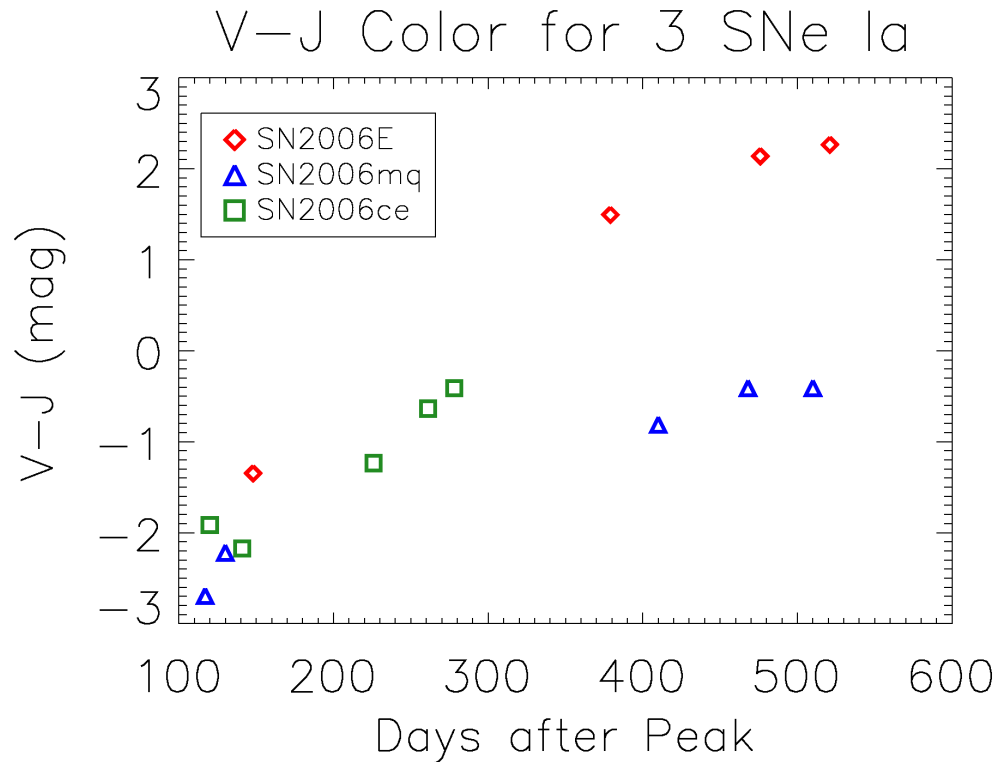


Figure 3.5 The color evolution as characterized by the  $V-J$  magnitudes for SNe 2006E (red diamonds), 2006mq (blue triangles), and 2006ce (green squares). In each SN except 2006mq, the color transitions from negative (greater shorter wavelength importance) to positive (greater NIR significance).

importance (more positive), however, SN2006mq does it more slowly than the others. This means that the  $V$ -band fades less quickly compared to the other SNe or that 2006mq's NIR band has a greater decline rate, or some combination of the two.

### 3.3 Bolometric Flux

By itself, one band's observations can tell us only about a small part of the bolometric power. In pairs we can tell something about the color evolution, but by incorporating all bands, we get a more complete picture. Figure 3.6 is a spectrum reproduced from Leloudas et al. (2009) and is a combination of their 320 day visible spectrum, and Motohara et al. (2006)'s 394 day NIR spectrum flux-scaled to 350 days. Overlaid on this are the passbands for the  $B, V, R, I, J, H$  filters. In order to account for a greater portion of the power - vis-

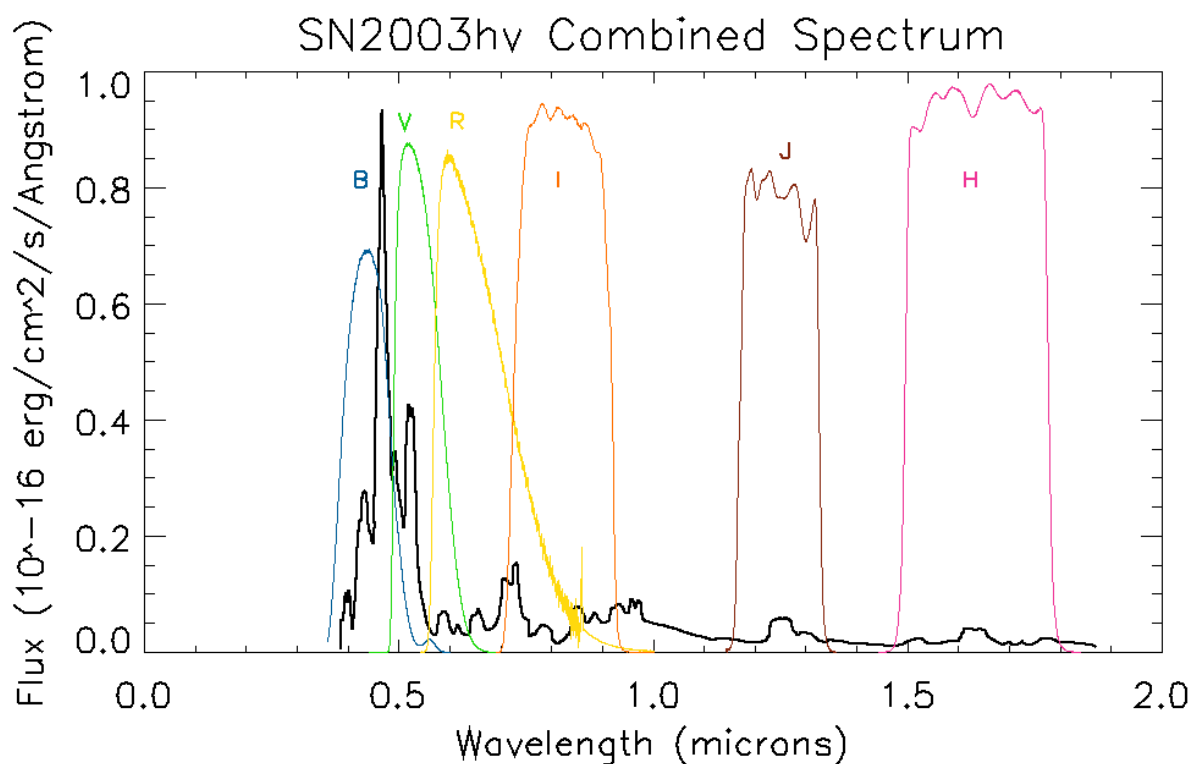


Figure 3.6 SN2003hv combined 394 day NIR and 320 day visible spectrum overlaid with  $B, V, R, I$  pass bands indicating what fraction of light at a particular wavelength is transmitted.

ible and NIR, we will first convert our observed magnitudes to flux. We use the formula



comparing to Vega (or an average of  $A_0$  stars),

$$m_{SN} - m_{vega} = -2.5 \log \left( \frac{F_{SN}}{F_{vega}} \right). \quad (3.1)$$

The magnitude of Vega (or the  $A_0$  stars) is by definition zero, thus we can solve for the SN flux if we know the flux of Vega in each band. Cox (2000) provides the measurements which are reproduced in Table 3.1 The flux calculated in this way accounts for only the

Table 3.1 Vega and  $A_0$  Star Fluxes by Band from Cox (2000)

Band	$F_{A_0}$ (erg/s/cm <sup>2</sup> /Å)	FWHM <sub>λ</sub> (Å)
B	6.40x10 <sup>-9</sup>	1000
V	3.75x10 <sup>-9</sup>	900
R	1.75x10 <sup>-9</sup>	2200
I	8.40x10 <sup>-10</sup>	2400
J	3.31x10 <sup>-10</sup>	2600
H	1.15x10 <sup>-10</sup>	2900

light measured by the respective filter. As seen in Figure 3.6, this does not account for all the flux in the SN Ia spectrum. One would get a more accurate measure of the total SN flux by integrating an observed SN spectrum over all wavelengths. Unfortunately there are no spectra of these three SNe available. Spectra of other SNe Ia do exist - even out to late times and in the NIR. We will use some of these at multiple epochs to approximate the distribution of flux. Because there are only a few epochs of observed spectra, and because uniformity of late behavior has not yet been established for SNe Ia, we will use the flux calculated from measured magnitudes to scale the SN spectrum at each observed epochs. First, we choose a SN Ia spectrum observed at an epoch as similar as possible to that of our observation, e.g., Figure 3.6 shows a visible spectrum taken at 320 days and a NIR spectrum taken at 394 days after the maximum light of SN2003hv. For a given filter, we integrate the flux of the chosen SN Ia spectrum over the wavelengths of that filter. For the

V band, this would be:

$$F_{\text{spec}V} = \int_{\lambda_{V\text{begin}}}^{\lambda_{V\text{end}}} F_{\lambda} d\lambda \quad (3.2)$$

The ratio of the flux calculated from a magnitude measurement in a given filter, e.g.,  $F_{\text{SN}V}$ , to that of the integrated spectrum over the wavelengths of that filter, e.g.,  $F_{\text{spec}V}$  provides a scale factor for the SN spectrum at the epoch of that measurement. For a single epoch, we can calculate the scale factor from each filter observed, and take the average to be that epoch's scale factor. We treat the visible separately from the NIR. The calculation for the visible scale factor of a certain epoch would be,

$$A_{\text{visible}} = (A_B + A_V + A_R + A_I) / 4 = \left( \frac{F_{\text{SN}B}}{F_{\text{spec}B}} + \frac{F_{\text{SN}V}}{F_{\text{spec}V}} + \frac{F_{\text{SN}R}}{F_{\text{spec}R}} + \frac{F_{\text{SN}I}}{F_{\text{spec}I}} \right) / 4. \quad (3.3)$$

The spectra used in this way are a 110 day visible spectrum of SN2003hv from Leloudas et al. (2009), a 221 day visible spectrum of SN2003du from Gerardy (2005), and a 320 day visible spectrum from Leloudas et al. (2009). The NIR spectrum included a 214 day spectrum of SN2005w, a 297 day spectrum of SN2003du – both from Motohara et al. (2006), and a 394 day spectrum of SN2003hv from Leloudas et al. (2009). For each of our three SNe, only epochs were chosen that had NIR and visible observations at similar times. Once scalings were determined for the appropriate spectrum, that spectrum was integrated separately for the visible and NIR,

$$F_{\text{visible}} = A_{\text{visible}} * \int_{\lambda_i}^{\lambda_f} F_{\lambda} d\lambda \quad (3.4)$$

$$F_{\text{NIR}} = A_{\text{NIR}} * \int_{\lambda_i}^{\lambda_f} F_{\lambda} d\lambda \quad (3.5)$$

$$F = F_{\text{visible}} + F_{\text{NIR}}. \quad (3.6)$$

The total flux is just the addition of the NIR and visible flux at that epoch. While this still does not account for all the energies at which light is emitted from the SN ejecta, it at least accounts for the continuous visible B to NIR H band wavelengths. Plotted in Figures 3.7 – 3.9 are the resulting light curves for SNe 2006E, 2006ce, and 2006mq.

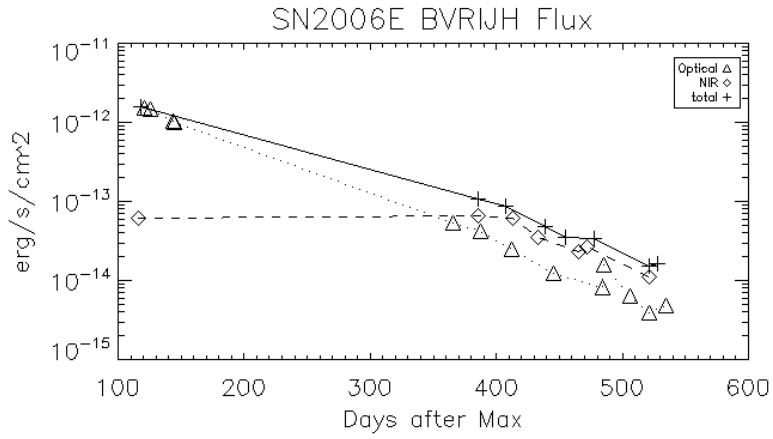


Figure 3.7 SN2006E visible (dotted line) and NIR Power (dashed line) as derived from observed magnitudes. The total flux (solid line) was built using only epochs where NIR and visible observations were taken at similar times.

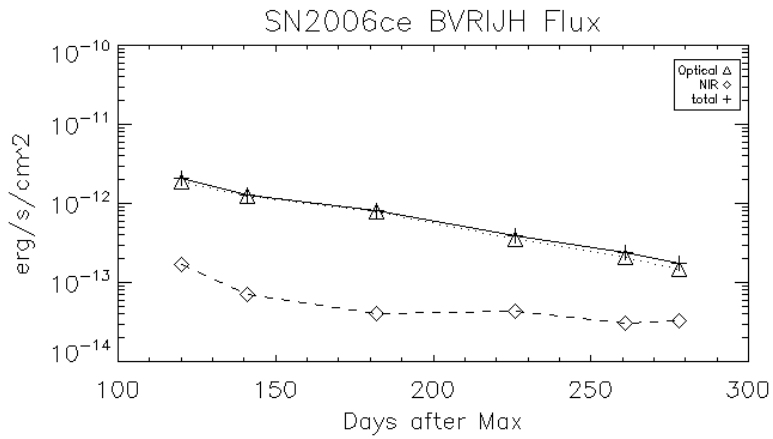


Figure 3.8 SN2006ce visible (dotted line) and NIR Power (dashed line) as derived from observed magnitudes. The total flux (solid line) was built using only epochs where NIR and visible observations were taken at similar times.

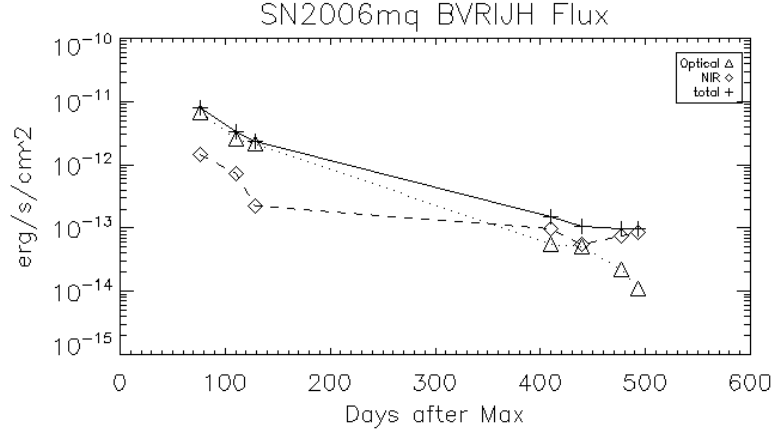


Figure 3.9 SN2006mq visible (dotted line) and NIR Power (dashed line) as derived from observed magnitudes. The total flux (solid line) was built using only epochs where NIR and visible observations were taken at similar times.

At first glance, the gap between the visible and NIR luminosities of SN2006ce appears larger than between those of 2006mq and 2006E. However, this is because 2006ce was observed only out to just shy of 300 days and the scale of the plot is different than the others. All three SNe show that the visible continues a steady decline while the NIR flattens in its decline rate. This brings the NIR and visible to a comparable level just before 400 days. After 400 days, SN2006E shows both the NIR and visible declining, while in SN2006mq, the NIR seems to continue its plateau even as the visible maintains its decline rate.

We convert the flux into luminosity, using the host galaxy distance recorded in the NASA/IPAC Extragalactic Database (NED<sup>1</sup>), and the simple relationship to flux,

$$F = \frac{L}{4\pi d^2}, \quad (3.7)$$

where  $d$  is the distance to the host galaxy. The distances used were 12.8 Mpc and 17.8 Mpc for the host galaxies of SN2006E and SN2006ce respectively. The single measurement for

---

<sup>1</sup> The NASA/IPAC Extragalactic Database (NED) is operated by the Jet Propulsion Laboratory, California Institute of Technology, under contract with the National Aeronautics and Space Administration.

the distance of the SN2006mq host galaxy 6.46 Mpc had a large error associated with it and the luminosity measurement was low compared to the other SNe. We used the value, 8.55 Mpc, which was the upper limit allowed by the distance measurement error.

The SN luminosities are plotted in Figure 3.10 where you can see they have a similar but not identical behavior in the visible and NIR decline.

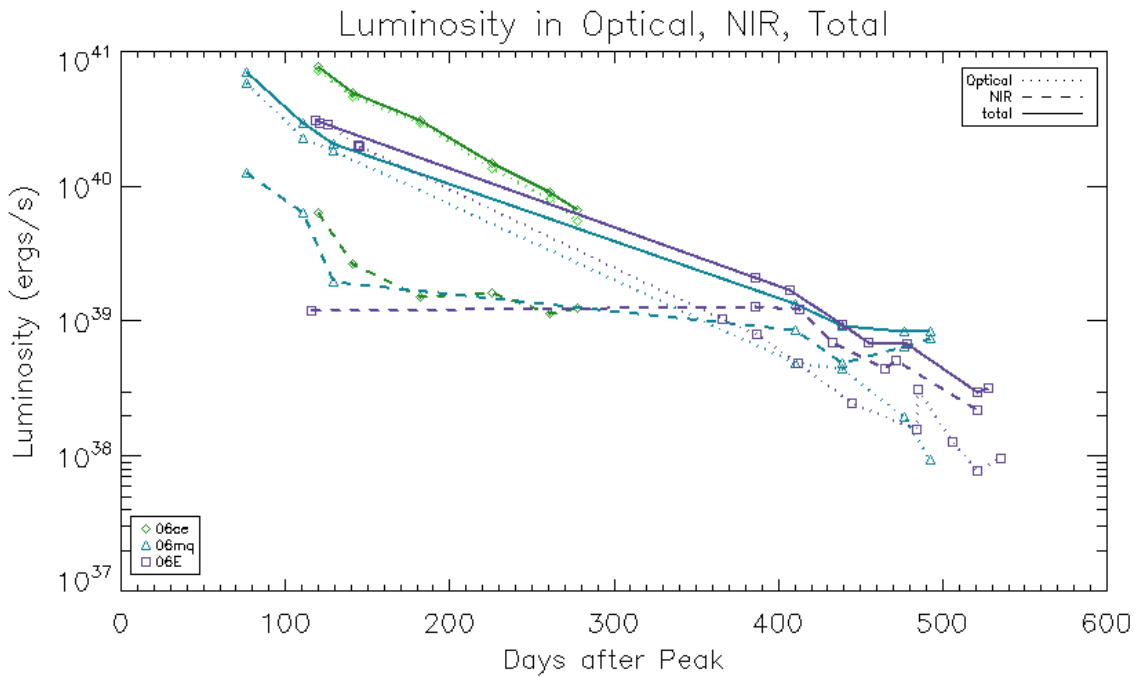


Figure 3.10 The combined  $B, V, R, I, J, H$  luminosities for SNe 2006E (purple squares), 2006ce (green diamonds), and 2006mq (blue triangles). For each, the visible (dotted line) and NIR (dashed line) contributions are also included.

However, there does appear to be a range of decline rates in the late NIR luminosities from 06E's shallow decline to 06mq's steeper loss of power. Much like previously observed SNe in late NIR epochs, our SNe enter a NIR plateau phase, and in SN2006E we seem to have caught the end of it after 413 days

We can compare the NIR portion of these late light curves to other SNe. In order to put these SNe on a scale independent of distance, we plot the NIR magnitudes of each SN relative to its respective peak  $V$ -band magnitude. We correct for extinction wherever possible. Figure 3.11 shows a uniformity in plateau shape, though the magnitude difference from  $V$  peak can differ by 4 magnitudes from SN to SN.

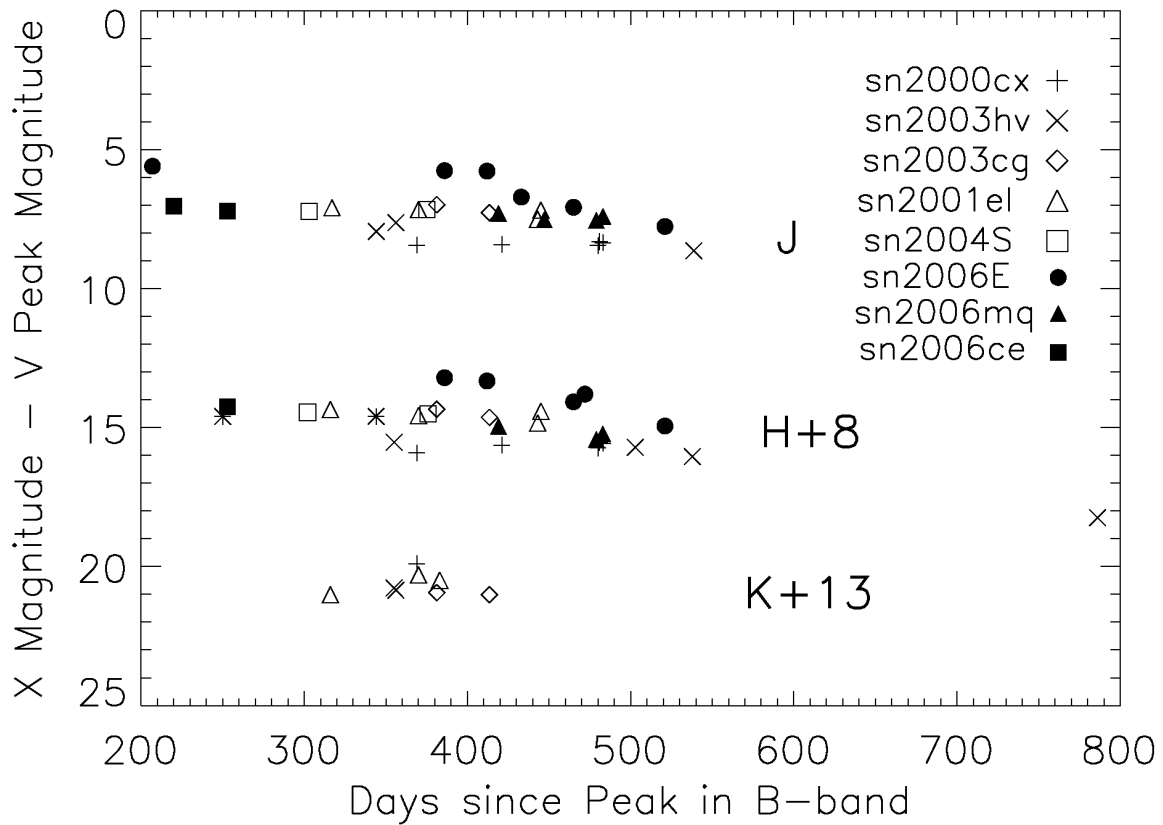


Figure 3.11 The NIR magnitudes of eight SNe Ia starting after 200 days normalized to their respective peak magnitude in  $V$  band. Our three SNe are designated by their filled symbols – circles for SN2006E, triangles for SN2006mq, and squares for SN2006ce. The different bands are offset arbitrarily for better viewing.

### 3.4 Deposited Positron Energy

Because at late times all products of the  $^{56}\text{Ni}$  radioactive decay chain easily escape except for positrons, we will look chiefly at their contribution to the energy of the ejecta.

The numbers of atoms of  $^{56}\text{Ni}$ ,  $^{56}\text{Co}$ , and  $^{56}\text{Fe}$  over time are given by

$$N_{\text{Ni}}(t) = N_{\text{Ni}0} e^{-\frac{t}{\tau_{\text{Ni}}}} \quad (3.8)$$

$$N_{\text{Co}}(t) = N_{\text{Ni}0} \frac{\tau_{\text{Co}}}{\tau_{\text{Co}} - \tau_{\text{Ni}}} \left( e^{-\frac{t}{\tau_{\text{Co}}}} - e^{-\frac{t}{\tau_{\text{Ni}}}} \right) \quad (3.9)$$

$$N_{\text{Fe}}(t) = N_{\text{Ni}0} \left( 1 + \frac{\tau_{\text{Ni}}}{\tau_{\text{Co}} - \tau_{\text{Ni}}} e^{-\frac{t}{\tau_{\text{Ni}}}} - \frac{\tau_{\text{Co}}}{\tau_{\text{Co}} - \tau_{\text{Ni}}} e^{-\frac{t}{\tau_{\text{Co}}}} \right), \quad (3.10)$$

and the rate of decays by

$$\frac{dN_{\text{Ni}}}{dt}(t) = \frac{N_{\text{Ni}0}}{\tau_{\text{Ni}}} e^{-\frac{t}{\tau_{\text{Ni}}}} \quad (3.11)$$

$$\frac{dN_{\text{Co}}}{dt}(t) = \frac{N_{\text{Ni}0}}{\tau_{\text{Co}}} \frac{\tau_{\text{Co}}}{\tau_{\text{Co}} - \tau_{\text{Ni}}} \left( e^{-\frac{t}{\tau_{\text{Co}}}} - e^{-\frac{t}{\tau_{\text{Ni}}}} \right), \quad (3.12)$$

where,  $N_{\text{Ni}0}$  is the initial number of  $^{56}\text{Ni}$  atoms,  $\tau_{\text{Ni}} = 5.5$  days is the lifetime of  $^{56}\text{Ni}$ , and  $\tau_{\text{Co}} = 111.3$  days is the lifetime of  $^{56}\text{Co}$  (Nadyozhin, 1994).

As discussed in section 1.2, positrons result from 19% of  $^{56}\text{Co}$  decays and with a typical kinetic energy of 0.632 MeV. The amount of power potentially available to the SN from radioactive decay via positrons at any given time can be calculated as the number of  $^{56}\text{Co}$  decays that result in positrons times the kinetic energy of the positron,

$$E_{\text{Pos}} = \frac{N_{\text{Ni}0}}{\tau_{\text{Co}}} \frac{\tau_{\text{Co}}}{\tau_{\text{Co}} - \tau_{\text{Ni}}} \left( e^{-\frac{t}{\tau_{\text{Co}}}} - e^{-\frac{t}{\tau_{\text{Ni}}}} \right) * 0.19 * \text{KE}_{\text{pos}}, \quad (3.13)$$

where  $\text{KE}_{\text{pos}} = 0.632$  MeV.

We do adopt the calculated gamma-ray contribution from Milne et al. (2001). Both this gamma-ray energy deposition and potential positron kinetic energy deposition are shown in Figure 3.12 for a SN that synthesizes  $0.6 M_{\odot}$  of  $^{56}\text{Ni}$ .

The positron energy shown in Figure 3.12 will vary depending on how many positrons escape with what fraction of their kinetic energy. We fit the column depth encountered by our positrons as a distance from their creation location to the surface. The greater the column depth, the less likely the positrons are to escape with any of their kinetic energy. At the same time, we fit a scale factor to the calculated  $\gamma$ -ray deposition.

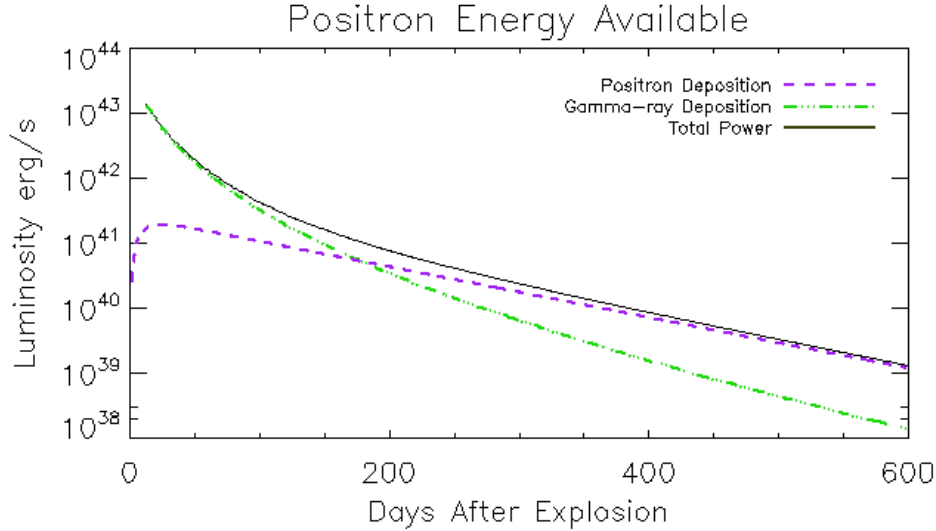


Figure 3.12 The power provided by positrons (blue dashed line) and  $\gamma$ -rays (green dot-dashed line) in a SN Ia. The total combined power is shown as a solid black line. This assumes an initial  $^{56}\text{Ni}$  mass of  $0.6M_{\odot}$  and that all positrons are produced with a kinetic energy of 0.632 MeV.

The slowing of positrons as they traverse the ejecta is done chiefly by ionization and excitation processes. Figure 3.13 shows the continuous-slowng-down approximation for the range (in column density) of electrons in Fe. Electrons that start out with a particular kinetic energy (x-axis) will encounter a particular amount of column density (y-axis) before losing all of their energy. This same effect also applies to positrons.

To get an idea of what kind of energy is donated to the SN ejecta by the positrons at late time, we can employ a very simple model of a one-zone SN Ia. This SN, previously made of only C and O, just reaches the Chandrasekhar mass of  $1.39 M_{\odot}$  before igniting and synthesizing  $0.6 M_{\odot}$  of  $^{56}\text{Ni}$ . It expands outward from a WD the size of the Earth, to an ejecta moving at  $v=1 \times 10^9$  cm/s. In our one-zone model, this gives us a density of  $\rho = \frac{m}{4/3\pi(vt)^3}$  and a column density of  $\xi = \frac{m}{4/3\pi(vt)^3} * vt = \frac{m}{4/3\pi(vt)^2} = 1.576 \times 10^{14}$  g/cm<sup>2</sup>/t<sup>2</sup> from the center of the ejecta to the surface (plotted in Figure 3.14).



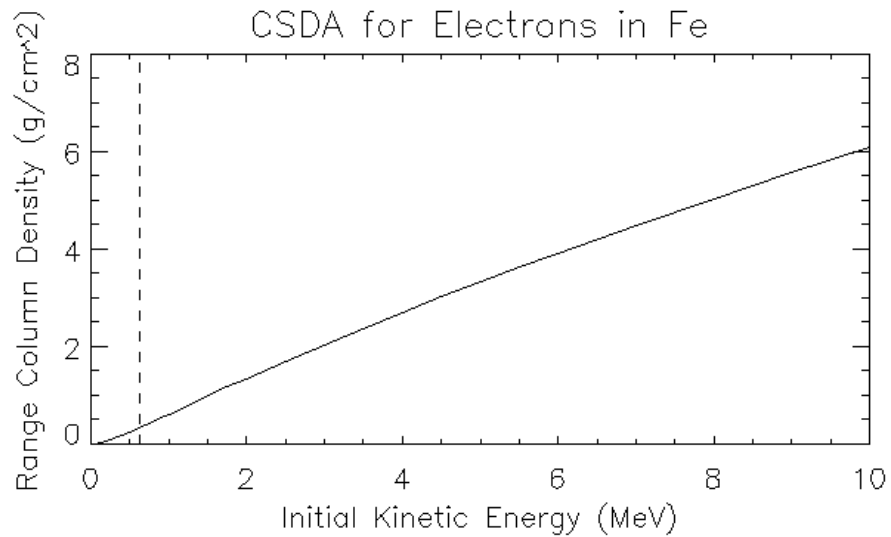


Figure 3.13 The continuous slowing down approximation range for electrons in a sea of Iron. Reproduced from data provided by NIST. The dashed line shows the average kinetic energy of positrons produced in  $^{56}\text{Co}$  decay.

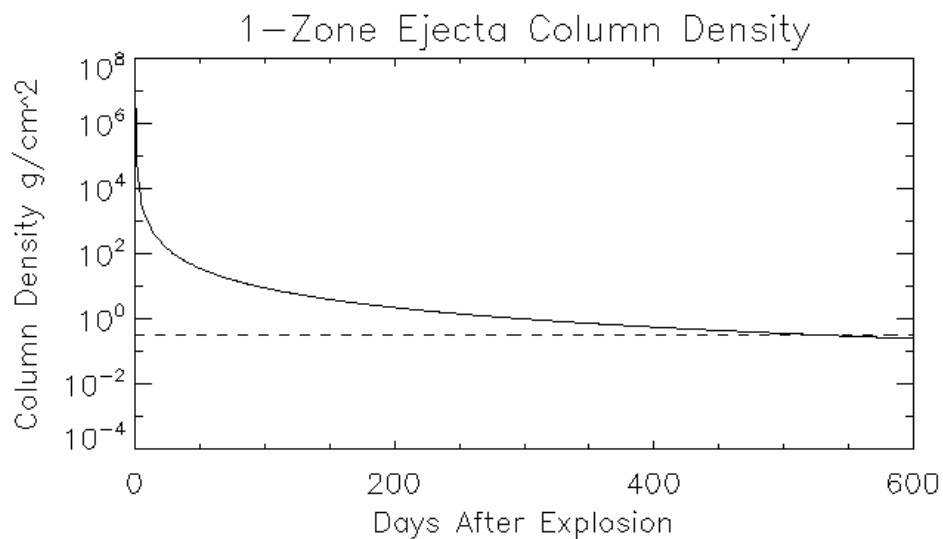


Figure 3.14 The column density in a one zone model of a SN Ia ejecta containing  $1.39 M_{\odot}$  and expanding with a velocity of  $v=1 \times 10^9$  cm/s

Assuming the all our positrons are produced with the typical value of 0.632 MeV (Nadyozhin, 1994), then the positrons lose all their energy to the ejecta as long as the column density along their path is greater than  $0.3232 \text{ g/cm}^2$  (according to Figure 3.13). If, however, the column density is less than this, the positron will escape the ejecta but will deposit an amount of energy proportional to the column density it passed through. We can calculate this by again referring to Figure 3.13.

Positrons created closer to the surface pass through less material than those that are deeper. To account for this, I vary the distance the positrons travel to the surface. If all the positrons started from halfway to the surface, and took shortest distance paths to escape, the positron deposition energy would look like Figure 3.15 and no positron would escape until after 350 days. Thus the amount of energy deposited by positrons is equal to that of the curve shown in 3.12 until that point.

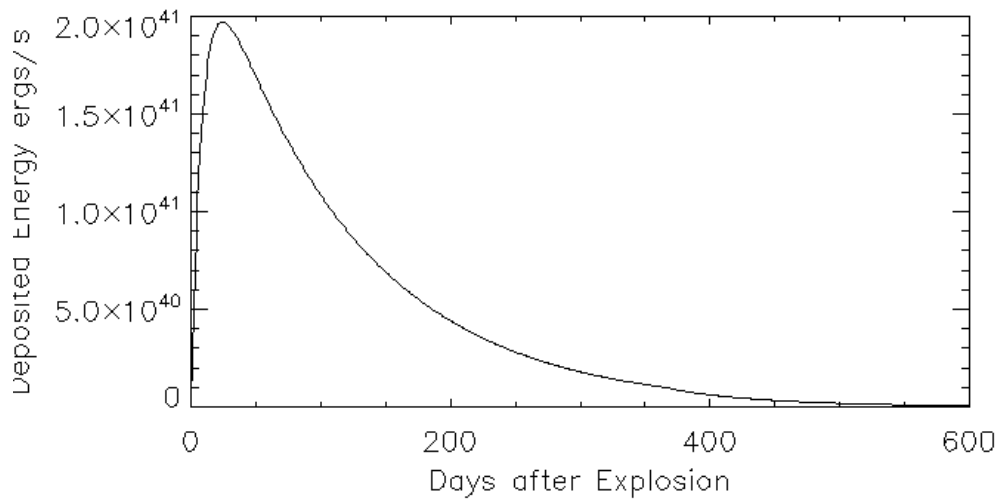


Figure 3.15 The positron energy deposition over time if positrons, located at half the distance to the surface took shortest path trajectories out. This differs from Figure 3.12 at late times when the ejecta is thin enough for the positrons to escape, and take some of their kinetic energy with them.

We do not consider any magnetic field configuration as this would only make trapping more successful. Thus we ignore magnetic fields and understand that any conclusions drawn from our model comparison would be a lower limit to the energy deposited by positrons.

We can compare this to the luminosity of our three SNe and vary the distance of the positrons to the surface in our one-zone model. Figures 3.17 through 3.18

Using the distances mentioned in Section 3.3 to determine luminosity made it impossible to compare to our model. Thus we allow the distance to vary as a free parameter to fit the observed luminosity around the 100 day epoch to the model luminosity. This resulted in deriving much larger distances than reported by NED, 35 Mpc for SN2006E, 34 Mpc for SN2006ce, and 26 Mpc for SN2006mq. These can each vary by  $\pm 3$  Mpc without a great change in fit.

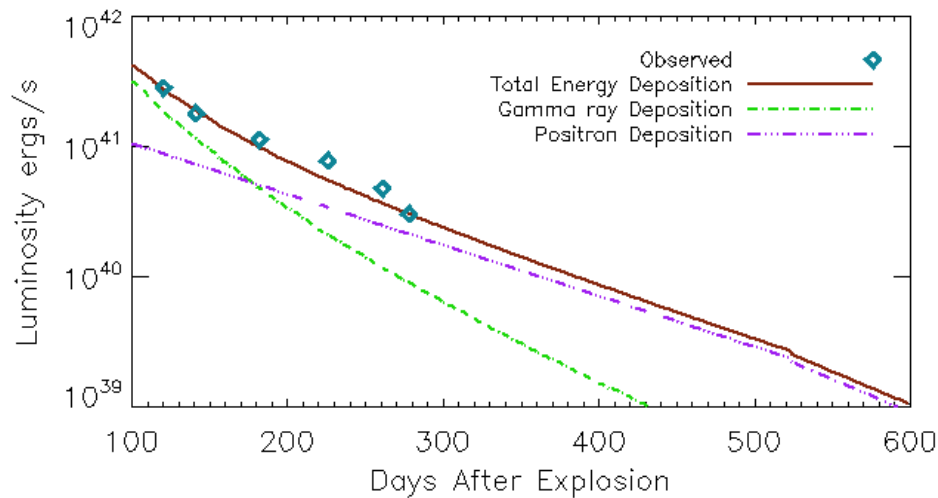


Figure 3.16 SN2006ce total observed flux (blue diamonds) compared to the power deposited by positrons (purple dash-triple-dotted line),  $\gamma$ -rays (green dot-dashed line) and total power (solid red line) in our simple 1-D model.

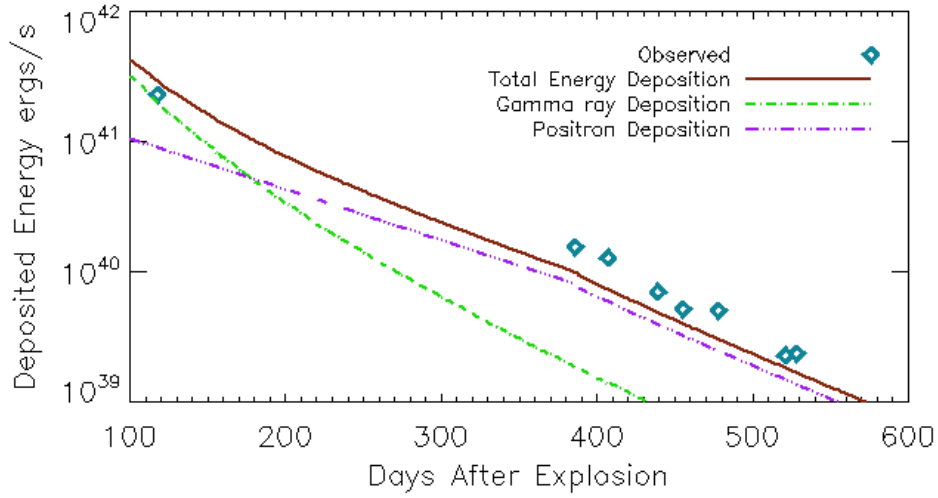


Figure 3.17 SN2006E total observed flux (blue diamonds) compared to the power deposited by positrons (purple dash-triple-dotted line),  $\gamma$ -rays (green dot-dashed line) and total power (solid red line) in our simple 1-D model.

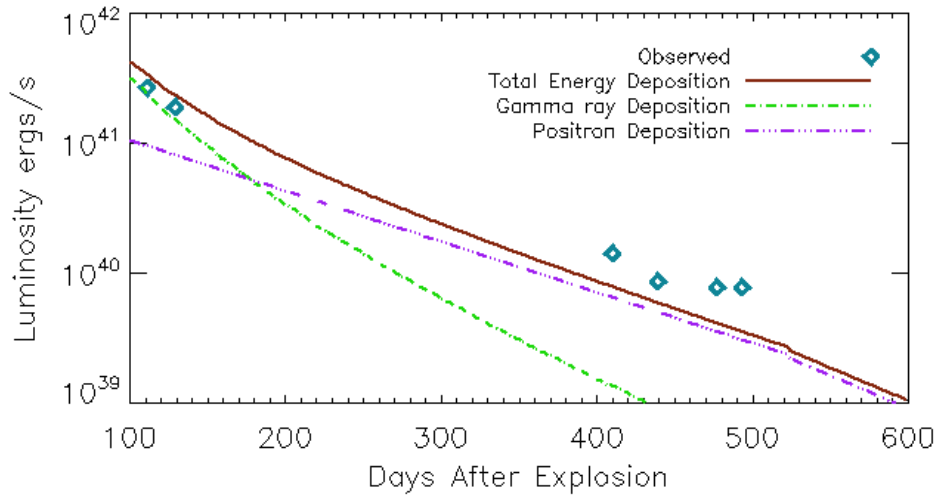


Figure 3.18 SN2006mq total observed flux (blue diamonds) compared to the power deposited by positrons (purple dash-triple-dotted line),  $\gamma$ -rays (green dot-dashed line) and total power (solid red line) in our simple 1-D model.

No useful data about positron escape came from SN2006ce as it was not observed late enough for positron escape to occur. Both SNe 2006E and 2006mq have abundant energy at late times to account for positron trapping. However, the decline rate of SN2006E was more shallow than that of positron trapping and was better fit by a decline rate shaped by positrons beginning to escape around 400 days (or placing them half a radius away from the surface). The fit was not particularly good for SN2006mq, with its steeper early decline, and more shallow late decline.

We built our own *BVRIJH* luminosity curve from Leloudas et al. (2009) observations of SN2003hv just as we did with the three 2006 SNe. Plotted in Figure 3.19 is a comparison of those four SNe NIR, visible, and total luminosities.

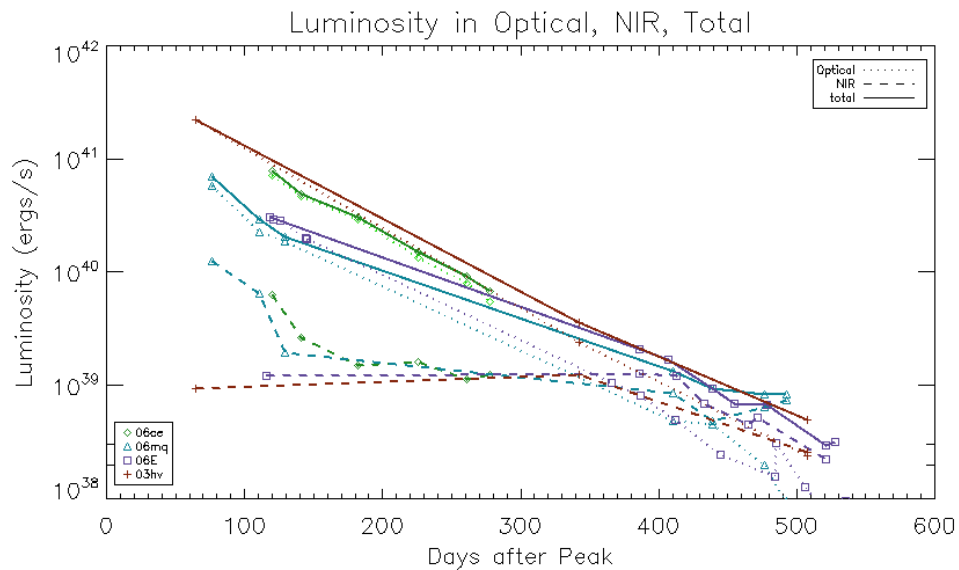


Figure 3.19 Comparing the *BVRIJH* visible, NIR, and composite luminosities of SNe 2006E (squares), 2006mq (triangles), and 2006ce (diamonds) to those of SN2003hv (X's) built from observations by Leloudas et al. (2009).

While Leloudas et al. (2009) built a UVOIR light curve for SN2003hv, building our own allowed us to confirm our procedures produced similar results and allowed us to see the behavior of the NIR and visible portions of the luminosity separately. The total luminosity

of our two late 2006 SNe match an overall general decline rate after 350 days. However, the visible decline rates seem steeper than that of 2003hv.

Leloudas et al. (2009) noticed the "slowdown of visible decay" – especially in the V-band. In fact, Sollerman et al. (2004) noticed this too – that around 550 - 693 days, SN2000cx's V band decline slope was much more shallow. It is possible that this resulted from a light echo (peak SN light reaching us later after scattering off of nearby dust), however there does not seem to be much evidence for dust near the SNe. Our visible observations do not go out as late as these two SNe, however the luminosity in *BVRI* for the SN2006 SNe is already at a lower value than 2000cx and 2003hv at 500 days.

The UVOIR light curves of both SN2003hv and SN2000cx have late decline rates that mirror the decay rate of  $^{56}\text{Co}$ . The change in magnitudes is related to the flux as,

$$\Delta m = -2.5 \log \left( \frac{F_i}{F_f} \right). \quad (3.14)$$

The flux is proportional to  $e^{-t/\tau}$ , thus

$$\Delta m = -2.5 \log \left( e^{-\Delta t/\tau} \right) = 1.085 \frac{\Delta t}{\tau}, \quad (3.15)$$

The lifetime of  $^{56}\text{Co}$  is about 111 days, so

$$\frac{\Delta m}{\Delta t} = \frac{1.085}{111 \text{days}} \sim \frac{1 \text{mag}}{100 \text{days}} \quad (3.16)$$

Fitting the decline rate in "bolometric" magnitudes for our SNe and comparing to SN2003hv, we get a very shallow 0.58 mag/100days for SN2006mq, a steep 1.50 mag/100days, and 1.29 mag/100days for SN2003hv. The fits can be seen in Figure 3.20. The 1.29 measured decline rate for 2003hv is steeper than the 0.98 mag/100 days measured by Leloudas et al. (2009) when including the *U* and *K* band which are missing from our "bolometric" magnitudes.

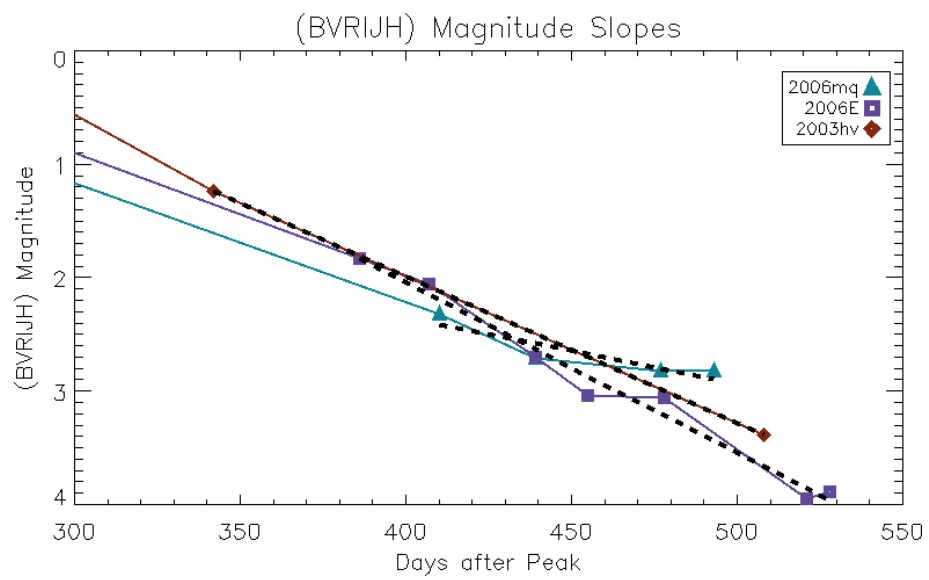


Figure 3.20 Comparing the late “bolometric” (*BVRIJH*) magnitudes of SNe 2006E (purple squares), 2006mq (blue triangles), and SN2003hv (maroon X’s).

## CHAPTER 4

### CONCLUSIONS

We observed 3 normal SNe Ia from just before 100 days out past 500 days in visible *BVRI* and NIR *JH* wavelengths. We combined these observations and studied the behavior of the late time power – comparing them to a simple model and to another well observed SN Ia.

Unfortunately, each of the SNe were discovered post peak, so early measurements of peak date, decline rate, and synthesized  $^{56}\text{Ni}$  estimates are not available. SN2006E was assigned two different ages. We were able to use early Super-LOTIS observations to fit to the normal SN1992A light curve and recover its peak date. Images for host galaxy subtraction were used to rid SN2006E of any contaminating host galaxy light in apparent magnitude measurements.

We used the apparent magnitudes to compare to the decline rates of other SNe (Lair et al., 2006), and found that the visible bands conformed to the typical decline rates very well. The *V-J* color (Figure 3.5) varied some in each of our three SNe, but the overall trend was to a much redder SN ejecta. Eight SNe (including the three from this thesis) have been observed in the NIR after 200 days. We compared each *J* and *H* magnitude to the SN's respective *V* magnitude at peak, and saw that each SN seems to plateau - has a very small or nonexistent decline rate - sometime over the epochs of 200 - 500 days.

We converted the observed magnitudes to flux using SNe spectra observed at various epochs. We examined the behavior of the visible and NIR. While the flux is initially greater in the visible bands than in the NIR, the visible declines steadily as the NIR plateaus from around 200 days to 400 days. At around 400 days, the contributions from the visible and NIR are roughly equal. After this, the NIR does seem to steepen its decline, though SN2006mq may still be roughly in plateau. The fact that the visible flux doesn't fall off, but instead maintains a steady decline rate indicates an infrared catastrophe is not occurring, or, at the most, is only a local phenomenon.



After using the rough host galaxy distance measurements to convert to luminosity, we were able to compare the SNe luminosities to each other. The total *BVRIZH* luminosities are comparable once distance errors are taken into account. It is apparent that the late evolution is slightly different among the three SNe. SN2006ce exhibits the approach to the NIR plateau phase, as does the beginning of the 2006mq NIR. SN2006E exhibits first, a flatter plateau at 200-400 days than 2006mq, but then, after 400 days, steps quickly down to a steeper decline rate, while 2006mq seems to be experiencing its NIR plateau phase.

Comparisons with previously observed SN2003hv shows an intermediate late total decline rate. However, the 2003hv visible light curve is always brighter than those of the 2006 SNe. The NIR plateaus of SNe 2006E, 2006mq, and 2006ce line up in luminosity around 300 days.

We built a 1-zone model that included  $\gamma$ -ray deposition from Milne et al. (2001) and positron escape to compare with the luminosities of our observations. We first fit the distance by matching the total ( $\gamma$ -ray + positron energy deposition) model luminosity to the observed luminosity at the roughly 100 day epoch. Then we varied the depth of the positron creation location in the SN ejecta in order to fit the late luminosities. A positron starting deeper would have farther to travel in column depth, meaning it would deposit more of its kinetic energy before leaving (or even be trapped completely) than a positron starting closer to the surface. For SNe 2006E and 2006mq, the luminosity was high enough to require all positrons to be trapped. However, the shape of the late light curve of SN2006E fit the decline rate of a model where positrons were created half an ejecta radius away from the surface and began to escape the ejects at 400 days. Thus, if the distance were found to actually be closer than derived positron escape would not be ruled out.

Our single zone model is, of course, an imperfect one. All our positrons were created with a uniform kinetic energy, and moved in straight line trajectories toward the surface. In an actual SN ejecta, a magnetic field may be present. It would, however, only increase the length of the path of travel for the positron, keeping it in the ejecta for a longer time and increasing the amount of material the positron runs into. Thus the positron formation location at 50% of the radius is merely a lower limit. Were we to incorporate any modification due to magnetic fields, this would necessarily require the positron starting

position to be closer to the outer edges to match our observations. Similarly, adding more zones would only delay positron escape and give the positron a chance to scatter more before it reached the surface, making it again necessary to start the positrons even closer to the surface.

If the distances, and thus luminosities, are incorrect, we would not be able to rule out positron escape as an explanation for the steeper slope of SN2006E. However, there may be other explanations. It could be that the color evolution is such that light is emerging in other wavelengths have not observed. Leloudas et al. (2009) used a visible/NIR/MIR spectrum to determine that there was an additional  $34 (\pm 17)\%$  extra energy in the MIR compared to the observed UBVOIR light curve. There may also be additional power elsewhere, as many Fe fine structure lines are red-ward of the MIR.

If it is the shift of energy that accounts for the difference in luminosity, it is interesting that the shift may not be uniform across all SNe Ia. The NIR plateau seems to occur at different times, and with different luminosities. In SNe 2000cx and 2003hv the visible light curve slows in its decline after 400 days, though it doesn't in SNe 2006E and 2006mq.

#### 4.1 Future Work

Additional SNe Ia have been observed in the 200+ day epochs in the visible, NIR, and even mid-IR. Incorporating longer wavelength information lead to an improved accounting for the power, where we can better hope to constrain positron creation location, and answer more accurately if they are trapped or escape the ejecta. A greater number of SNe Ia observed in these wavelengths at late epochs will also allow us to see how varied SN Ia late color evolution can be, and define “normal” late behavior. Are there 2 tracks - one with slower declining late visible luminosity and one with steadily declining visible luminosity? Is there a correlation with early behavior?

We would also like to extend these observations beyond normal SNe to more luminous and sub-luminous SNe. The late light curve could help us understand the causes behind the differences in SNe Ia, and perhaps help to refine the Ia standardization process and improve SN distance measurements.

## APPENDICES

## Appendix A

### DATA REDUCTION How-To's

Below are the step by step tutorials on how to reduce images, including standard images (Section A.1), multi-extension fits files (Section A.2), and NIR images (Section A.3). Also included is how to do photometry on reduced images (Section A.4).

#### A.1 Standard Image Reduction

## Using IRAF to Reduce Images by Ginger Bryngelson

This tutorial steps you through the process of preliminary reductions of CCD data, including overscan subtraction, bias or zero level subtraction, dark subtraction, and flat fielding. This exercise assumes that you have worked through Exercise 1 and feel comfortable with the basics of IRAF. A summary of all steps is included at the end of this tutorial. At each step, be sure to take a look at the images you're working with using ds9. As in all these exercises, the commands after the prompt (either "\$" or "cl>") are meant to be typed by the user; the #-sign indicates a comment. Go to the directory with your raw ccd images in it.

```
$ cd path/imagefolder
```

Log into IRAF in an xgterm window, and set up a ds9 window to display images.

1) First we need to do some preliminary set-up

Let's load some iraf packages:

```
cl> images
```

```
cl> imutil
```

```
cl> tv
```

a) Take a look at the images you have

```
cl> imhead *.fits
```

or

```
cl> hselect *.fits $I,object,filter,exptime
```

If you don't see the image name, object observed, filter, and exposure time, then look at the image header to make sure we have the right keyword (exptime might actually be exp\_time).

In fact, let's write a file that contains all this information, and call it "obslog."

```
cl> hselect *.fits $I,object,filter,exptime > obslog
```

You should be able to view the contents of this file by typing

```
cl> !more obslog
```

and hitting return or spacebar to scroll down and the scrollbar to scroll up.

You can also open the file in another window/terminal. The "!" tells iraf that this is just a terminal command, and to pass the command on to the terminal and then return to iraf when finished. Some terminal commands, like "ls" and "cd" have been incorporated into iraf, so you don't have to use the escape character "\!" when issuing it.

You should have some images of each:

Object (science field)

Bias or Zero (5-10)

Dark (5-10 at each of the same exposure times as your science and flat images)

Flat (5-10 for each filter you have for your science images)

Let's make a list of each type of the images using the "grep" and "awk" commands.

```
cl> !grep dark obslog
```

#you should see a list of images that are darks. If you see nothing, then "grep" is finding no line of text that has "dark" in it. Try looking again with variations of capital letters, e.g. Dark or DARK.

Now, instead of printing to the screen, we can print to a file. Let's pipe the results of grep to the "awk" command to print just the first column (expressed as "\$1") to a file listdark.

```
cl> !grep dark obslog | awk '{print $1}'
```

```
cl> !grep dark obslog | awk '{print $1}' > listdark
```

Do this for the flats and zeros/bias and objects. For the objects, you may want to do something like:

```
cl> !grep SN2010gh obslog | awk '{print $1}' > listobj
```

b) Let's make sure we have the appropriate labels for each image type in the IMAGETYP keyword. We can edit the header keywords (e.g. IMAGETYP) and values (e.g. dark) with the iraf task "hedit." The "add+" adds the keyword to the header if it doesn't exist, and "verify-" or a shortened "ver-" makes it so that you don't have to confirm your choice for every single individual image. Adding the "@" at the beginning of the word, tells iraf it is the name of a file that contains a list of the images you want

```
cl> hedit @listdark IMAGETYP "dark" add+ verify-
```

```
cl> hedit @listflat IMAGETYP "flat" add+ ver-
```

```
cl> hedit @listzero IMAGETYP "zero" add+ ver-
```

```
cl> hedit @listobj IMAGETYP "object" add+ ver-
```

Make sure you take a look at each of these kinds of images with ds9. Look at the values of the pixels, the shape of the varying background, and any odd pixel behavior.

2) Now we can actually start reducing images with iraf.

a) The first step in processing images, involves using the task ccdproc to trim images and fix bad pixels and subtract the overscan if there is one.

Let's load the packages needed for ccdproc

```
cl> help ccdproc
```

#look at the packages required for ccdproc (written at the very top middle) then quit by hitting "q"

```
cl> noao
cl> imred
cl> ccdred
```

ccdproc is capable of doing lots of steps at once, but for now we will do things one step at a time. Let's epar ccdproc and change things so that we are only fixing pixels, trimming, and overscan correcting.

```
cl> epar ccdproc
```

Put "no" for everything except "fixpix," "oversca," and "trim." Put the name of your bad pixel file for "fixfile," and just write "image" for both "biassec" and "trimsec" - this tells iraf to look at the image header information to find the appropriate pixel range. If you do not have a bad pixel file, then either ask for one or leave the "fixfile" blank and choose "no" for fixpix . Here's what the changes should look like:

```

      I R A F
Image Reduction and Analysis Facility
PACKAGE = ccdred
TASK = ccdproc

images =
) List of CCD images to correct
(output =
) List of output CCD images
(ccdtype=
) CCD image type to correct
(max_cac=
0) Maximum image caching memory (in Mbytes)
(noproc =
no) List processing steps only?

(fixpix =
yes) Fix bad CCD lines and columns?
(oversca=
yes) Apply overscan strip correction?
(trim =
yes) Trim the image?
(zeroeor=
no) Apply zero level correction?
(darkcor=
no) Apply dark count correction?
(flatcor=
no) Apply flat field correction?
(illumco=
no) Apply illumination correction?
(fringec=
no) Apply fringe correction?
(readcor=
no) Convert zero level image to readout correction?
(scancor=
no) Convert flat field image to scan correction?

(readaxi=
line) Read out axis (columnline)
(fixfile=
badpixfile) File describing the bad lines and columns
(biassec=
image) Overscan strip image section
(trimsec=
image) Trim data section
(zero =
) Zero level calibration image
(dark =
) Dark count calibration image
(flat =
) Flat field images
(illum =
) Illumination correction images
(fringe =
) Fringe correction images
(minrepl=
1.) Minimum flat field value
(scantyp=
shortscan) Scan type (shortscan/longscan)
(nscan =
1) Number of short scan lines

(interac=
no) Fit overscan interactively?
(funcio=
legendre) Fitting function
(order =
1) Number of polynomial terms or spline pieces
(sample =
*) Sample points to fit
(naverag=
1) Number of sample points to combine
(niterat=
1) Number of rejection iterations
(low_rej=
3.) Low sigma rejection factor
(high_re=
3.) High sigma rejection factor
(grow =
0.) Rejection growing radius
(mode =
q1)
```

**ESC-?** for HELP

Use ":q" to quit.

Now let's call this command with some specific parameters.

```
cl> ccdproc @listzero ccdtype=zero
cl> ccdproc @listdark ccdtype=dark
cl> ccdproc @listflat ccdtype=flat
cl> ccdproc @listobj ccdtype=object
```

b) Now, we need to combine all the zeros into a master Zero.fits using zerocombine. Look at an lpar to see the kind of options you have.

```
cl> lpar zerocombine
cl> zerocombine @listzero
```

Let's look at an individual zero/bias image as well as the master Zero image with ds9.

c) Now we can run ccdproc, and include zero subtraction.

```
cl> epar ccdproc
#Edit the parameter file to look like below. Use ":q" to quit when
done.
```

```

      I R A F
Image Reduction and Analysis Facility
PACKAGE = ccdred
TASK = ccdproc

images = List of CCD images to correct
(output = ) List of output CCD images
(ccdtype= ) CCD image type to correct
(max_cac= 0) Maximum image caching memory (in Mbytes)
(inoproc = no) List processing steps only?

(fixpix = no) Fix bad CCD lines and columns?
(oversca= no) Apply overscan strip correction?
(trim = no) Trim the image?
(zeroeor= yes) Apply zero level correction?
(darkcor= no) Apply dark count correction?
(flatcor= no) Apply flat field correction?
(illumco= no) Apply illumination correction?
(fringec= no) Apply fringe correction?
(readcor= no) Convert zero level image to readout correction?
(scancon= no) Convert flat field image to scan correction?

(readaxi= line) Read out axis (column|line)
(fixfile= badpixfile) File describing the bad lines and columns
(biassec= image) Overscan strip image section
(trimsec= image) Trim data section
(zero = Zero.fits) Zero level calibration image
(dark = ) Dark count calibration image
(flat = ) Flat field images
(illum = ) Illumination correction images
(fringe = ) Fringe correction images
(minrepl= 1.) Minimum flat field value
(scantyp= shortscan) Scan type (shortscan|longscan)
(nscan = 1) Number of short scan lines

(interac= no) Fit overscan interactively?
(function= legendre) Fitting function
(order = 1) Number of polynomial terms or spline pieces
(sample = *) Sample points to fit
(naverag= 1) Number of sample points to combine
(niterat= 1) Number of rejection iterations
(low_rej= 3.) Low sigma rejection factor
(high_re= 3.) High sigma rejection factor
(grow = 0.) Rejection growing radius
(mode = ql)
```



Now run ccdproc for flats, darks, and object images.

```
cl> ccdproc @listdark ccdtype=dark
cl> ccdproc @listflat ccdtype=flat
cl> ccdproc @listobj ccdtype=object
```

d) Next, we combine the darks into a master Dark for each exposure time. To do this, we need to make different lists of images for each exposure time. First, look at all the darks to see what exposure times you need.

```
cl> !grep dark obslog
```

Now, type this command for each exposure time (where 60 is the example exposure time):

```
cl> !grep dark obslog | grep 60 | awk '{print $1}' > listdark60
```

Now combine the darks by exposure time:

```
cl> darkcombine @listdark60 output=Dark60.fits
      #do this for each exposure time.
```

e) In order to process the correct exposed images with ccdproc, we will have to make lists of flats and objects that have the same exposure times as the master darks. Here, 60 is just a stand-in for the exposure times.

```
cl> !grep obslog flat | grep 60 | awk '{print $1}' > listflat60
```

```
cl> !grep listobj object | grep 60 | awk '{print $1}' > listobj60
etc...
```

Now, edit the ccdproc to say yes for "darkcor" as below, then exit with ":q"

```
cl> epar ccdproc
```

```

                                I R A F
                                Image Reduction and Analysis Facility

PACKAGE = ccdred
TASK = ccdproc

images =           List of CCD images to correct
(output =         ) List of output CCD images
(ccdtype=        ) CCD image type to correct
(max_cac=        0) Maximum image caching memory (in Mbytes)
(noproc =        no) List processing steps only?

(fixpix =        no) Fix bad CCD lines and columns?
(oversca=       no) Apply overscan strip correction?
(trim =         no) Trim the image?
(zeroeor=       no) Apply zero level correction?
(darkcor=       yes) Apply dark count correction?
(flatcor=       no) Apply flat field correction?
(illumco=       no) Apply illumination correction?
(fringec=       no) Apply fringe correction?
(readcor=       no) Convert zero level image to readout correction?
(scancor=       no) Convert flat field image to scan correction?

(readaxi=       line) Read out axis (column/line)
(fixfile=      badpixfile) File describing the bad lines and columns
(biassec=      image) Overscan strip image section
(trimsec=      image) Trim data section
(zero =        Zero.fits) Zero level calibration image
(dark =        ) Dark count calibration image
(flat =        ) Flat field images
(illum =       ) Illumination correction images
(fringe =      ) Fringe correction images
(minrepl=      1.) Minimum flat field value
(scantyp=      shortscan) Scan type (shortscan/longscan)
(nscan =       1) Number of short scan lines

(interac=      no) Fit overscan interactively?
(funcio=      legendre) Fitting function
(order =       1) Number of polynomial terms or spline pieces
(sample =      *) Sample points to fit
(naverag=      1) Number of sample points to combine
(niterat=     1) Number of rejection iterations
(low_rej=     3.) Low sigma rejection factor
(high_rej=    3.) High sigma rejection factor
(grow =       0.) Rejection growing radius
(mode =       ql)

```

Run ccdproc for each exposure time:  
 cl> ccdproc @listobj60 dark=Dark60.fits  
 cl> ccdproc @listflat60 dark=Dark60.fits  
 etc...

f) Now we will do something similar for the flats, where we separate by filter.

First, look at all the filters observed in for the flats, and your object (it will probably be different than SN2010gh):

```

cl> !grep obslog flat
cl> !grep obslog SN2010gh

```

Most likely it is something like "B", "V", "R", "I", but sometimes the filters are actually longer strings.

```

cl> !grep obslog flat | grep B | awk '{print $1}' > listflatB
cl> !grep obslog SN2010gh | grep B | awk '{print $1}' > listobjB

```

Do each of these for each filter.

Now combine all flats by their filter.

```
cl> flatcombine @listflatB output=FlatB.fits
etc...
```

g) Now divide the object images by the appropriate master Flat using ccdproc with the appropriate parameters.

```
cl> epar ccdproc
```

```

      I R A F
Image Reduction and Analysis Facility

PACKAGE = ccdred
TASK = ccdproc

images =
(output =
(ccdtype=
(max_cac=
(noproc =
(fixpix =
(oversca=
(trim =
(zerocon=
(darkcon=
(flatcon=
(illumco=
(fringec=
(readcon=
(scancor=
(readaxi=
(fixfile=
(biassec=
(trimsec=
(zero =
(dark =
(flat =
(illum =
(fringe =
(minrepl=
(scantyp=
(nscan =
(interac=
(funcio=
(order =
(sample =
(naverag=
(niterat=
(low_rej=
(high_re=
(grow =
(mode =

      List of CCD images to correct
      ) List of output CCD images
      ) CCD image type to correct
      0) Maximum image caching memory (in Mbytes)
      no) List processing steps only?

      no) Fix bad CCD lines and columns?
      no) Apply overscan strip correction?
      no) Trim the image?
      no) Apply zero level correction?
      no) Apply dark count correction?
      yes) Apply flat field correction?
      no) Apply illumination correction?
      no) Apply fringe correction?
      no) Convert zero level image to readout correction?
      no) Convert flat field image to scan correction?

      line) Read out axis (column\line)
      badpixfile) File describing the bad lines and columns
      image) Overscan strip image section
      image) Trim data section
      Zero.fits) Zero level calibration image
      ) Dark count calibration image
      ) Flat field images
      ) Illumination correction images
      ) Fringe correction images
      1.) Minimum flat field value
      shortscan) Scan type (shortscan\longscan)
      1) Number of short scan lines

      no) Fit overscan interactively?
      legendre) Fitting function
      1) Number of polynomial terms or spline pieces
      *) Sample points to fit
      1) Number of sample points to combine
      1) Number of rejection iterations
      3.) Low sigma rejection factor
      3.) High sigma rejection factor
      0.) Rejection growing radius
      ql)

:q
```

Run ccdproc on object images for each filter:

```
cl> ccdproc @listobjB flat=FlatB.fits
Etc...
```

3) At this point, all your object images have been reduced. Now, you can combine them all into one master science image by filter. We will use the task `imcombine`, in the `immatch` package. Let's use a median value of each pixel instead of averaging.

```
cl> immatch
```

```
cl> imcombine @listobjB output=ObjB.fits combine=median
```

Do this for each filter observed.

Now you should have a single image per filter that represents all the observations you've taken of this particular object. Please look at them using `ds9`, and compare it to the individual images.

#### Quick Summary of Image Reduction Steps

1. Preliminary Set-up
  - a. Make lists of each image type.
  - b. Establish `IMAGETYP` keyword for each image.
2. Prepare images.
  - a. Trim images, fix bad pixels, and subtract overscan.
  - b. Combine all zeros to master Zero.
  - c. Subtract Zero from darks, flats, object images.
  - d. Combine all darks into master Darks by exposure time.
  - e. Subtract Darks from flats and object images.
  - f. Combine all flats into master Flats by filters.
  - g. Divide out Flats from object images.
3. Combine reduced object images into master science images by filter.

## A.2 Multi-Extension Fits Image Reduction

## IRAF Tutorial Reducing MEF images (Multi-Extension-Fits)

0) Install the external package "mscred"

I) This is how my structure was setup when I installed linux under a new user called "iraf",  
/iraf/iraf/local

The version of iraf I installed used the archetype "redhat", even though I chose a linux version. This may or may not have any effect on your installation. You can check what type of archetype your current version of iraf uses by typing the below into an open session of iraf:

```
cl> show arch
.ssun
```

II) I ended up downloading 3 things in total, though I'm not sure if you need all three or not. I downloaded the following:

```
ftp://iraf.noao.edu/iraf/extern/mscdb/mscdb.tar.Z
ftp://iraf.noao.edu/iraf/extern/mscred/mscred.tar.Z
ftp://iraf.noao.edu/iraf/extern/mscred/mscred-bin.redhat.tgz
```

III) within the first /iraf mentioned above, create these directories:

```
mkdir -p /iraf/extern/mscred
mkdir /iraf/extern/mscdb
```

IV) place both the mscred.tar.Z & mscred-bin.redhat.tgz in the newly created mscred folder and:

```
tar -zxvf mscred.tar.Z
tar -zxvf mscred-bin.redhat.tgz
```

V) place the mscdb.tar.Z into the newly created mscdb folder and:

```
tar -zxvf mscdb.tar.Z
```

VI) Now go to hlib in local and edit extern.pkg:

```
cd $hlib
vi extern.pkg
```

extern.pkg should include the following:

```
reset  mscred      = /iraf/extern/mscred/
reset  mscdb       = /iraf/extern/mscdb/
task   mscred.pkg  = mscred$mscred.cl
```

Near the end of the hlib\$extern.pkg file, update the definition of helpdb so it includes the mscred help database, copying the syntax already used in the string. Add this line before the line containing a closing quote:

```
    ,mscred$hlib/helpdb.mip\
```

I think everything should work by now - assuming I've remembered all the steps I've done. Feel free to delete the .tgz and .tar.Z files after you've untarred them.

VI) Now go to the directory which contains the multi-extension fits files you will be working with, and do a mkiraf  
mkiraf

Then start up iraf and try to load the package we just installed to test if everything worked:

```
cl
```

```
cl> mscred
```

It worked if you received no error messages.

Now, the steps of image reduction are much the same as Exercise 2. Following along in Exercise 2, this tutorial will point out the different commands or extra actions needed for each step.

1) only load the mscred package

```
cl> mscred
```

Notice all of the tasks it loads. Many should look familiar - e.g. ccdproc, darkcombine, flatcombine, zerocombine. These tasks all do the same as we would expect from our previous use of them, they have just been modified a bit to deal with MEF fits files.

a) For these commands, we have to specify which extension of the fits file we want the information about. Usually it doesn't really matter which, though sometimes the 0th extension has more general header information about the whole image. In this case, the commands would look like:

```
cl> imhead *fits[0]
```

```
cl> hselect *fits[0] $!,object,filter,exptime yes
```

Notice when you examine the obslog made this way, the names of the images all will have the "[0]" after them. This will offer some complications later. To avoid this, one can make lists of images without the "[0]" using the sed command when creating lists:

```
cl> !grep Bias obslog | awk '{print $1}' | sed 's/s\[0\]/s/g' > listBias
```

```
cl> !grep 06E obslog | awk '{print $1}' | sed 's/s\[0\]/s/g' > list2006E
```

etc...

Here, the sed command takes the string 's[0]' and replaces it with 's'.

We'll also make some lists for creating bad pixel masks, e.g.:

```
cl> !more listBias | sed s/.fits/_bpm/ > listBiasMasks
```

```
cl> !more listObject | sed s/.fits/_bpm/ > listObjectMasks
```

```
cl> !more listFlat | sed s/.fits/_bpm/ > listFlatMasks
```

b) Since we've made separate lists of the different image types, we won't bother to edit the IMAGETYP in our image headers. When we call our tasks, we'll leave the "ccdtype" spot blank, or in our command line, we can say ccdtype- to tell the task not to look for a certain type of image by keyword. The task will just trust that we've put the appropriate images in the list we give it. Just be sure your lists are trustworthy - check them to make sure the images you think are in there actually are.

When visually examining your images, you'll need a special command to display these MEF images correctly. To see just a single extension image from IRAF, you can use the "display" command as long as you specify the extension # in square brackets at the end of the image name:

```
cl> display obj104.fits[2]
```

To see all extensions fitted together in one image, use the MEF specific command:

```
cl> msdisplay obj104.fits
```

You can also manually open your MEF image through ds9 by going into file -> open other -> open Mosaic IRAF and then choosing the desired image. Sometime this is the best way to do it, since IRAF sometimes limits the display settings.

If you want to perform tasks like measure a radial profile or find the centroid of an object, you would normally use the iraf task "imexam" however with MEF images, you can perform these same things with "mscexam". All the commands are the same.

2) Now we'll use the mscred version of the ccdproc task which doesn't want a list of images with extensions at the end, so we'll use the list we created without the "[0]".

a) You can go in and edit the options with

```
cl> epar ccdproc
PACKAGE = mscred
TASK = ccdproc
```

```
images =      @listBias) List of Mosaic CCD images to process
(output =      ) List of output processed images
(bpmasks=    @listBiasMasks) List of output bad pixel masks
(ccdtype=     ) CCD image type to process
(noproc =     no) List processing steps only?
(xtalkco=     yes) Apply crosstalk correction?
(fixpix =     yes) Apply bad pixel mask correction?
(oversca=     yes) Apply overscan strip correction?
(trim =       yes) Trim the image?
(zeroacor=    no) Apply zero level correction?
(darkcor=     no) Apply dark count correction?
(flatcor=     no) Apply flat field correction?
(sflatco=     no) Apply sky flat field correction?
(split =      no) Use split images during processing?
(merge =      no) Merge amplifiers from same CCD?

(xtalkfi=     xtalk0303) Crosstalk file
(fixfile=     BPM) List of bad pixel masks
(saturat=     !SATURATE) Saturated pixel threshold
(sgrow =      1) Saturated pixel grow radius
(bleed =      20000.) Bleed pixel threshold
(btrail =     15) Bleed trail minimum length
(bgrow =      1) Bleed pixel grow radius
(biassec=     image) Overscan strip image section
(trimsec=     image) Trim data section
(zero =       ) List of zero level calibration images
(dark =       ) List of dark count calibration images
(flat =       ) List of flat field images
```



```

(sflat =          ) List of secondary flat field images
(minrepl=        1.) Minimum flat field value
(interac=        no) Fit overscan interactively?
(funcio=         minmax) Fitting function
(order =         1) Number of polynomial terms or spline piece
(sample =        *) Sample points to fit
(naverag=       1) Number of sample points to combine
(niterat=       1) Number of rejection iterations
(low_rej=       3.) Low sigma rejection factor
(high_re=       3.) High sigma rejection factor
(grow =         0.) Rejection growing radius
(fd =           )
(fd2 =          )
(mode =         ql)

```

or you can put all the important parts in a one-line command:

```

cl> ccdproc @listBias ccdtype- xtalkco+ fixpix+ oversca+ trim+ merge- zerocor- darkcor- flatcor-
bpmasks=listBiasMasks fixfile=badpix_mosaic2 biassec=image trimsec=image xtalkfi=xtalk0303
saturat=!SATURATE sgrow=1 bleed=20000. btrail=15 bgrow=1
etc...

```

Here, I've specified files and header keywords that are used for MOSAIC-1 images. Your files/ keyword names may be different. You may need to supply the crosstalk file and badpixel file. For MOSAIC images they can be found here: <http://www.noao.edu/noao/mosaic/calibs.html>

#### **A note on Bad Pixel Masks:**

Bad Pixels can be "bad" in multiple ways:

- i) For a certain ccd, pixels can be non-responsive or unpredictably responsive to the photons that hit them. A list of them are usually provided at the telescope - e.g. for the newest version of MOSAIC it can be found here: <http://www.noao.edu/noao/mosaic/calibs.html> .
- ii) For a given image, pixels can be saturated (this is where a single pixel has been hit by so many photons that the value for that pixel will not increase - no matter how many more photons hit it) or they can contain bleed trails (this is where extra charge from those saturated pixels bleeds over into neighboring pixels creating spikes in the positive and negative x and y directions).

\*) For saturated pixels, we specify either a numeric value or a header keyword (e.g. "saturat=!SATURATE" for MOSAIC) that tells "ccdproc" that pixel with a value equal to or larger than that number is saturated and not to be trusted. Here I've set sgrow=1 which means that pixels which are 1 within 1 pixel of the saturated pixel will also be flagged as "bad" pixels.

\*\*) For bleed trail pixels, we will similarly use a minimum threshold. Any pixel of value greater than the number specified by the "bleed" parameter is eligible to be tagged as a bleed trail pixel (another kind of bad pixel). It must also be physically in line with at least "btrail" other pixels who also have a value greater than "bleed". "btrail" is a parameter specifying that number of pixels that must be present in a column in order for them to be flagged as bleed trail pixels. The parameter "bgrow" is analogous to "sgrow".

If you specify a list of output names (as we have by pointing to our list, e.g.: "bpmasks = listBiasMasks"), subdirectories will be created with these names, each containing generated

multiple bad pixel masks (one for each CCD), named bpm\_im\*.pl, where \*=1-8. These masks would have whatever bad pixel mask is provided by the keyword BPM plus all the pixels determined to be saturated or bleed trails. Thus during the process, all these pixels will have their values replaced with an average for those around them

b) Zerocombine will be the same as before:

```
cl> zerocombine @listBias output=Zero combine=median reject=reject ccdtype= process-
delete- rdnoise=RDNOISE gain=GAIN
```

c) Then we do ccdproc again, but this time only zero-subtracting - e.g.:

```
cl> ccdproc @listFlat ccdtype= xtalkco- fixpix- oversca- trim- merge- zerocor+ darkcor- flatcor-
zero=Zero.fits saturat=SATURATE
etc....
```

d)&e) Then, similarly for the master Darks, and dark correction with ccdproc, keeping in mind one needs to match up exposure times.

f) And then again for the flats, but by filter.

```
cl> flatcombine @listFlat output=Flat combine=average reject=avsigclip ccdtype= process-
delete- rdnoise=RDNOISE gain=GAIN
```

If you set "subsets = yes" then it will automatically combine by filter so you don't have to make lists individually for each band.

Once you've made the flats, there is sometimes an extra step that is necessary depending on the instrument you're using and your scientific goals. If you're using MOSAIC images, then the U, B, and I filter images will have a pupil ghost - this is light that reflects off of the filters, off the back surface of the corrector, and returns through the filters to your science detectors. It appears as additional light that looks like an image of the telescope pupil. To remove this and fringing, you can follow the steps detailed here: <http://www.noao.edu/noao/noaodeep/ReductionOpt/frames.html>

For MOSAIC, as long as we have done a good job of placing our SN and field stars well away from the center of the ccds, we do not need to do this.

g) Run ccdproc for flat fielding images by filter.

3) a) Before stacking your images into one image, it might be prudent to trim off some the unnecessary parts of the image. If we feel that we have enough field stars and the supernova centered up on one ccd, we can split apart the image and leave the others behind.

```
cl> mscsplit @listObject
```

Now remove the unwanted images

```
cl> !rm obj100_0.fits obj100_1.fits obj100_3.fits etc...
```

You can even do something like the following to keep only the extension you need (number 7 in the following example). You may also want to keep the 0th extension which contains all the header information too.

```

cl> !ls 11011*_fits | grep -v 7 | grep -v 0 | awk '{print "rm",$1}' > do_rm
cl> !chmod a+x do_rm
cl> !./do_rm

```

b) Before we combine our images, we need to assign a world coordinate system (WCS) to each image. Most likely a WCS was assigned at the telescope, but chances are good that it is not accurate enough to be able to find stars and align our images. Luckily it is not difficult to improve.

We will use the mscrd task "mscsmatch". It needs a list of accurate object coordinates (this would be the actual RA & Dec of stars). This would be tedious for us to write, but luckily there is another task called "mscgetcatalog" that will pull up a catalog and grab the coordinates of stars. Here is an epar of mscgetcatalog that will use an optical catalog: usnob1@noao.

```

      I R A F
      Image Reduction and Analysis Facility
PACKAGE = mscrd
  TASK = mscgetcatalog

input =           List of Mosaic files
output =          Output file of sources
(magmin =           9.) Minimum magnitude
(magmax =           17.5) Maximum magnitude
(catalog=           usnob1@noao) Catalog
(rmin =            21.) Minimum radius (arcmin)
(mode =            ql)

```

You can use the task "mscsmatch" to call "mscgetcatalog" and it will use that list of object coordinates to try to match up with the objects it finds in your image. It will then calculate the necessary offsets and rotation of the coordinate system to correctly assign a WCS to your image, and then it will do so. Here's an epar of mscsmatch

```

                                I R A F
                                Image Reduction and Analysis Facility
PACKAGE = mscrd
TASK = mscmatch
input = 2009ig_110110_B.fits List of input mosaic exposures
coords = !mscgetcat $I $C Coordinate file (ra/dec)
(outcoor= coordlist_09ig_110110B) List of updated coordinate files
(usebpm = no) Use bad pixel masks?
(verbose= yes) Verbose?

# Coarse Search
(nsearch= 60) Maximum number of positions to use in search
(search = 60.) Translation search radius (arcsec)
(rsearch= 0.2) Rotation search radius (deg)

# Fine Centroiding
(cbox = 11) Centering box (pixels)
(maxshif= 5.) Maximum centering shift to accept (arcsec)
(csig = 0.1) Maximum centering uncertainty to accept (arcsec)
(cfrac = 0.5) Minimum fraction of accepted centers
(listcoo= yes) List centered coordinates in verbose mode?

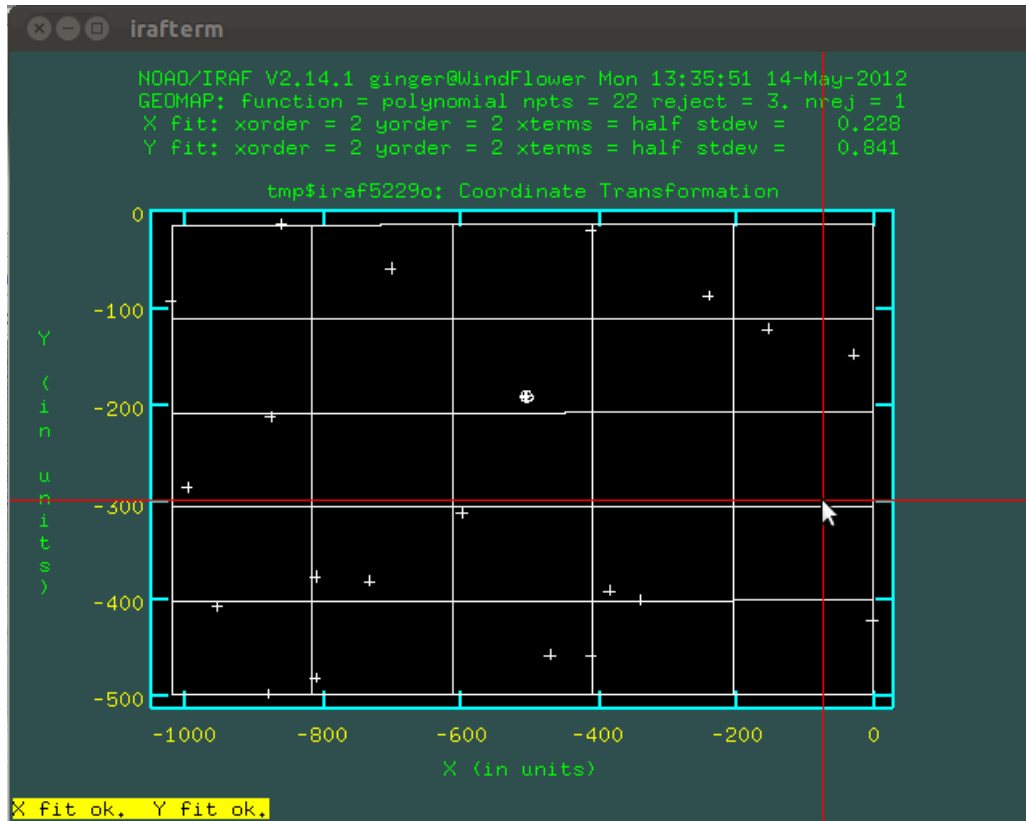
# MCS Fitting
(nfit = 4) Min for fit (>0) or max not found (<=0)
(rms = 2.) Maximum fit RMS to accept (arcsec)
(fitgeom= general) Fitting geometry
(reject = 3.) Fitting rejection limit (sigma)
(update = yes) Update coordinate systems?
(interac= yes) Interactive?
(fit = yes) Interactive fitting?
(graphic= stdgraph) Graphics device
(cursor = ) Graphics cursor

accept = yes Accept solution?
(mode = ql)

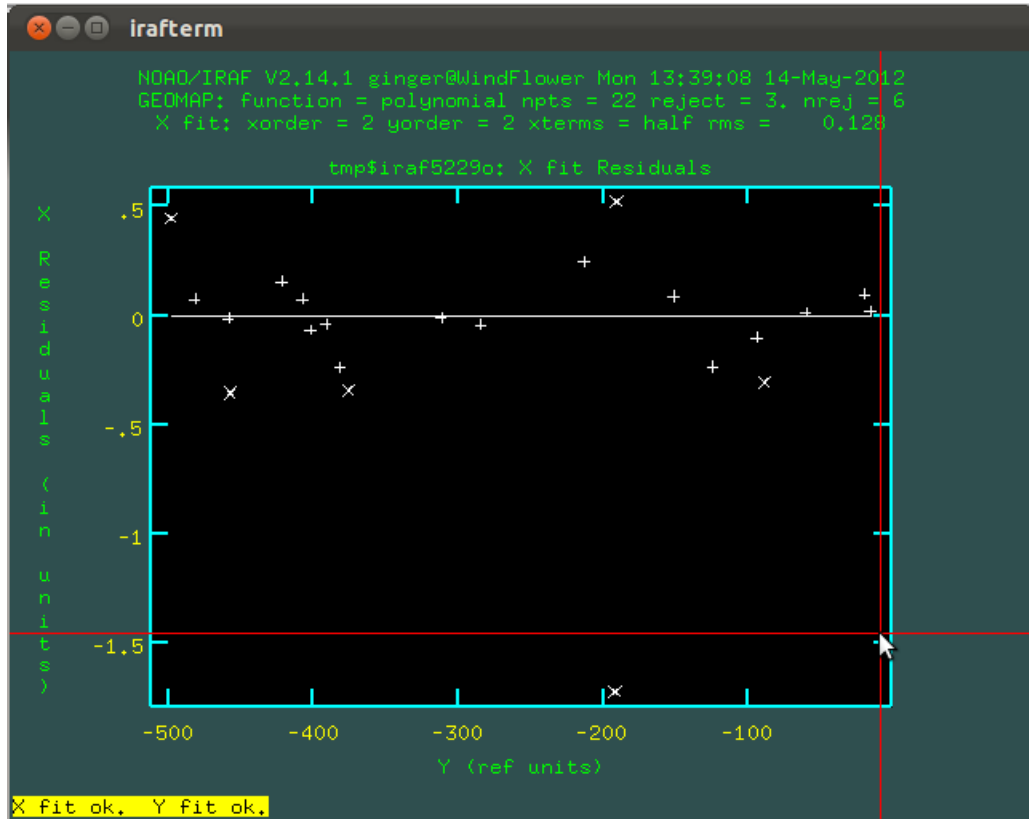
```

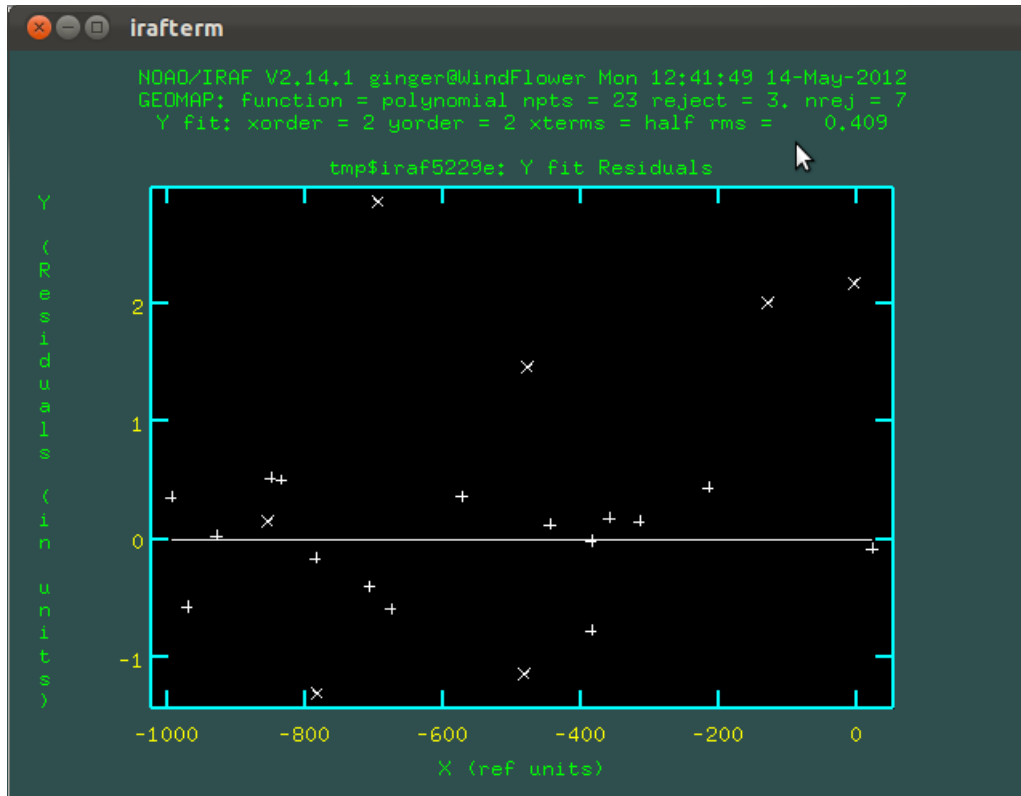
The line that reads "!mscgetcat \$I \$C" is calling the task mscgetcatalog - fancy, eh?

"mscmatch" will show you the best fit for the the WCS to your image, plotting the objects it has found as plus signs.



You can look at the residuals to the fit by typing "x" and "y". Delete the points that are far away from the fit by hovering over a plus sign and typing "d". Always follow this up with "r", and "f" for re-plot, and recalculate-the-fit respectively. I would start with deleting the farthest point away vertically from the center of the group (especially if it is obviously off by itself) and keep going until all points are at least between 1 and -1, paying attention to how each deletion affects the new fit. You can un-delete a point by typing "u" with your cursor over that point (don't forget to re-fit/re-plot).





When you are satisfied, type "q", and then, in the terminal, type yes to accept the solution. It may give you a warning like "Warning: Cannot open file (!mscgetcat\$!\$C)" and claim that "ERROR: MSCCMATCH failed for 2009ig\_110110\_B.fits" But it seems to work just fine. Your image should have a WCS on it. You can test it by opening your image, then use the Analysis -> Catalogs -> to pull up an optical catalog. Did it accurately circle objects in your field?

c) Now we have to take our MEF fits and merge it into one image using the task "mscimage" It is fairly straightforward - just give it the name of the MEF image and the name you want for the output single-extension-fits image, e.g.:  
`c> mscimage 2009ig_110110_B.fits comb09ig_110110B.fits`  
 Tada! In fact, you can also give it a list of input images and a list of output image names.

d) We also need to calculate the scaling for each image going into the final image. We do that using the task "mscimatch". First, run mscgetcatalog to get a list of sources:

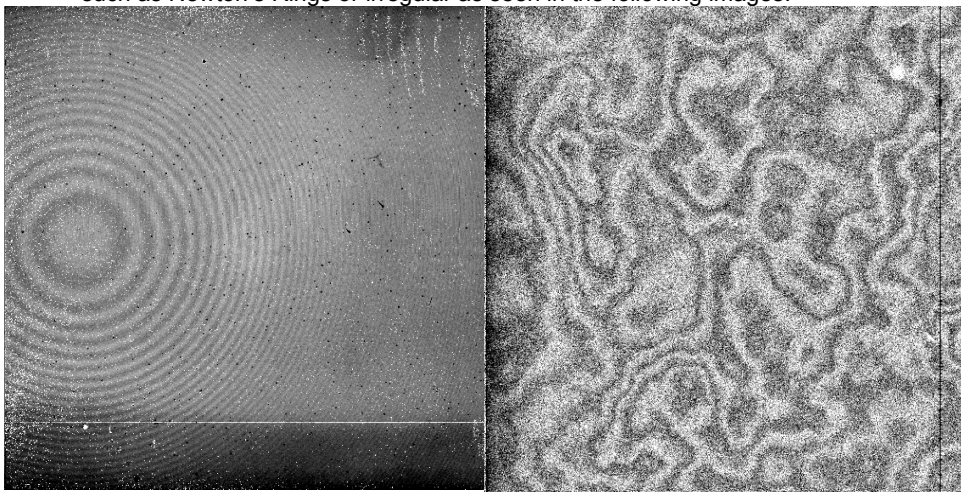
### A.3 NIR Image Reduction



## NIR Reduction

By: Ginger Bryngelson

0. Install the IRAF external package "xdimsum"
1. Do initial corrections just like in the general image reduction tutorial, including: fix bad pixels, overscan correct, trim, bias subtract, dark subtract, and flat correct. If you do not have bias images or dark images, don't worry too much, as this will be corrected in the next step.
2. Fringe correct your image. Likely your image will have fringing - light interference patterns from the optics of your telescope instrument set-up. Fringing can be regular such as Newton's Rings or irregular as seen in the following images:



We'd like to remove this extra signal which is usually sitting on top of our science field. To do this, we will take advantage of the fact that NIR observations are usually taken as dithers. This is where the telescope is moved in between each exposure. Thus a particular star is on a different part of the CCD from image to image. Likewise, in a string of images, a pixel may alternately reflect stellar signal and background noise. However, from image to image, there will still be the same amount of fringe signal on each pixel. Thus, if we combine a collection of images of the same object in the same filter choosing the keep only the median pixel value, the result should be only the fringe. So, let's do that using the IRAF task *imcombine*, e.g.

```
cl> imcombine @list09nrH fringe09nrH combine=median reject=minmax
```

Check out the image *fringe09nrH*. It should look like the above.

Now, if you see any bright areas that look suspiciously like stars or a galaxy, that may mean the dithering did not use a large enough offset, and there were multiple images in a row where a pixel experienced stellar or galactic signal. Those areas of pixels will have a much larger value of counts than just fringing. When we fringe correct, we want to use an image of only the fringing - we don't want to cut out any star or galaxy counts. We can cut out the non-fringe areas by excluding the very high (and very low) count pixels from our fringe template. We will create a pixel mask using "ccdmask" as such:

```
cl> ccdmask fringe09nrH.fits fringemask09nrH ncsig=40 lsigma=5 hsigma=5
```

Check out your mask in a ds9 section, by typing in your iraf section:

```
cl> display fringemask09nrH 1
```

You should see some darker areas and light areas. See if you can tell which are the pixels we are masking (dark or light?).

Next, we'll correct those pixels in our fringe template. *fixpix* will take the mask of "bad pixels" and replace those specified pixels with the value of pixels that are nearby.

```
cl> fixpix fringe09nrH.fits fringemask09nrH
```

Hopefully now when you look at `fringe09nrH.fits` again, you'll see a more smooth fringe image.

Now, we want to fix the fringing, and we'll use the *mscred* task *rmfringe*.

```
cl> rmfringe @list09nrH fringe=fringe09nrH.fits fringem=fringemask09nrH.pl
```

Go through and look at your images. Does it look like they have any fringe left?

3. Make a dummy bad pixel image. The last steps of NIR reduction require a bad pixel file in a certain format in order to work. Namely, it should be the same size as each of your images, and each pixel should have a value of either 1 or 0 - 1 meaning a good pixel, and 0 meaning a bad pixel. You may have a bad pixel file already in this format, but even if you do, you've already done bad pixel correction in the first step, so it won't hurt to go ahead and use a dummy file. Using the task *imarith*, I copy any image from the night I'm working on, and manipulate it to get an image entirely of pixels of value 1 (signifying that every pixel is a "good" pixel).

```
cl> imarith SN2009nr.0034.fits * 0 blah.pl
```

```
cl> imarith blah.pl + 1 fakebadpixel.fits
```

Check it out, does `fakebadpixel.fits` have all 1's?

4. Subtract the sky from each image and combine.

The next step actually rolls a large number of steps into one IRAF task: *xmosaic*. This task will first take all your dithered images of a certain object in a given filter, and combine them into one image to get a measure of the sky background level. This is similar to how we did get the fringe except it creates a sky image for every individual image. For each image, it looks at a number of images (like 8) nearby in the list, and combines only those. It will then try to find any outlier pixels (bad pixels and cosmic rays) in the background templates, and create masks for them. Then it will subtract the respective sky image from each individual science image. Then it will try to align all the stars and features in the images, though you will be involved heavily in this part. Once it thinks it knows the offsets for each image of the dither, it will combine the images according to those offsets, and show you the result. You then have to help it determine where all the objects are (stars and galaxies, etc) in this combined image by choosing a pixel value. Any pixel with a value above this is considered an object, and a mask will be made of these. Then *xmosaic* will calculate backward, based on the known offsets, where the objects are in the individual images. It will then recombine these images again - except for the pixels where the known objects are. This way it has an even better measure of the background level.

Look at an epar of *xmosaic*, and you'll notice a list of things you can choose to do or not.

**I R A F**

Image Reduction and Analysis Facility

```

PACKAGE = xdmsum,
TASK = xmosaic

inlist = @list09nrH The list of input images
referenc= SN2009nr_0001.fits The reference image in input image list
output = SN2009nrH Root name for output combined images
expmap = .exp Root name for output exposure map image or suffix

(fp_xslm= yes) Do the first pass sky subtraction step ?
(fp_mask= yes) Do first pass bad pixel correction step ?
(fp_xzap= yes) Do first pass cosmic ray correction step ?
(fp_badp= yes) Do first pass bad pixel mask update ?
(fp_mksh= yes) Determine first pass shifts interactively ?
(fp_xnre= yes) Do first pass image combining step ?

(np_mkma= yes) Create the combined image object mask ?
(np_mask= yes) Deregister masks ?
(np_xslm= yes) Do the mask pass sky subtraction step ?
(np_mask= yes) Do mask pass bad pixel correction step ?
(np_xzap= yes) Do mask pass cosmic ray correction step ?
(np_badp= yes) Do mask pass bad pixel mask update ?
(np_xnre= yes) Do mask pass image combining step ?

(statsec= ) The image section for computing sky stats
(nsigrej= 3.) The nsigma rejection for computing sky stats
(maxiter= 20) The maximum number of iterations fo computing sky stats

(sslist = .sub) The output sky-subtracted images or suffix
(hmasks = .hom) The output holes masks or suffix
(newxslm= no) Use new version of xslm ?
(forcesc= yes) Force recalculation of image medians ?
(nmean = 8) Number of images to use in sky image
(nreject= 1) Number of pixels for sky image minmax reject
(nskymin= 3) Minimum number of image to use for sky image
(cache = yes) Enable cacheing in new version of xslm ?
(np_useo= yes) Use object mask to compute sky statistics ?

(bpmask = fakebadpixel.fits) The input pixel mask image
(forcefi= no) Force bad pixel fixing ?

```

**More**

**ESC-?** for HELP

Here, we'll say yes to practically everything, and we'll point it to our fake bad pixel image. Notice I tell it not to force bad pixel fitting (there's no point since we're giving it a fake bad pixel file). The reference image is just the first image in the list of images you gave it.

In the second half of the parameters, we'll say yes to some interactive steps, and give it the name of a shifts file where it can print out the shifts once it calculates them. If everything runs smoothly the first time you run *xmosaic* you won't ever need them. But often something can go wrong, and it is nice to not have to calculate them again if that has already successfully been done.

```

(crmasks=      .crm) The output cosmic ray masks or suffix
(newxzap=      no) Use new version of xzap ?
(nrepeat=      3) Number of repeats for bad pixel status

(fp_chks=      yes) Check and confirm new shifts ?
(fp_crad=      5.) Centroiding radius in pixels for mkshifts
(fp_maxs=      5.) Maximum centroiding shift in pixels for mkshifts

(rmasks =      .rjm) The output rejection masks or suffix
(mp_npre=      0) Number of previous object masks to combine
(mp_blkrc=     yes) Use block replication to magnify the image ?
(mp_mag =      4.) Magnification factor for mask pass output image
(shiftli=      shiftslist09nrH) Input or output shifts file
(section=      .corners) The output sections file or suffix
(fractio=      no) Use fractional pixel shifts if mag = 1 ?
(pixin =      yes) Are input coords in ref object pixels ?
(ab_sens=      yes) Is A through B counterclockwise ?
(xscale =      1.) X pixels per A coordinate unit
(yscale =      1.) Y pixels per B coordinate unit
(a2x_ang=      0.) Angle in degrees from A CCW to X
(ncoavg =      1) Number of internal coaverages per frame
(secpexp=      1.) Seconds per unit exposure time
(y2n_ang=      0.) Angle in degrees from Y to N N through E
(rotatio=      yes) Is N through E counterclockwise?

(omask =      .msk) The output combined image mask or suffix
(mp_chkm=      yes) Check the object masks ?
(mp_kpch=      yes) Keep checking the object masks ?
(mp_stat=      ) The combined image section for computing mask stats
(mp_nsig=      1.5) The nthreshold factor for cosmic ray masking
(mp_nsig=      1.1) The nthreshold factor for object masking
(mp_negt=      no) Set negative object masking threshold ?
(mp_ngro=      0) Object region growing radius in pixels

(ocrmask=     .ocm) The output cosmic ray unzapping masks or suffix
(objmask=     .obm) The output object masks or suffix
(del biq=     no) Delete combined image masks at task termination ?
(del_sma=     no) Delete the individual object masks at task termination ?

(mode =      ql)

```

Before you execute this, make sure a ds9 image is open. It won't need you for a while. You'll see updates to the screen about each step on each image. The first interactive thing that will require your attention will be determining shifts. An image will appear in your ds9 window (the first image in the list you gave it), and instructions will appear in the iraf terminal. You will basically be clicking on the same star in each of the images. The first thing *xmosaic* wants you to do is pick out a star that has a good signal and go through each image to make sure it stays within the field of view and is never saturated. Use the commands detailed in the iraf terminal. In the ds9 window, type "n" and "p" to go to the next or previous image. When you have decided on your star, type "q" to go to the next part. Now *xmosaic* wants you to give it the coords of that star in each image. Do this by going to ds9 and hovering over the center of the star and typing "a". Then hit "n" to go to the next image. Repeat until you get back to the first image - you'll have to keep an eye out for it because iraf doesn't automatically quit. Once you've done this for each image, type "q" and it will let you do the next part. Now *xmosaic* wants you to click on that same star and a number of other non-saturated, reasonably bright stars in **only the first image**. Type "q" when done.

*xmosaic* will dump you out into a vi session where you can see the coordinates you reported for each image. If you know you made a mistake somewhere, you can edit it out. When done, quit with a ":wq". If all went well, *xmosaic* will have calculated the appropriate offset for each image,

and will show you another vi session of all of these. Quit with another “:wq”, and *xmosaic* will continue on to the next task.

You will be needed again when it comes time to determine the object mask. *xmosaic* will show you the combined image in ds9, and let you play around with an *imexam* session. You can use all manner of things commands to determine a good pixel value for objects. Any pixels with a value equal or higher to this will be classified as having star or galaxy signal. Once you think you have a good idea for the value, quit out of *imexam* with a “q”, and *xmosaic* will show you a suggested object level. Your number will probably be close to this. I’ve found the suggestion is usually pretty good, though I usually choose a number slightly less than the suggestion. Type in your chosen level, and hit enter. After thinking a bit, *xmosaic* will show you the calculated mask. Compare this to the combined image, and you should see everything that you thought was an object blocked out in the mask. If not, pick a different value. Tell *xmosaic* if you want to try again or not.

When you’ve told *xmosaic* that you’re satisfied, it will continue on to do the rest of its tasks. It will deregister the object mask based on the offsets previously calculated to match each individual image. Next it will make new sky background images again by combining pixels of adjacent images - ignoring the values where the object mask tells it to. Afterwards it look for more badpixels and cosmic ray hits to throw out. Then it subtracts the new sky images from the respective original science images, and combines each of those into one final image. When all is finished, you will have a number of badpixel masks (“.pl” files), a sky image, and sky-subtracted image for each image. You also have a “.fp.fits” image which is the first pass combined image - the one you saw when determining the object level - and a “mp.fits” which is the mask pass (and final) combined image. Additionally there will be “.exp.fits” image that shows you how many images (or exposures) contributed to each part of your final image. Likely the middle part of your image is where your images overlapped the most.

Hopefully it all went smoothly, but it’s more likely that something went wrong. If anything does go wrong and *xmosaic* quits somewhere in the middle of its work. If you know what you already accomplished, you can *epar xmosaic* and tell it not to do the stuff it already did. Depending on when it stopped, this may or may not work. If it doesn’t, you can try deleting any “tmp\*” files and “\_\*” files and trying it again. If it still doesn’t work, then I suggest you rerun it from the beginning again, with perhaps one change - if you have already successfully done the calculating of offsets, and it successfully saved to the filename you specified in the parameter file, then set “fp\_mksh” to “no”, and you shouldn’t have to do that part again.

Compare your individual images to the original images and to your final image - it’s amazing how much signal is uncovered after getting rid of the sky background!

## A.4 Photometry

## Photometry

1. For each field, there will be a number of stars whose instrumental magnitude you need to measure. In a field of standard stars, you will measure the instrumental magnitude of those stars with known apparent magnitude. Also, you'll measure the interesting star/SN of unknown magnitude. Additionally, one might want to calibrate multiple other stars (local standard stars) in the science image. As you are choosing which stars to use as local standards, make sure that for each night you pick a number of stars that can be seen in each band, and not saturated in any bands. You can check for saturation using ds9 to open an image of the field, and using the IRAF task, "imexamine" in the images.tv packages. Simply hover your mouse (the cursor should be a blinking donut) over the star of interest and type "s" or "r".

It will be helpful to have a region file you can pull up on your images when you do photometry. This will be an overlay that helps you keep track of which star is which:

- a. Open an image of the field in ds9. As accurately as possible (you may want to zoom in), click on each star whose coordinates you want. A green circle should appear around them as you click. If you accidentally click somewhere you didn't want, just delete the green circle by selecting it and hitting "delete." If you double click on the green circle, you can add a label. Use this to number or name your standard stars. Be sure to also include your object of unknown magnitude (the SN). If you are calibrating local stars, it's good to have something like 30 - the more (non-saturated) stars the better of a range of magnitudes.
  - b. Now, in the "Region" pull down menu at the top, choose "Save Region". In the bottom line of the window that opens, choose what to call this list of coordinates. The default suffix is ".reg", which, if kept, will enable you to load your regions onto any image. (Note: If your images have an accurate WCS, you might want to choose to format your regions file as "WCS" instead of "image" or "physical". This will make it work on any of your images that have accurate WCS)
  - c. I suggest you try loading these regions onto your other images of the same field to make sure they still match up well with the stars. Otherwise you may want to make region files for each image/night, or align and crop your images so that the coordinates work for each image of that field. Often you may have a different region file for each night.
  - d. Repeat these steps for each field (SN field and standard fields if calibrating your field - only science field if doing relative photometry).
2. Make a file called "imsets" which is a list of the images you want to do photometry with or on. This includes both the object fields and the standard fields. Usually you have a different imsets file for each night. Be careful, this file needs to be in a specific format. Below is an example of a file called imsets:

```

field      B      V      R      I
sn06D : sn06D_mar23_B.fits sn06D_mar23_V.fits sn06D_mar23_R.fits sn06D_mar23_I.fits
stdA : StdA_mar23_B.fits StdA_mar23_V.fits StdA_mar23_R.fits StdA_mar23_I.fits
stdB : StdB_mar23_B.fits StdB_mar23_V.fits StdB_mar23_R.fits StdB_mar23_I.fits
~
~
~
~
~
~
~
"imsets" 4L, 259C

```

Notice that there are only single spaces in between each name, and before and after the ":". The "sn06D", "stdA", and "stdB" indicate what field each of the images is of. (i.e. the first four images are of the sn field, while the next four are images of our first field of standard stars, and the last four are images of the second field of standard stars). If you are doing relative photometry, you will only need the one science field (in this case sn06D)

- Now, in iraf (via packages: noao.digiphot.photcal) one needs to do "mkcatalog". I call the output file "stds." This is a list of the standard stars located in each field and their known apparent magnitudes in each band you've observed. It's ok to put in extra information (i.e. magnitudes in bands you haven't observed), because later you'll specify exactly which information you need. If you have several standard star fields, go ahead and include the stars from each one in this file. It is tedious to make the catalog file this way, but I have tried to outsmart it before, and have never succeeded. It's best to do it this way so that it is in the exact format iraf likes.

The mkcatalog script will first prompt you for what you want to call each column and how wide you want each column. Many times it will suggest the title with the phrase, "<CR>=ID" and if you like that name, just hit "return" to accept. Generally 10 or 15 characters is plenty of space for each column. When you're done entering the titles, and specifying widths, hit "ctrl+d" which is what iraf means by "<EOF>=quit entry". Here's an example of this first part:

```

photcal> mkcatalog
The name of the output catalog (stds):

Enter the id column name (name, <CR>=ID, <EOF>=quit entry):
  Enter width of id column (width, <CR>=15):
Enter a name for column 2 (name, <CR>=COL2, <EOF>=quit entry): V
  Enter width of column 2 (width, <CR>=10):
Enter a name for error column 3 (name, <CR>=error(V), <->=skip):
  Enter width of column 3 (width, <CR>=10):
Enter a name for column 4 (name, <CR>=COL4, <EOF>=quit entry): B
  Enter width of column 4 (width, <CR>=10):
Enter a name for error column 5 (name, <CR>=error(B), <->=skip):
  Enter width of column 5 (width, <CR>=10):
Enter a name for column 6 (name, <CR>=COL6, <EOF>=quit entry): R
  Enter width of column 6 (width, <CR>=10):
Enter a name for error column 7 (name, <CR>=error(R), <->=skip):
  Enter width of column 7 (width, <CR>=10):
Enter a name for column 8 (name, <CR>=COL8, <EOF>=quit entry): I
  Enter width of column 8 (width, <CR>=10):
Enter a name for error column 9 (name, <CR>=error(I), <->=skip):
  Enter width of column 9 (width, <CR>=10):
Enter a name for column 10 (name, <CR>=COL10, <EOF>=quit entry): ^D

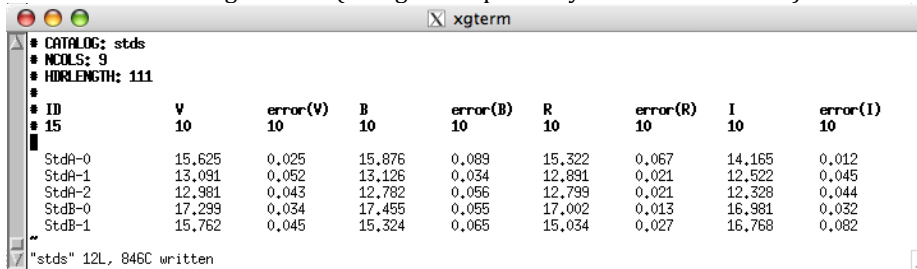
```

Now, finally, you must specify the values you want to put in. The "ID" values will be the similar to the field id's you used in the "imsets" files,



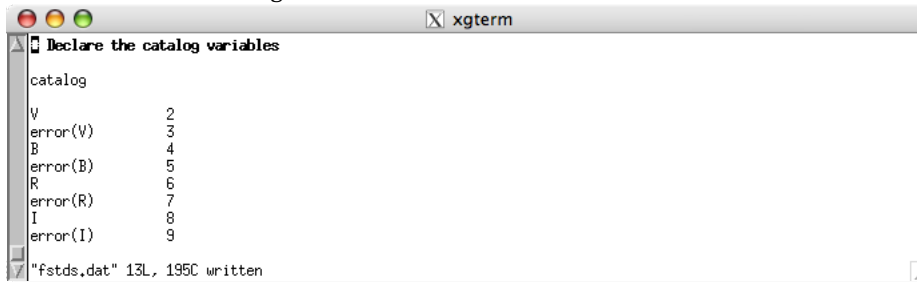
except they will also include a label for each star.

If you happen to make a mistake while entering data, don't worry. After you tell it you're finished ("ctrl+d") it will spit you out into a vi session of your file, "stds", so that you can fix anything you might need to. When you need to quit, use ":q". The finished product should look something like this (though with probably more rows of stars):



```
CATALOG: stds
# NCOLS: 9
# ROWLENGTH: 111
#
# ID      V      error(V)  B      error(B)  R      error(R)  I      error(I)
# 15      10      10        10      10        10      10        10      10
StdA-0    15.625  0.025    15.876  0.089    15.322  0.067    14.165  0.012
StdA-1    13.091  0.052    13.126  0.034    12.891  0.021    12.522  0.045
StdA-2    12.981  0.043    12.782  0.056    12.799  0.021    12.328  0.044
StdB-0    17.299  0.034    17.455  0.055    17.002  0.013    16.981  0.032
StdB-1    15.762  0.045    15.324  0.065    15.034  0.027    16.768  0.082
..
"stds" 12L, 846C written
```

"mkcatalog" will also create a file called "fstds.dat":



```
Declare the catalog variables
catalog
V          2
error(V)  3
B          4
error(B)  5
R          6
error(R)  7
I          8
error(I)  9
"fstds.dat" 13L, 195C written
```

which records what columns the appropriate information is on.

Note: If you know apparent magnitudes in terms of V,B-V, V-R, etc., or some variation thereof, you may enter this information into mkcatalog instead, but your column names will be different, and certain steps will be different when we do "mkconfig" (step 6).

4. Next, we will do "phot" (which is located in "noao.digiphot.apphot") on each set of images including standard star field images. This calculates *instrumental* magnitudes. Before we use "phot," there are several parameters we need to specify to make sure photometry is done correctly. These parameters can either be specified explicitly, or you can point to the appropriate image header keyword. We will do the latter. Do an "epar datapars" to edit the file so that the parameters with "image header keyword" in the description reflect the appropriate header values. You may have to examine the header of the image to confirm the names of the values. In some cases you may have to use the "hedit" task to add the appropriate header keywords.

```

xgterm
IRAF
Image Reduction and Analysis Facility
PACKAGE = apphot
TASK = datapars

(scale =          1.) Image scale in units per pixel
(fwhmpsf=        2.5) FWHM of the PSF in scale units
(emissio=        yes) Features are positive ?
(sigma =         INDEF) Standard deviation of background in counts
(datanin=        INDEF) Minimum good data value
(datanax=        INDEF) Maximum good data value
(noise =         poisson) Noise model
(ccdread=        RDNNOISE) CCD readout noise image header keyword
(gain =          GAIN) CCD gain image header keyword
(readnoi=        0.) CCD readout noise in electrons
(epadu =         1.) Gain in electrons per count
(exposur=        EXPTIME) Exposure time image header keyword
(airmass=        AIRMASS) Airmass image header keyword
(filter =        FILTER) Filter image header keyword
(obstime=        TIME_OBS) Time of observation image header keyword
(itime =         1.) Exposure time
(xairmas=        INDEF) Airmass
(ifilter=        INDEF) Filter
(otime =         INDEF) Time of observation
(mode =         ql)

```

**ESC-Q** for HELP  We will

also edit the “centerpars” parameter file. Here, the most important parameter is “maxshif” which tells the phot task how much leeway it has to find the center of the star when you give it coordinates. A good value is 3 pixels. The default values are probably fine for the rest.

```

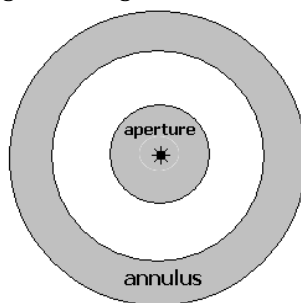
xgterm
IRAF
Image Reduction and Analysis Facility
PACKAGE = apphot
TASK = centerpars

(calgori=        centroid) Centering algorithm
(cbox =          5.) Centering box width in scale units
(cthresh=        0.) Centering threshold in sigma above background
(minsnra=        1.) Minimum signal-to-noise ratio for centering algorithm
(cmaxite=        10) Maximum number of iterations for centering algorithm
(maxshif=        3.) Maximum center shift in scale units
(clean =         no) Symmetry clean before centering ?
(rclean =        1.) Cleaning radius in scale units
(rclip =         2.) Clipping radius in scale units
(kclean =        3.) Rejection limit in sigma
(mkcente=        no) Mark the computed center on display ?
(mode =         ql)

```

The next

3 parameters we will edit determine the size of the aperture and annulus that measure the star and background brightness.



You may want to look carefully at the stars in your image (using ds9 and "imexam") to determine how large the aperture and annulus should be. Edit the parameter file "photpars" with an epar. The parameter "aperture" refers to the radius (in pixels) of the aperture.

```

xgterm
IRAF
Image Reduction and Analysis Facility
PACKAGE = apphot
TASK = photpars

(weight= constant) Photometric weighting scheme for wphot
(aperture= 5.) List of aperture radii in scale units
(zmag = 25.) Zero point of magnitude scale
(mkapert= no) Draw apertures on the display
(mode = ql)
  
```

Now

edit "fitskypars" with an epar. The "annulus" parameter specifies how many pixels (radially) away from the centroid of the star the annulus should start. The "dannulus" is how wide the annulus should be.

```

xgterm
IRAF
Image Reduction and Analysis Facility
PACKAGE = apphot
TASK = fitskypars

(salgori= centroid) Sky fitting algorithm
(annulus= 10.) Inner radius of sky annulus in scale units
(dannulu= 10.) Width of sky annulus in scale units
(skyvalu= 0.) User sky value
(smaxite= 10) Maximum number of sky fitting iterations
(sloclip= 0.) Lower clipping factor in percent
(shiclip= 0.) Upper clipping factor in percent
(snrejec= 50) Maximum number of sky fitting rejection iterations
(sloreje= 3.) Lower K-sigma rejection limit in sky sigma
(shireje= 3.) Upper K-sigma rejection limit in sky sigma
(khist = 3.) Half width of histogram in sky sigma
(binsize= 0,1) Binsize of histogram in sky sigma
(smooth = no) Boxcar smooth the histogram
(rgrow = 0.) Region growing radius in scale units
(mksky = no) Mark sky annuli on the display
(mode = ql)
  
```

Now we will edit the actual task, “phot”. Also, you may specify a file with a list of x,y coordinates for each star in a given field, but probably this won’t work. Our “.reg” file is not in the right format, so just leave the “coords” parameter blank unless you have made you own coordlist and have reason to think you can get iraf to accept it. Every time I’ve tried, IRAF has shut me down. Here’s an “lpar” of phot for an example:

```

xgterm
IRAF
Image Reduction and Analysis Facility

PACKAGE = apphot
TASK = phot

image =          @2006Dlist The input image(s)
skyfile =        The input sky file(s)
(coords = █      SN06D.reg) The input coordinate files(s) (default: image,coo,?)
(output =        default) The output photometry file(s) (default: image,mag,?)
(plotfil=        ) The output plots metacode file
(datapar=        ) Data dependent parameters
(centerp=        ) Centering parameters
(fitskyp=        ) Sky fitting parameters
(photpar=        ) Photometry parameters
(interac=        no) Interactive mode ?
(radplot=        no) Plot the radial profiles in interactive mode ?
(icomman=        ) Image cursor: [x y wcs] key [cmd]
(gcomman=        ) Graphics cursor: [x y wcs] key [cmd]
(wcsin =         )_wcsin) The input coordinate system (logical,tv,physical,world)
(wcsout =        )_wcsout) The output coordinate system (logical,tv,physical)
(cache =         )_cache) Cache the input image pixels in memory ?
(verify =        )_verify) Verify critical parameters in non-interactive mode ?
(update =        )_update) Update critical parameters in non-interactive mode ?
(verbose=        )_verbose) Print messages in non-interactive mode ?
(graphic=        )_graphics) Graphics device
(display=        )_display) Display device
(mode =         ql)

```

Unlike above, you will want to put “interac” to “yes”, open a ds9 with the image you are doing the photometry on, and then start phot. You will be able to specify each star directly on the image. Just hover your cursor over the stars and hit spacebar. MAKE sure you click on them in order! An algorithm will be used to find the exact centroid (within the 3 pixels we specified when editing the centerpars parameter file). Then go to the next star and do the same thing. Just remember, order is important. When you are finished, type “q”. If you run phot on multiple images, it will prompt you to hit n for the next image. Make sure you also change images in ds9 before you start clicking again.

Running phot will produce a text file for each image in the list “sn06Dlist” called \*.mag.1 (1 = if it’s your first time running phot) which contains a plethora of information including the instrumental magnitude for each star whose coordinates are specified in the file, “sn06.reg”. Here’s an excerpt from an example file. Make sure all the header keywords we set in “datapars” were picked up correctly. If you see any INDEF among the data, or zero values for exposure times, etc., something went wrong.

```

pmlne@kaboom: ~/proposals/swift/gi8
#K SALGORITHM = mode          algorithm  Z-23s
#K ANNULUS = 23.              scaleunit Z-23.7g
#K DANNULUS = 5.              scaleunit Z-23.7g
#K SKYVALUE = 0.              counts    Z-23.7g
#K KHIST = 3.                 sigma     Z-23.7g
#K BINSIZE = 0.1              sigma     Z-23.7g
#K SMOOTH = no                switch    Z-23b
#K SMAXITER = 10              number    Z-23d
#K SLOCLIP = 0.               percent   Z-23.7g
#K SHICLIP = 0.               percent   Z-23.7g
#K SNREJECT = 50              number    Z-23d
#K SLOREJECT = 3.             sigma     Z-23.7g
#K SHIREJECT = 3.             sigma     Z-23.7g
#K RGRW = 0.                  scaleunit Z-23.7g
#
#K WEIGHTING = constant       model     Z-23s
#K APERTURES = 18.            scaleunit Z-23s
#K ZMAG = 25.                 zeropoint Z-23.7g
#
#N IMAGE          XINIT  YINIT  ID  COORDS          LID  \
#U imagename     pixels pixels ## filename     ##  \
#F Z-23s         Z-10.3f Z-10.3f Z-5d Z-23s      Z-5d \
#
#N XCENTER  YCENTER  XSHIFT  YSHIFT  XERR  YERR  CIER  CERROR  \
#U pixels   pixels   pixels   pixels pixels pixels ##  errors  \
#F Z-14.3f  Z-11.3f  Z-8.3f  Z-8.3f  Z-8.3f Z-15.3f Z-5d Z-9s \
#
#N NSKY      STDEV      SSKEW      NSKY  NSREJ  SIER  SERROR  \
#U counts    counts    counts    npix  npix  ##  errors  \
#F Z-18.7g   Z-15.7g   Z-15.7g   Z-7d  Z-9d  Z-5d Z-9s \
#
#N ITIME      XAIRMASS  IFILTER      OTIME          \
#U timeunit   number    name          timeunit       \
#F Z-18.7g   Z-15.7g   Z-23s        Z-23s          \
#
#N RPAPERT  SUM      AREA      FLUX      MAG      MERR  PIER  PERROR  \
#U scale    counts    pixels    counts    mag     mag  ##  errors  \
#F Z-12.2f  Z-14.7g   Z-11.7g   Z-14.7g  Z-7.3f Z-6.3f Z-5d Z-9s \
#
#
sn2001c_V      547,000  498,000  1  nullfile      0  \
549,747  498,596  2,747  0,596  0,046  0,044  0  NoError  \
1338,225  21,04508  17,39355  437  366  0  NoError  \
600,0001  1,14  2  600, \
18,00  1442549,  1018,21  79955,06  19,688  0,017  0  NoError \
sn2001c_V      439,000  342,000  2  nullfile      0  \
438,509  344,712  -0,491  2,712  0,006  0,005  0  NoError  \
1303,955  9,142126  -4,695602  696  99  0  NoError  \
600,0001  1,14  2  600, \
18,00  1605518,  1018,182  277855,6  18,336  0,003  0  NoError \
sn2001c_V      675,000  394,000  3  nullfile      0  \
676,531  393,658  1,531  -0,342  0,009  0,009  0  NoError  \
1329,693  9,377841  4,382178  784  15  0  NoError  \
600,0001  1,14  2  600, \
18,00  1466531,  1017,78  113195,8  19,311  0,005  0  NoError \
sn2001c_V      627,000  454,000  4  nullfile      0  \
625,266  454,361  -1,734  0,361  0,004  0,004  0  NoError  \
1330,89  14,11741  11,62749  615  185  0  NoError  \
600,0001  1,14  2  600, \
18,00  1924655,  1018,105  569668,9  17,556  0,002  0  NoError \
sn2001c_V      645,000  632,000  5  nullfile      0  \
645,587  630,576  0,587  -1,424  0,007  0,006  0  NoError  \
1330,207  9,152436  -2,792799  803  3  0  NoError  \
600,0001  1,14  2  600, \
18,00  1561610,  1017,559  208047,1  18,650  0,003  0  NoError

```

- The “mknobsfile” task in “noao.digiphot.photcal” pulls out the pertinent information from the \*.mag.1 files and the imsets file we made earlier. It includes calculated coordinates of the star, airmass, time, instrumental magnitude, and error. Here’s the epar of my “mknobsfile”:

```

xgterm
IRAF
Image Reduction and Analysis Facility

PACKAGE = photcal
TASK = mknobsfile

photfile= *.mag.1 The input list of APPHOT/DAOPHOT databases
idfilter= B,V,R,I The list of filter ids
insets = insets The input image set file
observat= sobs The output observations file
(wrap = yes) Format output file for easy reading ?
(obspara= ) The input observing parameters file
(obscolu= 2 3 4 5) The format of obsparams
(minmage= 0,001) The minimum error magnitude
(shifts = ) The input x and y coordinate shifts file
(apercor= ) The input aperture corrections file
(apertur= 1) The aperture number of the extracted magnitude
(toleran= 0.) The tolerance in pixels for position matching
(allfilt= no) Output only objects matched in all filters
(verify = no) Verify interactive user input ?
(verbose= yes) Print status, warning and error messages ?
(mode = ql)

```

The “idfilters” are a list of the different filters you’ve observed your fields in – they should match the values of “filter” in the fits headers. Setting the tolerance to zero makes iraf match the stars in each image by the order in which they are measured rather than by their calculated coordinates. Here’s what the resultant “sobs” looks like:

```

xgterm

# FIELD      FILTER      OTIME AIRMAGS XCENTER YCENTER  MAG  MERR
sn06D-1     R           11:36:31.3  1.840 1398.037 1909.541 15.511 0.001
*           V           11:50:19.3  1.870 1396.009 1902.346 15.387 0.003
*           B           12:10:13.2  1.900 1392.125 1912.234 15.002 0.002
*           I           12:30:23.9  1.950 1389.036 1919.531 14.356 0.006
sn06D-2     R           11:36:31.3  1.840 1420.391 1799.123 17.679 0.003
*           V           11:50:19.3  1.870 1396.009 1902.346 15.387 0.003
*           B           12:10:13.2  1.900 1392.125 1912.234 15.002 0.002
*           I           12:30:23.9  1.950 1389.036 1919.531 14.356 0.006
sn06D-3     R           11:36:31.3  1.840 1466.401 1714.994 15.568 0.001
*           V           11:50:19.3  1.870 1396.009 1902.346 15.387 0.003
*           B           12:10:13.2  1.900 1392.125 1912.234 15.002 0.002
*           I           12:30:23.9  1.950 1389.036 1919.531 14.356 0.006
sn06D-SN    R           11:36:31.3  1.840 1360.634 1963.275 20.195 0.067
*           V           11:50:19.3  1.870 1396.009 1902.346 15.387 0.003
*           B           12:10:13.2  1.900 1392.125 1912.234 15.002 0.002
*           I           12:30:23.9  1.950 1389.036 1919.531 14.356 0.006
StdA-0      B           12:32:11.0  1.350  821.053 1309.114 14.514 0.001
*           V           11:50:19.3  1.870 1396.009 1902.346 15.387 0.003
*           R           12:10:13.2  1.900 1392.125 1912.234 15.002 0.002
*           I           12:30:23.9  1.950 1389.036 1919.531 14.356 0.006
StdA-1      B           12:32:11.0  1.350 1238.343 1001.009 15.731 0.004
*           V           11:50:19.3  1.870 1396.009 1902.346 15.387 0.003
*           R           12:10:13.2  1.900 1392.125 1912.234 15.002 0.002
*           I           12:30:23.9  1.950 1389.036 1919.531 14.356 0.006
"sobs" 90L, 7130C

```

- You will need to edit “sobs” to make the labels match the ones in “stds”. “mknobsfile” also results in a file called “fsobs.dat” which just keeps track of what column what information is in. Here’s what it looks like:

```

xterm
Declare the observations file variables

observations

TV 3      # time of observation in filter V
XV 4      # airmass in filter V
xV 5      # x coordinate in filter V
yV 6      # y coordinate in filter V
mV 7      # instrumental magnitude in filter V
error(mV) 8 # magnitude error in filter V

TR 10     # time of observation in filter R
XR 11     # airmass in filter R
xR 12     # x coordinate in filter R
yR 13     # y coordinate in filter R
mR 14     # instrumental magnitude in filter R
error(mR) 15 # magnitude error in filter R

TB 10     # time of observation in filter B
XB 11     # airmass in filter B
xB 12     # x coordinate in filter B
yB 13     # y coordinate in filter B
mB 14     # instrumental magnitude in filter B
"fsobs.dat" 26L, 919C

```

- Now we use the task "mkconfig" to create pointers to variables and formulas with which to calculate the actual apparent magnitudes. Here, we will use the landolt transformation equations.

```

xgterm
IRAF
Image Reduction and Analysis Facility
PACKAGE = photcal
TASK = mkconfig

config =          config  The new configuration file
catalog =         stds    The source of the catalog format specification
observat=         sobs    The source of the observations file format speci
transfor=         landolt The source of the transformation equations
(template=       )      An existing template configuration file
(catdir =        )_catdir The standard star catalog directory
(verify =        no)    Verify each new entry
(edit =          yes)   Edit the new configuration file
(check =         yes)   Check the configuration file
(verbose=        no)    Verbose output
(mode =          ql)

ESC-? for HELP

```

Running "mkconfig" makes a file called "config" and spits you out into a vi session on this file. You will need to edit it to include only the information you need. For instance, this file output:

```

xterm
# Declare the catalog variables

catalog
V          2
error(V)   3
BV         4
error(BV)  5
VR         6
error(VR)  7
VI         8
error(VI)  9

# Declare the observations file variables

observations

TB         3          # time of observation in filter B
XB         4          # airmass in filter B
xB         5          # x coordinate in filter B
yB         6          # y coordinate in filter B
mB         7          # instrumental magnitude in filter B
error(mB)  8          # magnitude error in filter B

TV         10         # time of observation in filter V
XV         11         # airmass in filter V
xV         12         # x coordinate in filter V
yV         13         # y coordinate in filter V
mV         14         # instrumental magnitude in filter V
error(mV)  15         # magnitude error in filter V

TR         17         # time of observation in filter R
XR         18         # airmass in filter R
xR         19         # x coordinate in filter R
yR         20         # y coordinate in filter R
mR         21         # instrumental magnitude in filter R
error(mR)  22         # magnitude error in filter R

TI         24         # time of observation in filter I
XI         25         # airmass in filter I
xI         26         # x coordinate in filter I
yI         27         # y coordinate in filter I
mI         28         # instrumental magnitude in filter I
error(mI)  29         # magnitude error in filter I

# Sample transformation section for the Landolt UBVRI system

transformation

fit  u1=0.0, u2=0.65, u3=0.000
const u4=0.0
UFIT : mU = (UB + BV + V) + u1 + u2 * XU + u3 * UB + u4 * UB * XU

fit  b1=0.0, b2=0.35, b3=0.000
const b4=0.0
BFIT : mB = (BV + V) + b1 + b2 * XB + b3 * BV + b4 * BV * XB

fit  v1=0.0, v2=0.17, v3=0.000
const v4=0.0
VFIT : mV = V + v1 + v2 * XV + v3 * BV + v4 * BV * XV

fit  r1=0.0, r2=0.08, r3=0.000
const r4=0.0
RFIT : mR = (V - VR) + r1 + r2 * XR + r3 * VR + r4 * VR * XR

fit  i1=0.0, i2=0.03, i3=0.000
const i4=0.0
IFIT : mI = (V - VI) + i1 + i2 * XI + i3 * VI + i4 * VI * XI

```



has an equation for U observations, but none were taken for my images, so those 3 lines can be deleted. Make sure the variables used in the equations match those specified in the "observations" column. The landolt equations transform the instrumental magnitude of the field stars to the real apparent magnitude. Included in these equations is an offset (b1,r1,i1,etc.) the dependence of the instrumental magnitude on intrinsic color (these are the  $UB=U-B$ ,  $BV=B-V$ ,  $VR=V-R$ , and  $VI=V-I$ ), airmass ( $XB$ ,  $XV$ , etc.), and a combination of the two (the last term in the equations). Once you quit and save the file "config", IRAF will compile the script and report how many if any errors are present. Errors can occur if any of the variables in the equations do not match the variables listed under observations, or if they do not match the id's specified in the "stds" file.

If you entered information into standards that contained B-V, V-I, etc., then you needn't change the landolt equations too much. However, if you entered the apparent magnitude individually in each of the filters, you will need to make the landolt equations look like below:

```

xterm
# Declare the catalog variables

catalog
V          2
error(V)   3
B          4
error(BV)  5
R          6
error(VR)  7
I          8
error(VI)  9

# Declare the observations file variables

observations
TB          3          # time of observation in filter B
XB          4          # airmass in filter B
xB          5          # x coordinate in filter B
yB          6          # y coordinate in filter B
mB          7          # instrumental magnitude in filter B
error(mB)   8          # magnitude error in filter B

TV          10         # time of observation in filter V
XV          11         # airmass in filter V
xV          12         # x coordinate in filter V
yV          13         # y coordinate in filter V
mV          14         # instrumental magnitude in filter V
error(mV)   15         # magnitude error in filter V

TR          17         # time of observation in filter R
XR          18         # airmass in filter R
xR          19         # x coordinate in filter R
yR          20         # y coordinate in filter R
mR          21         # instrumental magnitude in filter R
error(mR)   22         # magnitude error in filter R

TI          24         # time of observation in filter I
XI          25         # airmass in filter I
xI          26         # x coordinate in filter I
yI          27         # y coordinate in filter I
mI          28         # instrumental magnitude in filter I
error(mI)   29         # magnitude error in filter I

# Sample transformation section for the Landolt UBVR system

transformation

fit  b1=0.0, b2=0.35, b3=0.000
const b4=0.0
BFIT : mB = B + b1 + b2 * XB + b3 * (B - V) + b4 * (B - V) * XB

fit  v1=0.0, v2=0.17, v3=0.000
const v4=0.0
VFIT : mV = V + v1 + v2 * XV + v3 * (B - V) + v4 * (B - V) * XV

fit  r1=0.0, r2=0.08, r3=0.000
const r4=0.0
RFIT : mR = R + r1 + r2 * XR + r3 * (V - R) + r4 * (V - R) * XR

fit  i1=0.0, i2=0.03, i3=0.000
const i4=0.0
IFIT : mI = I + i1 + i2 * XI + i3 * (V - I) + i4 * (V - I) * XI
~
~
~

```

8. The task “fitparams” tries to fit each of the constants for the stars where the instrumental magnitude and actual apparent magnitude is known. Note above, certain constants are listed in the row “fit” and given some initial value to start with (usually the defaults work well). The 4<sup>th</sup> constant is usually left at zero, because the addition of the airmass\*color term is most often negligible. If you had any errors in the config file, “fitparams” will not run.

```

xgterm
IRAF
Image Reduction and Analysis Facility
PACKAGE = photcal
TASK = fitparams
observat= sobs List of observations files
catalogs= stds List of standard catalog files
config = config Configuration file
paramete= params Output parameters file
(weighti= uniform) Weighting type (uniform,photometric,equations)
(addscat= yes) Add a scatter term to the weights ?
(toleran= 3.000000000000000E-5) Fit convergence tolerance
(maxiter= 15) Maximum number of fit iterations
(nreject= 0) Number of rejection iterations
(low_rej= 3.) Low sigma rejection factor
(high_re= 3.) High sigma rejection factor
(grow = 0.) Rejection growing radius
(interac= yes) Solve fit interactively ?
(logfile= STDOUT) Output log file
(log_unm= yes) Log any unmatched stars ?
(log_fit= no) Log the fit parameters and statistics ?
(log_res= no) Log the results ?
(catdir = _.)_catdir) The standard star catalog directory
(graphic= stdgraph) Output graphics device
(cursor = ) Graphics cursor input
(mode = ql)
ESC-? for HELP

```

Running this will open an interactive session where you can asses how well the task has fit the constants. Useful keystrokes (used on the irafterm window) are

- d = delete point
- u = undo delete
- f = redo fit (after you've deleted points)
- r = redraw
- q = finished with this fit/quit
- n = go to next fit

After you quit, if you've asked it to save the fit results, then it will output a file called "params" which saves the value of each constant, and information like what equation it was fitting. Below is the Bfit part of the "params" file:

```

Thu 15:47:59 02-Aug-2007
begin BFIT
  status 0      (Solution converged)
  variance 0.006224377
  stdeviation 0.07889472
  avsqerror 1.
  averror 1.
  avsqscatter 0.
  avscatter 0.
  chisqr 0.006224377
  msq 0.00544633
  rms 0.07379925
  reference mB
  fitting (BV+V)+b1+b2*XB+b3*Bv+b4*Bv*XB
  weights uniform
  parameters 4
    b1 (fit)
    b2 (fit)
    b3 (fit)
    b4 (constant)
  derivatives 4
    0.1
    0.1
    0.1
    0.1
  values 4
    1.162345
    1.568694
    0.002566711
    0.
  errors 4
    0.09834564
    0.06571188
    0.03911657
    0.

```

9. "Invertfit" then applies the fitting constants in the same equation to take the unknown (SN) from an instrumental magnitude to an actual apparent magnitude. Here's an lpar:

```

xgterm
  I R A F
Image Reduction and Analysis Facility
PACKAGE = photcal
TASK = invertfit
observat= sobs List of observations files
config = config Configuration file
paramete= params Fitted parameters file
calib = results Output calibrated standard indices file
(catalog= stds) List of standard catalog files
(errors = obserrors) Error computation type (undefined,obserrors,equation)
(objects= all) Objects to be fit (all,program,standards)
(print = ) Optional list of variables to print
(format = ) Optional output format string
(append = no) Append output to an existing file ?
(catdir = )_catdir The standard star catalog directory
(mode = ql)

ESC-? for HELP

```

This outputs a “results” file with the calculated actual apparent magnitudes of all the objects given in “sobs.”

10. Check through the “results” file to see if the calculated magnitudes for the standard stars match the known magnitudes we supplied at the beginning. Did the fit do a good job?

## BIBLIOGRAPHY

- ALDERING, G., BAILEY, S., BONGARD, S., KOCEVSKI, D., LEE, B. C., LOKEN, S., NUGENT, P., PERLMUTTER, S., SCALZO, R., THOMAS, R. C., WANG, L., WEAVER, B. A., BLANC, N., COPIN, Y., GANGLER, E., SMADJA, G., ANTILOGUS, P., GILLES, S., PAIN, R., PEREIRA, R., PECONTAL, E., RIGAUDIER, G., KESSLER, R., BALTAY, C., RABINOWITZ, D., AND BAUER, A. 2006. Classification of SN 2006E, a Postmaximum Type Ia Supernovae. *The Astronomer's Telegram* 690, 1.
- AXELROD, T. S. 1980. Late time optical spectra from the Ni-56 model for Type 1 supernovae. Ph.D. thesis, AA(California Univ., Santa Cruz.).
- BLACKMAN, J., SCHMIDT, B., AND KERZENDORF, W. 2006. Supernovae 2006ce and 2006ci. *Central Bureau Electronic Telegrams* 541, 1.
- BRANCH, D. 1982. Type I supernovae - Observational constraints. In *NATO ASIC Proc. 90: Supernovae: A Survey of Current Research*, V. L. Trimble, Ed. 267–279.
- BROWN, P. J., DAWSON, K. S., HARRIS, D. W., OLMSTEAD, M., MILNE, P., AND ROMING, P. W. A. 2012. Constraints on Type Ia Supernova Progenitor Companions from Early Ultraviolet Observations with Swift. *Astrophys. J.* 749, 18.
- BROWN, P. J., HOLLAND, S. T., JAMES, C., MILNE, P., ROMING, P. W. A., MASON, K. O., PAGE, K. L., BEARDMORE, A. P., BURROWS, D., MORGAN, A., GRONWALL, C., BLUSTIN, A. J., BOYD, P., STILL, M., BREEVELD, A., DE PASQUALE, M., HUNSBERGER, S., IVANUSHKINA, M., LANDSMAN, W., MCGOWAN, K., POOLE, T., ROSEN, S., SCHADY, P., AND GEHRELS, N. 2005. Ultraviolet, Optical, and X-Ray Observations of the Type Ia Supernova 2005am with Swift. *Astrophys. J.* 635, 1192–1196.
- COLGATE, S. A. AND MCKEE, C. 1969. Early Supernova Luminosity. *Astrophys. J.* 157, 623–+.
- COX, A. N. 2000. *Allen's Astrophysical Quantities*. Springer.
- ELIAS-ROSA, N., BENETTI, S., CAPPELLARO, E., TURATTO, M., MAZZALI, P. A., PATAT, F., MEIKLE, W. P. S., STEHLE, M., PASTORELLO, A., PIGNATA, G., KOTAK, R., HARUTYUNYAN, A., ALTAVILLA, G., NAVASARDYAN, H., QIU, Y., SALVO, M., AND HILLEBRANDT, W. 2006. Anomalous extinction behaviour towards the Type Ia SN 2003cg. *MNRAS* 369, 1880–1900.
- FILIPPENKO, A. V. 1997. Optical Spectra of Supernovae. *ARA&A* 35, 309–355.

- FILIPPENKO, A. V., RICHMOND, M. W., MATHESON, T., SHIELDS, J. C., BURBIDGE, E. M., COHEN, R. D., DICKINSON, M., MALKAN, M. A., NELSON, B., PIETZ, J., SCHLEGEL, D., SCHMEER, P., SPINRAD, H., STEIDEL, C. C., TRAN, H. D., AND WREN, W. 1992. The peculiar Type IA SN 1991T - Detonation of a white dwarf? *Astrophys. J. Lett.* *384*, L15–L18.
- GERARDY, C. L. 2005. Surprises from the Type Ia SN 2003du. In *1604-2004: Supernovae as Cosmological Lighthouses*, M. Turatto, S. Benetti, L. Zampieri, and W. Shea, Eds. Astronomical Society of the Pacific Conference Series, vol. 342. 250.
- HAMUY, M., PHILLIPS, M. M., SUNTZEFF, N. B., SCHOMMER, R. A., MAZA, J., SMITH, R. C., LIRA, P., AND AVILES, R. 1996. The Morphology of Type IA Supernovae Light Curves. *Astronom. J.* *112*, 2438.
- HILLEBRANDT, W. AND NIEMEYER, J. C. 2000. Type IA Supernova Explosion Models. *ARA&A* *38*, 191–230.
- HOEFLICH, P. AND KHOKHLOV, A. 1996. Explosion Models for Type IA Supernovae: A Comparison with Observed Light Curves, Distances, H 0, and Q 0. *Astrophys. J.* *457*, 500–+.
- HUBBLE, E. 1929. A Relation between Distance and Radial Velocity among Extra-Galactic Nebulae. *Proceedings of the National Academy of Science* *15*, 168–173.
- IMMLER, S., HOLLAND, S. T., BROWN, P. J., AND MILNE, P. 2006. Swift Observations of Supernova 2006E in NGC 5338. *The Astronomer's Telegram* *691*, 1.
- KASEN, D. 2006. Secondary Maximum in the Near-Infrared Light Curves of Type Ia Supernovae. *Astrophys. J.* *649*, 939–953.
- KHOKHLOV, A. M. 1991. Delayed detonation model for type IA supernovae. *A&A* *245*, 114–128.
- KNÖDLSER, J., JEAN, P., LONJOU, V., WEIDENSPÖTNER, G., GUESSOUM, N., GILLARD, W., SKINNER, G., VON BALLMOOS, P., VEDRENNE, G., ROQUES, J.-P., SCHANNE, S., TEEGARDEN, B., SCHÖNFELDER, V., AND WINKLER, C. 2005. The all-sky distribution of 511 keV electron-positron annihilation emission. *A&A* *441*, 513–532.
- KRISCIUNAS, K., GARNAVICH, P. M., STANISHEV, V., SUNTZEFF, N. B., PRIETO, J. L., ESPINOZA, J., GONZALEZ, D., SALVO, M. E., ELIAS DE LA ROSA, N., SMARTT, S. J., MAUND, J. R., AND KUDRITZKI, R.-P. 2007. The Type Ia Supernova 2004S, a Clone of SN 2001el, and the Optimal Photometric Bands for Extinction Estimation. *Astronom. J.* *133*, 58–72.
- LAIR, J. C., LEISING, M. D., MILNE, P. A., AND WILLIAMS, G. G. 2006. Late Light Curves of Normal Type Ia Supernovae. *Astronom. J.* *132*, 2024–2033.
- LEE, N. AND LI, W. 2006. Supernova 2006mq in ESO 494-G26. *Central Bureau Electronic Telegrams* *721*, 1.

- LELOUDAS, G., STRITZINGER, M. D., SOLLERMAN, J., BURNS, C. R., KOZMA, C., KRISCIUNAS, K., MAUND, J. R., MILNE, P., FILIPPENKO, A. V., FRANSSON, C., GANESHALINGAM, M., HAMUY, M., LI, W., PHILLIPS, M. M., SCHMIDT, B. P., SKOTTFELT, J., TAUBENBERGER, S., BOLDT, L., FYNBO, J. P. U., GONZALEZ, L., SALVO, M., AND THOMAS-OSIP, J. 2009. The normal Type Ia SN 2003hv out to very late phases. *A&A* 505, 265–279.
- MAZZALI, P. A., CHUGAI, N., TURATTO, M., LUCY, L. B., DANZIGER, I. J., CAPPELLARO, E., DELLA VALLE, M., AND BENETTI, S. 1997. The properties of the peculiar type IA supernova 1991bg - II. The amount of  $^{56}\text{Ni}$  and the total ejecta mass determined from spectrum synthesis and energetics considerations. *MNRAS* 284, 151–171.
- MILNE, P. A., THE, L.-S., AND LEISING, M. D. 2001. Late Light Curves of Type Ia Supernovae. *Astrophys. J.* 559, 1019–1031.
- MOTOHARA, K., MAEDA, K., GERARDY, C. L., NOMOTO, K., TANAKA, M., TOMINAGA, N., OHKUBO, T., MAZZALI, P. A., FESEN, R. A., HÖFLICH, P., AND WHEELER, J. C. 2006. The Asymmetric Explosion of Type Ia Supernovae as Seen from Near-Infrared Observations. *Astrophys. J. Lett.* 652, L101–L104.
- NADYOZHIN, D. K. 1994. The properties of NI to CO to Fe decay. *Astrophys. J. Suppl.* 92, 527–531.
- PERLMUTTER, S., GABI, S., GOLDHABER, G., GOOBAR, A., GROOM, D. E., HOOK, I. M., KIM, A. G., KIM, M. Y., LEE, J. C., PAIN, R., PENNYPACKER, C. R., SMALL, I. A., ELLIS, R. S., MCMAHON, R. G., BOYLE, B. J., BUNCLARK, P. S., CARTER, D., IRWIN, M. J., GLAZEBROOK, K., NEWBERG, H. J. M., FILIPPENKO, A. V., MATHESON, T., DOPITA, M., COUCH, W. J., AND THE SUPERNOVA COSMOLOGY PROJECT. 1997. Measurements of the Cosmological Parameters Omega and Lambda from the First Seven Supernovae at  $Z \geq 0.35$ . *Astrophys. J.* 483, 565–+.
- PHILLIPS, M. M. 1993. The absolute magnitudes of Type IA supernovae. *Astrophys. J. Lett.* 413, L105–L108.
- PINTO, P. A. AND EASTMAN, R. G. 2000. The Physics of Type IA Supernova Light Curves. II. Opacity and Diffusion. *Astrophys. J.* 530, 757–776.
- PONTICELLO, N. J., KHANDRIKA, H., MADISON, D. R., LI, W., NEWTON, J., CROWLEY, T., PUCKETT, T., MONARD, L. A. G., SEHGAL, A., AND (LOSS/KAIT). 2006. Supernovae 2006cb, 2006cc, 2006cd, 2006ce. *IAU Circ.* 8709, 1.
- PRIETO, J. 2006. Supernova 2006mq in ESO 494-G26. *Central Bureau Electronic Telegrams* 731, 1.
- PUCKETT, T., REDDY, V., AND LI, W. 2006. Supernova 2006E in NGC 5338. *Central Bureau Electronic Telegrams* 363, 1.



- RIESS, A. G., FILIPPENKO, A. V., CHALLIS, P., CLOCCHIATTI, A., DIERCKS, A., GARNAVICH, P. M., GILLILAND, R. L., HOGAN, C. J., JHA, S., KIRSHNER, R. P., LEIBUNDGUT, B., PHILLIPS, M. M., REISS, D., SCHMIDT, B. P., SCHOMMER, R. A., SMITH, R. C., SPYROMILIO, J., STUBBS, C., SUNTZEFF, N. B., AND TONRY, J. 1998. Observational Evidence from Supernovae for an Accelerating Universe and a Cosmological Constant. *Astronom. J.* *116*, 1009–1038.
- RIESS, A. G., PRESS, W. H., AND KIRSHNER, R. P. 1996. A Precise Distance Indicator: Type IA Supernova Multicolor Light-Curve Shapes. *Astrophys. J.* *473*, 88–+.
- SOLLERMAN, J., LINDAHL, J., KOZMA, C., CHALLIS, P., FILIPPENKO, A. V., FRANSSON, C., GARNAVICH, P. M., LEIBUNDGUT, B., LI, W., LUNDQVIST, P., MILNE, P., SPYROMILIO, J., AND KIRSHNER, R. P. 2004. The late-time light curve of the type Ia supernova 2000cx. *A&A* *428*, 555–568.
- STRITZINGER, M. AND SOLLERMAN, J. 2007. Late-time emission of type Ia supernovae: optical and near-infrared observations of SN 2001el. *A&A* *470*, L1–L4.
- WATSON, L., DEPOY, D., PRIETO, J. L., AND GARNAVICH, P. M. 2006. Supernovae 2006mp and 2006mq. *Central Bureau Electronic Telegrams* *724*, 1.
- YAMAOKA, H. AND ITAGAKI, K. 2006. Supernova 2006E in NGC 5338. *IAU Circ.* *8666*, 3.